الجمهورية الجزائرية الديمقراطية الشعبية
People's Democratic Republic of Algeria
وزارة التعليم العالي والبحث العلمي
Ministry of Higher Education and Scientific Research

University Center
Abdelhafid Boussouf – Mila

المركز الجامعي
عبد الحفيظ بوالصوف ميلة

Institute: Mathematics and Computer Sciences
Department: Mathematics
Order N° : …….
Matricule : M99/2021
Field: Mathematics
Specialty: Applied mathematics

www.centre-univ-mila.dz

Thesis

Presented for the degree of
Doctorate LMD

Numerical study of boundary problems for partial differential equations

Presented by: Laouar Zineb
Supervised by: Dr. Arar Nouria

Abdelouahab Mohammed-Salah	**Prof**	**Centre Universitaire Mila**	**Chairman**
Arar Nouria	**MCA**	**Université Constantine 1**	**Supervisor**
Halim Yacine	**Prof**	**Centre Universitaire Mila**	**Examiner**
Laouira Widad	**MCA**	**Centre Universitaire Mila**	**Examiner**
Laib Hafida	**MCA**	**Centre Universitaire Mila**	**Examiner**
Abada Nadjet	**MCA**	**ENS Constantine**	**Examiner**

University year : 2023/2024

Acknowledgments

Firstly, I would like to express my deepest gratitude to my thesis supervisor, Dr. ARAR Nouria, who has advised and guided me throughout the entire journey of this PhD research. Her availability and wise observations have been of precious help in the realization of the present work. Her assistance has been instrumental in shaping my research skills and academic growth.

I am immensely thankful to the members of my doctoral committee, Prof. ABDELOUAHAB Mohammed-Salah, Prof. HALIM Yacine, Dr. ABADA Nadjet, Dr. LAIB Hafida, and Dr. LAOUIRA Widad, for taking time to read and giving their constructive feedback and expertise, which significantly enriched the quality of my thesis.

Special thanks go to my parents for their unwavering support and encouragement throughout this challenging and rewarding academic journey. Their advice, love and understanding have been my source of strength.

Abstract

The aim of this work is to study various problems of mathematical equations using spectral methods. It develops *four numerical techniques* suitable for every studied problem and shows efficiency throughout different numerical illustrations. This study proposes a *Legendre Galerkin method coupled with finite differences technique* for the advection-diffusion equation with perturbed Robin boundary conditions. The obtained results provide two ways to confirm the efficiency: firstly, by calculating the error of approximation, and simultaneously by comparing the obtained approximate solution to the exact solution of the problem with Dirichlet boundary conditions. For the same equation, a second scheme is proposed using the spectral *Galerkin method* for both temporal and spatial discretizations. On the same axis, a transition to integral/integro-differential equations is introduced. A novel way of writing the basis functions as compact combinations of orthogonal polynomials using the set of initial conditions is elaborated in a *Galerkin method* for the integral and integro-differential equations, depending on the order of derivation. Additionally, some numerical techniques, such as using Gauss types quadrature, are also investigated for more accuracy. The last set of results pertains to the study of integro-differential equations of fractional order. Some interesting estimations are formulated to approximate the solution using orthogonal polynomials in a *collocation method*. All the presented techniques are supported by numerical examples that cover a vast range of cases, to demonstrate the efficiency of the proposed algorithms.

Key words/phrases: Partial differential equations, spectral approximation, Galerkin method/Collocation method, finite differences scheme, Integral/integro-differential equations, Fractional equations, Legendre/Chebyshev polynomials, Gauss types quadrature.

Résumé

Le but de ce travail est d'étudier quelques problèmes d'équations mathématiques à l'aide des méthodes spectrales. On développe *quatre techniques numériques* adaptées aux équations étudiées et on démontre leur efficacité. On propose une *méthode de Galerkin Legendre* pour l'équation d'advection-diffusion, avec des conditions aux limites perturbées de type Robin. Les résultats obtenus offrent deux façons de confirmer l'efficacité de la méthode: d'abord, en calculant l'erreur d'approximation, puis en comparant la solution approximative obtenue à la solution exacte du problème avec des conditions aux limites de Dirichlet. Pour la même équation, un second schéma est proposé en utilisant *une méthode de Galerkin* pour les discrétisations temporelles et spatiales. Sur le même axe, une transition vers les équations intégrales/intégro-différentielles est introduite. Une nouvelle méthode d'écrire les fonctions de base, sous forme de combinaisons compactes de polynômes orthogonaux utilisant l'ensemble des conditions initiales est élaborée dans une *méthode de Galerkin*, en fonction de l'ordre de dérivation. Certaines techniques numériques telles que l'utilisation de la quadrature de Gauss sont également explorées pour plus de précision. Les derniers résultats sont liés à l'étude des équations intégro-différentielles d'ordre fractionnaire. Des estimations intéressantes sont formulées pour approximer la solution de tels problèmes en utilisant des polynômes orthogonaux dans une *méthode de collocation*. Toutes les techniques présentées sont étayées par des exemples numériques traitant le maximum de cas possibles afin de démontrer l'efficacité des algorithmes proposés.

Mots Clés: Equations différentielles partielles, Approximation spectrale, Méthode de Galerkin/collocation, Schéma de différences finies, Equations intégrales/integro-différentielles, Equations fractionnaires, Polynômes de Legendre/Chebyshev, Quadrature de Gauss.

ملخص

يهدف هذا العمل إلى دراسة مجموعة من المعادلات الرياضية باستعمال طرق التقريب الطيفي، حيث يطور أربع تقنيات رقمية مناسبة لكل نوع متطرق إليه، ويبرهن على فعاليتها من خلال مجموعة من الأمثلة. تطرح هذه الدراسة طريقة لاجندر غالركين مقترنة بتقنية الفروق المنتهية لمعادلة الانتشار المادي والحراري مع شروط حدية مضطربة من نوع روبن، حيث تسمح النتائج المتحصل عليها بتأكيد كفاءة الطريقة المقترحة باستعمال طريقتين، الأولى من خلال حساب خطأ التقريب الخاص بالطريقة المقترحة، والثانية بمقارنة الحل التقريبي بالحل الصحيح للمعادلة تحت شروط حدية من نوع ديريشليت من جهة أخرى. كما قد تم إقتراح مخطط ثان لدراسة نفس المعادلة باستعمال طريقة غالركين لكل من المتغيرات الزمانية والمكانية. على نفس المنوال، نقدم طريقة الانتقال إلى المعادلات التكاملية/التفاضلية التكاملية، حيث نستعرض طريقة جديدة لكتابة الدوال المركبة للأساس على شكل تركيبات متراصة من كثيرات الحدود المتعامدة باستعمال مجموعة الشروط الابتدائية على حسب رتبة الاشتقاق لبناء مخطط رقمي بطريقة غالركين. بالإضافة إلى استعمال بعض التقنيات العددية الهادفة إلى الحصول على المزيد من الدقة كتكاملات غاوس لحساب التكاملات بطريقة عددية. المجموعة الأخيرة من النتائج تتعلق بدراسة المعادلات التفاضلية التكاملية ذات الرتبة الكسرية، حيث قمنا بصياغة بعض التقديرات المهمة لتقريب حل المعادلة باستخدام كثيرات الحدود المتعامدة في طريقة التجميع. جميع التقنيات المقدمة مدعومة بأمثلة عددية تدرس مجموعة واسعة من الحالات لإثبات كفاءة الخوارزميات المقترحة.

الكلمات المفتاحية:

المعادلات التفاضلية الجزئية، التقريب الطيفي، طريقة غالركين، طريقة التجميع، مخطط الفروق المنتهية، المعادلات التكاملية، المعادلات التكاملية التفاضلية، المعادلات الكسرية، كثيرات حدود لاجندر/تشيبيتشاف، تكاملات غاوس.

Contents

Notations

- $L^2(I)$: the space of measurable functions on I with $\|u\|_{L^2(I)} < \infty$.
- $H^m(I)$: the Sobolev space which is the vector space where a function v with its distributional derivatives of order up to m belong to $L^2(I)$.
- $\mathscr{C}^m(I, \mathbb{R})$: the vector space where for each function $v : \bar{I} \to \mathbb{R}$, $D^\alpha v$ exists and is continuous for $0 \leq |\alpha| \leq m$.
- $\mathscr{C}^\infty(\bar{I})$: the space of the infinitely differentiable functions on $\bar{I}$.
- $\mathbb{P}_N$ the space of polynomials of degree less than or equal to N.
- $P_k^{(\alpha,\beta)}(x)$: Jacobi polynomials.
- $\mathscr{L}_k(x)$: Legendre polynomials.
- $\mathscr{V}_k(x)$: Chebyshev polynomials of the third kind.

General introduction

General introduction

The main issue when studying differential equations is that the majority lack explicit analytical solutions. As a result, many researchers turn to numerical methods to obtain approximate solutions effectively. Currently, the challenge for mathematicians is to develop suitable and accurate algorithms to obtain the required solutions.
The presented thesis aims to introduce some numerical approaches applicable to different types of differential equations, mainly focusing on partial differential equations. It develops different algorithms that encompass a wide range of equations and propose numerous schemes effectively used to approximate the solution.
Numerical analysis plays a crucial role in the development of calculation codes as well as solving simulation problems or conducting mathematical experiments. It has close links with information technology (IT). While the theoretical part is more mathematical, its practical application generally involves implementing algorithms on a computer. Its methods are based both on the search for exact solutions, as in the case of matrix analysis or symbolic calculus, and on approximate solutions, often stemming from discretization processes, as in the treatment of differential equations.

Throughout history, to solve differential equations, finite differences methods were the standard and most widely used numerical methods. These methods involve approximating the values of the unknown function at a set of discrete points, usually equally spaced within the interval of the study, using an appropriate step size. This approach is called "local" because the approximate solution in known only at a finite number of points.

Recently, another type of numerical methods has emerged and can be more effective in some situations. These methods are based on the finite expansion of a function using orthogonal polynomials, known as "spectral methods" which have gained significant interest in solving several types of equations. In spectral methods, the function $u(x)$ is represented as an infinite expansion $u(x) = \sum_{k=0}^{+\infty} \hat{u}_k \phi_k(x)$ where $\{\phi_k(x)\}$ is a sequence of basis functions (generally orthogonal polynomials or a combination of orthogonal polynomials[29, 16]). The idea is to express the solution as a finite sum of these special basis functions and compute as many coefficients as possible $\{\hat{u}_k\}$ to obtain the simplest system, where the solution is constructed from the coefficients of the approximation in the chosen basis [73]

$$u(x) \simeq u_N(x) = \sum_{k=0}^{N} \hat{u}_k \phi_k(x).$$

The main advantage of these methods is that once the spectral coefficients are determined, the approximate solution can be directly evaluated at any point within the study interval. This characteristic gives these methods a global approximation nature. Due to their straightforward application, spectral methods provide interesting results compared to other methods.

Thanks to the favourable properties of orthogonal polynomials (Legendre, Chebyshev, ...), spectral methods exhibit speed convergence. This implies that even with limited data, these methods achieve a hight rate of convergence and spectral accuracy [82]. The selection of appropriate basis functions plays a crucial role in the implementation of spectral methods [80]. By choosing the suitable basis [81], the resulting systems become simpler, with a special structure of matrices easy to invert. This reduction in complexity reduces the cost of the method, enhancing its efficiency and accuracy.

Spectral methods encompass different categories including Galerkin, collocation and tau methods. Galerkin and Tau methods are applied directly in terms of the expansion coefficients. In Galerkin method, the test functions are identical to the basis functions. An essential characteristic is that the basis functions are constrained to satisfy the boundary conditions of the problem. In contrast, for the

Tau method, basis functions do not satisfy the boundary conditions. As a result, other equations must be added to ensure that the global expansion does satisfy the boundary conditions.

On the other hand, collocation method utilizes also the finite expansion, similar to Galerkin and Tau methods, but it evaluates the solution at a specific number of discrete points $u_N(x_j)$. These points can be either equally spaced or not. The optima choices for these points include nodes corresponding to highest precision quadrature formulas or the zeros of orthogonal polynomials used as basis functions. The collocation method is becoming increasingly popular for solving a wide variety of differential equations. Notably, spectral collocation methods have been successfully applied to integral and integro-differential equations [49], for multi-order fractional differential equations [31], for multi-order fractional equations with multiple delays [22], two-dimensional fractional integro-differential equations with weakly singular kernels [9] and systems of fractional differential equations [4, 50, 51].

Another type of spectral methods that also employs discrete values of the unknown function and is regarded as a variation of the Galerkin method is the Galerkin method with numerical integration. The objective of this latter is to preserve the advantages of both the Galerkin and collocation methods. The integrals that arise in the weak formulation are approximated using a precise quadrature formula. For instance, we use in this thesis a Gauss-Lobatto integration formula.

As basis functions, spectral methods primarily utilize orthogonal polynomials (such as Legendre, Chebyshev, etc.) to represent the numerical solution through a finite expansion [32, 17]. Orthogonal polynomials, also known as eigenfunctions of the Sturm-Liouville problem, have a wide range of properties. The significance of Sturm-Liouville problems for spectral methods lies in the fact that the spectral approximation of the solution of a differential equation is usually regarded as a finite expansion of eigenfunctions of a suitable Sturm Liouville problem across the entire domain. We opt for orthogonal polynomials for their several properties depending on the interval of study, as they are the most common eigenfunctions [43, 73, 1, 79, 10, 83, 84]. Another option of basis functions is to create linear com-

binations of the orthogonal polynomials as a technical procedure. This involves the use of more properties of these orthogonal polynomials, allowing us to derive more benefits from them and potentially reduce the cost of the numerical method. Due to the special properties of the chosen basis functions, spectral methods achieve a rapid convergence rate and hight accuracy, ensuring spectral accuracy when compared to other numerical methods like finite differences and finite elements methods [53, 14, 82].

In this context, we chose two kinds of orthogonal polynomials as fundamental mathematical tools to elaborate the spectral schemes: Legendre and Chebyshev polynomials. This choice was deliberate, as among the numerous properties that characterise the orthogonal polynomials, these two kinds hold special importance. Indeed, Legendre polynomials are orthogonal with a unit weight function which makes easy their implementation. On the other hand, Chebyshev polynomials are famous for their direct association with the trigonometric functions "cosine" and "sine". However, unlike Legendre polynomials, the locations of their zeros are known analytically. Furthermore, the Chebyshev polynomials, like the Legendre polynomials, belong to a specific category of orthogonal polynomials known as Jacobi polynomials. These polynomials correspond to weight functions of the form $(1-x)^{\alpha}(1+x)^{\beta}$ and serve as solutions of Sturm-Liouville equations.

Given the fact that mathematics provide essential tools to explain various phenomena in the universe, differential equations were developed to establish connections between various influencing factors. The presented thesis aims to explore various types of differential equations using different numerical approaches within the same family of numerical methods, namely spectral methods. The leading families of equations which consist the subject of this thesis are the family of partial differential equations and the family of integral/integro-differential equations. These equations hold significant importance in modelling various real-world phenomena. We note here that there is a direct link between the two families of equations; every partial differential equation can be transformed to an integral equation by just integrating it with respect to one of its variables. This procedure aims to reduce the number of boundary conditions. Generally for evolution

equations, an integration for the temporal variable by making use of the initial condition is a commonly employed practice.

The first equation is a partial differential equation known as the Advection-diffusion equation. It is an evolution equation that is viewed as a prototype of parabolic equations.

The second type of equations is the family of integral and integro-differential equations. These equations involve an unknown function within the sign of the integration (including the two categories of equations based on the boundaries of integration) additionally, they also may contain the derivative of the unknown function (integro-differential equation) with the same order as the order of derivation appearing in the equation. These types of equations which are generally difficult to solve directly using classical methods and have been the main subject of numerous numerical methods that aim to approximate the solution through reliable algorithms [53].

The third type of equations is the family of fractional equations, more precisely integro-differential equations of fractional order. The concept of fractional calculus has attracted interest of mathematicians and physicists due to its effectiveness in describing various phenomena in biology [44, 55, 46], medicine [33, 74, 85, 30], physics [38, 37], finance [75]. A significant number of real world problems can be represented by differential equations involving fractional derivative. This notion of fractional derivation generalises the classical derivative of integer order to a derivation of a non-integer order. The two most commonly used definitions of fractional integration and derivation are the Riemann Liouville sense and the Caputo sense. These definitions are particularly valuable for their high explanatory power in capturing memory effects which is needed in different real-world problems, especially for medicine, physics, and finance.

Advection-diffusion equation

The advection and diffusion are two processes of significant importance in real world applications. They describe physical phenomena involving the trans-

port of particles such as mass, energy, heat, humidity, pollutant and more. The Advection-Diffusion equation has several engineering applications, including heat transfer, water transfer in soils, chemical engineering, biosciences, as well as the study of velocity, vorticity, and dispersion of tracers in porous media [41, 72, 20]. This equation is used to describe the transport of air and groundwater pollutants, capturing the behaviour of contaminant or pollutant concentration distribution through air, rivers, lakes and porous medium like aquifer.

This equation has been solved using many numerical methods, especially when the boundary conditions are from Dirichlet or Neumann types. Boundary conditions of Robin type, which consider a linear combination between the function and its derivative, are used to model important and vital problems of chemical engineering and heat transfer. Mojtabi and Deville [66] considered the time dependent one-dimensional linear advection-diffusion equation with Dirichlet homogeneous boundary conditions. They observed that when the advection becomes dominant, the analytical solution becomes ill-behaved and harder to evaluate.

The numerical simulation became very useful, easier, and more efficient in time, particularly for time-dependent problems. Hutomo et al. [39] studied the numerical solution of the advection-diffusion equation with variable coefficients. The results obtained from the Du-Fort Frankel method for the 2-D advection-diffusion equation align with those of the analytical solution.

Integral and integro-differential equations

In recent years, integral equations and integro-differential equations received significant interest from researchers in various scientific fields. Mathematicians and physicists have recognized the importance of this kind of equations, which are employed in fundamental problems in biology, medicine [77], chemistry, electrostatics, fluid dynamics, physics [86], economics [34], engineering [78], mechanics [6], potential theory [8], problems of gravitation [21] and more.

When discussing numerical methods for integral and integro-differential equations, many studies have shown interest in this area. Doha et al. [25] used shifted Ja-

cobi polynomials in spectral collocation method to solve integro-differential equations and systems of integro-differential equations. In [26], the authors developped a collocation procedure using cubic B-splines for linear and nonlinear Fredholm and Volterra integral equations. Fathy et al. [28] presented a Legendre-Galerkin method for the linear Fredholm integro-differential equations, while Nemati in [71] used the shifted Legendre polynomials to approximate the solution of Volterra-Fredholm integral equations. Other researchers, such as Černá et al. [18], Moghaddam et al. [62], [63] used B-spline wavelets; Maleknejad et al. [58] Haar wavelets and Lakestani et al. [48] utilized multi-wavelets to solve numerically integral and integro-differential equations. Moghaddam et al. in [64] developped fractional finite differences method, Biçer et al. [11] investigated Bernoulli polynomials, Doha et al. [23] used ultraspherical polynomials, Jalilian et al. [42] used the exponential spline method, Meng et al. [61] and El-Sayed et al. [27] employed alternative (shifted) Legendre polynomials, Mandal et al. [59] used the Bernstein polynomials, Machado et al. [56] employed the reduced differential transform, Loh et al. [52] used Laplace transform and resolvent kernel method, and Mokhtary et al. [67] used the spectral methods to solve numerically integro-differential equations.

Fractional integro-differential equations

In order to expand the field of study of fractional equations, numerous numerical methods were developed to encompass various types of these equations. For this, there has been significant interest in solving fractional integro-differential equations using many numerical methods [36, 57, 13, 5], with specific emphasis on collocation methods. In [12], the authors used a wavelet collocation method to solve Fredholm Fractional integro-differential equations. Doha et al. in [25] used a Shifted Jacobi polynomials to establish a Gauss collocation method for fractional integro-differential equations, encompassing linear and nonlinear Volterra, Fredholm, mixed Volterra-Fredholm, and system of Volterra equations. In [2], the authors investigated the first kind of Bessel polynomials in a collocation technique to approximate the solution of a linear Fredholm-Volterra fractional integro-differential equations of multi-hight order. Additionally, in [87], an implementation of a collocation method using shifted Legendre polynomials coupled with Gauss-Legendre quadrature is presented. Rahimkhani et al. [76] used alternative

Legendre functions for nonlinear fractional integro-differential equations. Other works, such as [89, 54, 88] also contribute to the exploration of numerical methods for solving fractional integro-differential equations.

Our motivation for the presented thesis is to elaborate a suitable numerical method based on spectral methods to approximate the solution of each proposed equation. The thesis is divided into four chapters.

- In chapter 1, we present some essential preliminaries of orthogonal polynomials and Gauss type quadratures and, illustrating their direct link with the numerical approximation through various numerical applications. The chapter emphasises basic properties crucial for the development of the numerical approach of each equation.

- In chapter 2, two spectral techniques are presented to study the advection-diffusion equation. In the first one, we propose a spectral method to approximate the solution of the advection-diffusion equation with Robin boundary conditions. The approximation relies on a special basis, involving a specific linear combination of Legendre polynomials that satisfy boundary conditions [43, 14, 82]. Analytical results in the form of stability and convergence theorems are also derived in this study to investigate and reinforce spectral accuracy [7, 19]. Moreover, the temporal solution is established using a Crank-Nicolson scheme with an appropriate temporal step [3]. In this study, we seek for taking the advantage of Legendre polynomials and Gauss types quadrature to apply Galerkin and Crank-Nicolson methods, in order to obtain the best approximate solution. To get the best results from spectral method, especially when calculating integrals, we introduce a Gauss type quadrature using Legendre-Gauss-Lobatto nodes and their corresponding weights. Due to their high accuracy, Gauss formulas play fundamental role in the theoretical analysis of spectral methods. The possibility of integrating polynomials just by knowing their values at M points will be widely used; in addition, the fact that the points $x = -1$ and $x = 1$ are included in the nodes is very important for imposed boundary conditions [29, 73].
  The second technique uses the spectral expansion for both spatial and tem-

poral discretizations. First, the problem is reduced to its integral form by taking into account the initial condition. Then, the same linear combination of Legendre polynomials that satisfy boundary conditions, as for the first approach, is used to approximate the solution. This technique calls upon using the Kronecker product to write the matrix form of the system, which will be next solved by a Gauss elimination method. The proposed scheme show applicability for integral equations as for partial differential equations.

- In chapter 3, we elaborate a spectral approximation governing both integral and integro-differential equations of linear and nonlinear forms. We apply the shifted-Legendre-Gauss collocation method with a specific combination of shifted-Legendre polynomials as basis functions and the nodes of shifted-Legendre-Gauss interpolation as collocation points. The form of the basis functions is determined according to the order of the equation. The initial condition of the problem influences the choice of the basis functions, leading to simple systems solvable in both linear and nonlinear cases. For linear systems, we solve directly by Gauss elimination method, and for nonlinear systems we use a Newton algorithm by calculating the Jacobian matrix. The proposed scheme holds significant practical value since it uses a distinctive set of basis functions, presented as a linear combination adapted to the order of the integro-differential equation. Moreover, the case of integral equations may be directly derived as a special case of the proposed study.

- In chapter 4, we propose an efficient spectral method: the shifted Chebyshev-Gauss collocation method, based on the zeros of Chebyshev polynomials of the third kind to approximate the solution of a mixed Volterra-Fredholm integro-differential equation of fractional order. We express the solution as a finite expansion of shifted Chbyshev polynomials of the third kind, after substituting the approximation in the studied problem and considering the collocation, and we evaluate integrals using Chebyshev-Gauss quadrature. Depending on the linearity of the term that contains the unknown function under the integration we study two cases. In the linear case, we obtain a simple algebraic system that we solve by a Gauss elimination algorithm. For the second case, we consider a power-type nonlinearity of the unknown func-

tion, and we obtain a nonlinear system for which we calculate the jacobian matrix and solve it using a Newton algorithm. This scheme is considered as a suitable method because of its simplicity and accurate results obtained for different examples. One of its advantages that it treats different types of integro-differential equation: Volterra, Fredholm, mixed Volterra-Fredholm in both linear and nonlinear cases. Moreover, the use of Chebyshev polynomials of the third kind is highly significant; due to their numerous properties. These polynomials simplify the calculations, serving as an orthogonal basis that can be written as a compact combination of Chebyshev polynomials of the second kind. This characteristic facilitates the development of an accurate algorithm of approximation to gain the spectral accuracy: the well-known advantage of spectral methods. Furthermore, an error analysis is conducted and numerical results are exposed to validate the effectiveness of the proposed method.

The tools used to produce this thesis are as follows:
References: all books and papers used in the elaboration of this study are cited at the end of this thesis in the reference section.
LaTeX: for the production of this thesis.
MATLAB: for all algorithms used in the numerical approximation and the production of all figures and results of tables. All the computations were carried out in double precision using Matlab 9.8.0 (R2020a), and executions were done on AMD Ryzen 5 5600X 6-Core, 3.70Ghz Desktop.

Chapter 1

Preliminaries

Chapter 1

Preliminaries

In spectral methods, the approximation of solutions is related to the use of orthogonal polynomials or their combinations as basis functions. Orthogonal polynomials gain their importance from the well-known Sturm Liouville problem. It is crucial to note that the Sturm Liouville problem manifests as an eigenvalue problem of the form

$$\begin{aligned} &-(pu')' + qu = \lambda wu \quad \text{in } I \\ &\text{with suitable boundary conditions for u} \end{aligned} \tag{1.1}$$

where I is an open interval in $\mathbb{R}$, the continuous functions $p : \bar{I} \to \mathbb{R}$, $q : I \to \mathbb{R}$, $w : I \to \mathbb{R}$ satisfying $p \geq 0$ in $\bar{I}$ and the weight function w is continuous, nonnegative and integrable over I.
When p vanishes for at least one point on the boundary, the problem (1.1) is considered singular. Particular importance is attributed to this kind of problems, where the eigenfunctions are algebraic polynomials, owing to the efficiency they provide in numerical evaluation. The exclusive set of polynomials eigenfunctions of a singular Sturm-Liouville problem comprises precisely the family of Jacobi polynomials.

This chapter addresses the fundamental aspects of orthogonal polynomials. First, our focus lies in the family of Jacobi polynomials. Then we introduce the basic properties of Legendre polynomials and Chebyshev polynomials, specifically the

Chebyshev polynomials of the third kind. It is noteworthy that we provide proofs for the most important properties used in the subsequent chapters.
We denote by $\mathbb{P}_N$ the space of polynomials of degree less than or equal to N and $I =]-1, 1[$.

1.1 Jacobi polynomials

The family of Jacobi polynomials encompasses all polynomials solutions of the singular Sturm-Liouville problem with $p(x) = (1-x)^{1+\alpha}(1+x)^{1+\beta}$, $q(x) = 0$, the weight function $w^{(\alpha,\beta)}(x) = (1+x)^{\alpha}(1-x)^{\beta}$, and the corresponding eigenvalues $\lambda_k = k(k+\alpha+\beta+1)$, where α and β are two indices characterizing the Jacobi polynomials $P_k^{(\alpha,\beta)}(x)$ of degree k.
These polynomials depend on the parameters $\alpha, \beta \in \mathbb{R}$ with $\alpha, \beta > -1$. An appropriate selection of these parameters leads to define some well-known families of orthogonal polynomials. Specifically, for $\alpha = \beta$, we retrieve ultraspherical polynomials (symmetric Jacobi polynomials). For the special cases $\alpha = \beta = 0$ and $\alpha = \beta = \mp 1/2$, we obtain standard Legendre polynomials and the Chebyshev polynomials of the first and the second kinds, respectively. The third and the fourth kinds of Chebyshev polynomials represent two significant special cases of nonsymmetric Jacobi polynomials with $\alpha = -\beta = \pm 1/2$.
Hereafter, we present some useful formulas and properties.

- Jacobi polynomials are the unique polynomial solutions of (1.1) with the normalization condition

$$P_k^{(\alpha,\beta)}(1) = \binom{k+\alpha}{k} \tag{1.2}$$

  and they can be expressed using the formula

$$P_k^{(\alpha,\beta)}(x) = \frac{1}{2^k} \sum_{l=0}^{k} \binom{k+\alpha}{l} \binom{k+\beta}{k-l} (x-1)^l (x+1)^{k-l}. \tag{1.3}$$

- Another representation is provided by the Rodriguez formula

$$P_k^{(\alpha,\beta)}(x) = \frac{(-1)^k}{2^k k!} (1-x)^{-\alpha}(1+x)^{-\beta} \frac{\mathrm{d}^k}{\mathrm{d}x^k}((1-x)^{\alpha+k}(1+x)^{\beta+k}). \tag{1.4}$$

- Jacobi polynomials satisfy two recurrence formulas:

$$P_0^{(\alpha,\beta)}(x) = 1, \quad P_1^{(\alpha,\beta)}(x) = \frac{1}{2}\left((\alpha-\beta)+(\alpha+\beta+2)x\right),$$
$$P_{k+1}^{(\alpha,\beta)}(x) = \frac{a_{2,k}}{a_{1,k}}P_k^{(\alpha,\beta)}(x) - \frac{a_{3,k}}{a_{1,k}}P_{k-1}^{(\alpha,\beta)}(x), \tag{1.5}$$

  where

$$a_{1,k} = 2(k+1)(k+\alpha+\beta+1)(2k+\alpha+\beta),$$
$$a_{2,k} = (2k+\alpha+\beta+1)(\alpha^2-\beta^2) + \frac{x\Gamma(2k+\alpha+\beta+3)}{\Gamma(2k+\alpha+\beta)},$$
$$a_{3,k} = 2(k+\alpha)(k+\beta)(2k+\alpha+\beta+2);$$

  and

$$\frac{\mathrm{d}}{\mathrm{d}x}P_k^{(\alpha,\beta)}(x) = \frac{b_{2,k}(x)}{b_{1,k}(x)}P_k^{(\alpha,\beta)}(x) + \frac{b_{3,k}(x)}{b_{1,k}(x)}P_{k-1}^{(\alpha,\beta)}(x), \tag{1.6}$$

  where

$$b_{1,k}(x) = (2k+\alpha+\beta)(1-x^2),$$
$$b_{2,k}(x) = k(\alpha-\beta-(2k+\alpha+\beta)x),$$
$$b_{3,k}(x) = 2(k+\alpha)(k+\beta).$$

- Jacobi polynomials satisfy the following relations:

$$P_k^{(\alpha,\beta)}(-x) = (-1)^k P_k^{(\alpha,\beta)}(x),$$
$$P_k^{(\alpha,\beta)}(-1) = \frac{(-1)^k\Gamma(k+\beta+1)}{k!\Gamma(\beta+1)}, \tag{1.7}$$
$$P_k^{(\alpha,\beta)}(1) = \frac{\Gamma(k+\alpha+1)}{k!\Gamma(\alpha+1)}.$$

- Additionally, the formula of their derivatives is given by:

$$\frac{\mathrm{d}^m}{\mathrm{d}x^m}P_k^{(\alpha,\beta)}(x) = 2^{-m}\frac{\Gamma(k+m+\alpha+\beta+1)}{\Gamma(k+\alpha+\beta+1)}P_{k-m}^{(\alpha+m,\beta+m)}(x); \tag{1.8}$$

  The special case for the first derivative is expressed as:

$$\frac{\mathrm{d}}{\mathrm{d}x}P_k^{(\alpha,\beta)}(x) = \frac{1}{2}(k+1+\alpha+\beta)P_{k-1}^{(\alpha+1,\beta+1)}(x). \tag{1.9}$$

- With the weight function $w^{(\alpha,\beta)}(x) = (1+x)^\alpha(1-x)^\beta$, we can define the weighted space $L^2_{w^{(\alpha,\beta)}}(I)$ with the following inner product and norm:

$$\langle u, v\rangle_{w^{(\alpha,\beta)}} = \int_I u(x)v(x)w^{(\alpha,\beta)}(x)\mathrm{d}x,$$

$$\|u\|_{w^{(\alpha,\beta)}} = \langle u, u\rangle^{1/2}_{w^{(\alpha,\beta)}}. \tag{1.10}$$

The set of Jacobi polynomials forms a complete $L^2_{w^{(\alpha,\beta)}}$ orthogonal system. This is why these polynomials play a key role in spectral methods.

- Any function $u(x)$ which is square integrable can be expressed using the Jacobi series as:

$$u(x) = \sum_{k=0}^{\infty} \hat{u}_k P_k^{(\alpha,\beta)}(x), \tag{1.11}$$

where

$$\hat{u}_k = \frac{2k+\alpha+\beta+1}{2^{\alpha+\beta+1}} \frac{k!\Gamma(k+\alpha+\beta+1)}{\Gamma(k+\alpha+1)\Gamma(k+\beta+1)} \times \int_{-1}^{1} u(x) P_k^{(\alpha,\beta)}(x)(1-x)^{\alpha}(1+x)^{\beta}\mathrm{d}x.$$

1.2 Legendre polynomials

Legendre polynomials are the eigenfunctions of the singular Sturm-Liouville problem (1.1) with $p(x) = 1 - x^2$, $q(x) = 0$ and $w(x) = 1$.
Let $\mathscr{L}_k(x), x \in I$ denotes the standard Legendre polynomial of degree k which is even when k is even and odd if k is odd.
Here is a collection of the essential properties for Legendre polynomials:

- The family of Legendre polynomials $\{\mathscr{L}_k(x)\}_{k\in\mathbb{N}}$ constitutes a Hilbert basis of $L^2(I)$.

- They are solutions of the following differential Legendre equation [29, 16]

$$\left(1-x^2\right)\mathscr{L}_k''(x) - 2x\mathscr{L}_k'(x) + k\,(k+1)\,\mathscr{L}_k(x) = 0, \quad k \geq 0. \tag{1.12}$$

- They satisfy the recurrence relations:

$$(1-x^2)\mathscr{L}_k'(x) = -kx\mathscr{L}_k(x) + k\mathscr{L}_{k-1}(x), \tag{1.13}$$

$$\mathscr{L}_{k+1}'(x) = (k+1)\mathscr{L}_k(x) + x\mathscr{L}_k'(x), \tag{1.14}$$

- They can be expressed in the Rodrigues formula:

$$\mathscr{L}_k(x) = \frac{(-1)^k}{2^k k!} \frac{\mathrm{d}^k}{\mathrm{d}x^k} (1-x^2)^k.$$

- The polynomial $\mathscr{L}_k(x)$ is of degree k for all $k \in \mathbb{N}$, and the coefficient of its highest degree term is $\dfrac{(2k)!}{2^k(k!)^2}$.

The principle property of Legendre polynomials is the orthogonality property. They satisfy the orthogonality relation with respect to the weight $w(x) = 1$ in $[-1, 1]$

$$\forall k \neq j \in \mathbb{N}, \quad \int_{-1}^{1} \mathscr{L}_k(x)\mathscr{L}_j(x)\,\mathrm{d}x = 0 \quad \text{and} \quad \int_{-1}^{1} \mathscr{L}_k^2(x)\,\mathrm{d}x = \frac{2}{2k+1}. \tag{1.15}$$

The first Legendre polynomials are given by:

$$\mathscr{L}_0(x) = 1, \quad \mathscr{L}_1(x) = x, \quad \mathscr{L}_2(x) = (3x^2 - 1)/2,$$

$$\mathscr{L}_3(x) = (5x^3 - 3x)/2, \quad \mathscr{L}_4(x) = (35x^4 - 30x^2 + 3)/8.$$

In particular cases, we have:

- $$\mathscr{L}_k(1) = 1, \quad \mathscr{L}_k(-x) = (-1)^k\, \mathscr{L}_k(x), \quad \mathscr{L}_k(-1) = (-1)^k. \tag{1.16}$$

- $$\mathscr{L}'_k(1) = \frac{k(k+1)}{2}, \quad \mathscr{L}'_k(-1) = \frac{k(k+1)}{2}(-1)^{k+1}. \tag{1.17}$$

We give also some other properties of Legendre polynomials:

- $\forall x \in I, \quad |\mathscr{L}_k(x)| \leqslant 1,$
- $\forall x \in I, \quad |\mathscr{L}'_k(x)| \leqslant \frac{k(k+1)}{2},$
- $$(k+1)\, \mathscr{L}_{k+1}(x) = (2k+1)x\, \mathscr{L}_k(x) - n\, \mathscr{L}_{k-1}(x). \tag{1.18}$$

- $$\mathscr{L}''_N(x) = \sum_{k=0}^{N-2} (k + \frac{1}{2})\, (N(N+1) - k(k+1))\, \mathscr{L}_k(x). \tag{1.19}$$

- A function u which is square integrable can be expressed in terms of the Legendre polynomials as:

$$u(x) = \sum_{k=0}^{\infty} \hat{u}_k \mathscr{L}_k(x), \tag{1.20}$$

where

$$\hat{u}_k = (k + \frac{1}{2}) \int_{-1}^{1} u(x) \mathscr{L}_k(x) \, \mathrm{d}x.$$

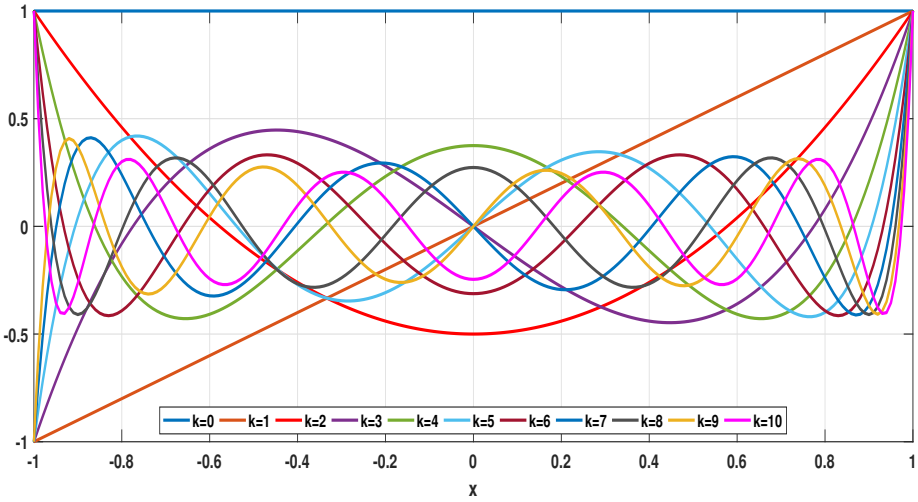

Figure 1.1: The first Legendre polynomials for $k = 0, \ldots, 10$.

1.2.1 Shifted Legendre polynomials

In order to generalize the use of these polynomials in any interval of the form $[0, \ell]$ and for the elaboration of numerical methods, the shifted Legendre polynomials are introduced by implementing the change of variable $t = \frac{2x}{\ell} - 1$, with the special case $t = 2x - 1$ for $[0, 1]$. The polynomial obtained, denoted as $\mathscr{L}_k(2x-1)$ by $\widetilde{\mathscr{L}_k}(t)$. Using basic properties of Legendre polynomials, the shifted Legendre polynomials are derived using the following recurrence formula:

$$\widetilde{\mathscr{L}_{k+1}}(t) = \frac{(2k+1)(2t-1)}{(k+1)} \widetilde{\mathscr{L}_k}(t) - \frac{n}{(k+1)} \widetilde{\mathscr{L}_{k-1}}(t), \; k = 1, 2, \ldots$$

and the first ones are

$$\widetilde{\mathscr{L}_0}(t) = 1, \quad \widetilde{\mathscr{L}_1}(t) = 2t - 1, \quad \widetilde{\mathscr{L}_2}(t) = 6t^2 - 6t + 1.$$

It is noteworthy to mention the special cases

$$\widetilde{\mathscr{L}_k}(0) = (-1)^k, \quad \widetilde{\mathscr{L}_k}(1) = 1.$$

These polynomials satisfy also the orthogonality condition with respect to the weight function $w(t) = 1$ on $[0, 1]$ with the inner product:

$$\langle \widetilde{\mathscr{L}_k}(t), \widetilde{\mathscr{L}_j}(t) \rangle = \int_0^1 \widetilde{\mathscr{L}_k}(t) \widetilde{\mathscr{L}_j}(t) \, \mathrm{d}t = \frac{1}{2k+1} \delta_{kj}, \tag{1.21}$$

where δ_{kj} is the well-known Kronecker delta function.

1.3 Chebyshev polynomials

What gives the various polynomials their power and relevance is their close relationship with the trigonometric functions "cosine" and "sine". We are all aware of the power of these functions and their appearance in the description of all kinds of natural phenomena, and this is undoubtedly the key to the versatility of the Chebyshev polynomials.
This property is the origin of their widespread popularity in numerical approximation. The transformation $x = \cos\theta$ enables many mathematical relations, as well as theoretical results, to be readily adapted to the Chebyshev system.
As mentioned before, there are four kinds of Chebyshev polynomials:
Chebyshev polynomials of the first kind

$$T_k(x) = \cos k\theta, \text{ with } x = \cos\theta. \tag{1.22}$$

Chebyshev polynomials of the second kind

$$U_k(x) = \sin(k+1)\theta / \sin\theta, \text{ with } x = \cos\theta. \tag{1.23}$$

Chebyshev polynomials of the third kind

$$\mathscr{V}_k(x) = \cos(k + \frac{1}{2})\theta / \cos\frac{1}{2}\theta, \text{ with } x = \cos\theta. \tag{1.24}$$

Chebyshev polynomials of the fourth kind

$$W_k(x) = \sin(k+\frac{1}{2})\theta / \sin\frac{1}{2}\theta, \text{ with } x = \cos\theta. \tag{1.25}$$

These polynomials have connections among each other, and we can mention some interesting formulas:

$$U_k(x) = \frac{1}{2}(\mathscr{V}_k(x) + W_k(x)); \tag{1.26}$$

$$\mathscr{V}_k(x) + \mathscr{V}_{k-1}(x) = W_k(x) - W_{k-1}(x) = 2T_k(x); \tag{1.27}$$

$$\mathscr{V}_k(x) = s^{-1}T_{2k+1}(s), \quad W_k(x) = U_{2k}(s); \tag{1.28}$$

where $s = (\frac{1}{2}(1+x))^{1/2} = \cos\frac{1}{2}\theta$.
It is worth mentioning that a new family of symmetric orthogonal polynomials was recently developed using a certain generalized Sturm-Liouville problem. This family includes some well-known classes of orthogonal polynomials like the four kinds of Chebyshev polynomials and generates new ones. Special mention is given to two new classes of orthogonal polynomials, which have some links with the first and second kinds of Chebyshev polynomials and are called Chebyshev polynomials of fifth and sixth kinds.
Hereafter, we choose to discuss Chebyshev polynomials of the third kind since they will be used next in this thesis.

1.3.1 Chebyshev polynomials of the third kind

We denote by $\mathscr{V}_k(x)$ the Chebyshev polynomials of the third kind of degree k, the polynomials defined for $x \in [-1, 1]$

$$\mathscr{V}_k(x) = \frac{\cos\left(k+\frac{1}{2}\right)\theta}{\cos\left(\frac{1}{2}\theta\right)}, \quad \text{where } \; x = \cos\theta \; \text{ and } \quad \theta \in [0, \pi].$$

Here are some principle properties of these polynomials:

- $\mathscr{V}_k(x)$ are orthogonal polynomials on $[-1, 1]$ with respect to the weight function $w(x) = (1+x)^{\frac{1}{2}}(1-x)^{-\frac{1}{2}}$

$$\int_{-1}^{1} \mathscr{V}_k(x)\mathscr{V}_j(x)(1+x)^{\frac{1}{2}}(1-x)^{-\frac{1}{2}}\mathrm{d}x = \pi\delta_{kj}. \tag{1.29}$$

- $\mathscr{V}_k(x)$ satisfies the recurrence relations:

$$\mathscr{V}_k(x) = 2x\mathscr{V}_{k-1}(x) - \mathscr{V}_{k-2}(x), \quad \text{for all } k \geq 2$$

with $\mathscr{V}_0(x) = 1$, and $\mathscr{V}_1(x) = 2x - 1$.

- $\mathscr{V}_k(x)$ are solutions of the differential equation:

$$(1 - x^2)\, y''(x) + (1 - 2x)\, y'(x) + k(k+1)\, y(x) = 0.$$

- The zeros of the polynomial $\mathscr{V}_k(x)$ are of the form:

$$x = x_i = \cos \frac{\left(i - \frac{1}{2}\right)\pi}{k + \frac{1}{2}}, \quad i = 1, 2, \ldots, k.$$

- $\mathscr{V}_k(1) = 1$, $\mathscr{V}_k(-1) = (-1)^k(2k+1)$.

- The analytical form of the Chebyshev polynomials of the third kind $\mathscr{V}_k(x)$ of degree k is

$$\mathscr{V}_k(x) = \sum_{i=0}^{\lfloor \frac{2k+1}{2} \rfloor} (-1)^i (2)^{k-i} \frac{(2k+1)\Gamma(2k-i+1)}{\Gamma(i+1)\Gamma(2k-2i+2)} (x+1)^{k-i}, \; k \in \mathbb{Z}^+. \quad (1.30)$$

- A connection between the different kinds of Chebyshev polynomials can be derived. Chebyshev polynomials of the third kind can be obtained from the Chebyshev polynomials of the second kind by the relation:

$$\mathscr{V}_k(x) = U_k(x) - U_{k-1}(x),$$

where $U_k(x)$ refers to the Chebyshev polynomial of the second kind of degree k.

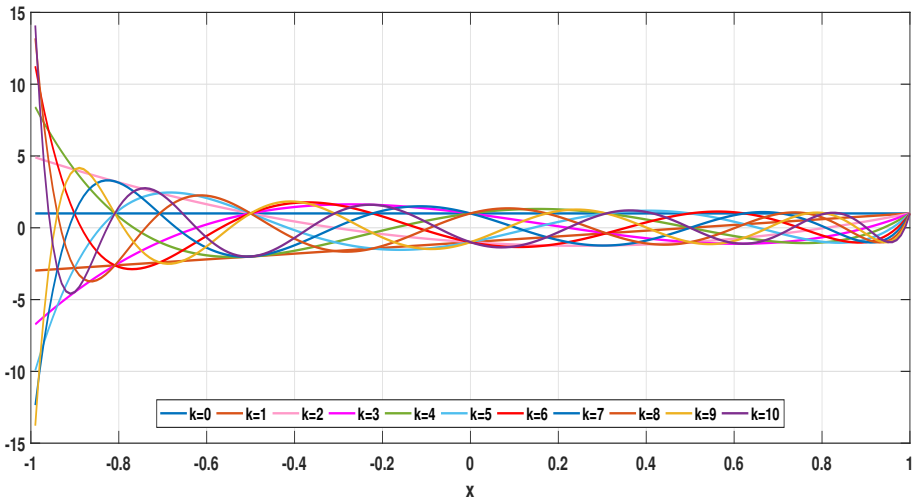

Figure 1.2: The first Chebyshev polynomials of the third kind for $k = 0, \ldots, 10$.

1.3.2 Shifted Chebyshev polynomials of the third kind

We define the shifted Chebyshev polynomials of the third kind using the change of variable $s = 2x - 1$ by $\widetilde{\mathscr{V}_k}(x) = \mathscr{V}_k(2x - 1)$.

- $\widetilde{\mathscr{V}_k}(x)$ are orthogonal polynomials on $[0, 1]$

$$\int_0^1 \widetilde{\mathscr{V}_k}(x)\widetilde{\mathscr{V}_j}(x)x^{\frac{1}{2}}(1-x)^{-\frac{1}{2}}\mathrm{d}x = \frac{\pi}{2}\delta_{kj}. \tag{1.31}$$

- $\widetilde{\mathscr{V}_k}(x)$ may be produced by employing recurrence relations:

$$\begin{cases} \widetilde{\mathscr{V}_k}(x) = 2(2x-1)\widetilde{\mathscr{V}_{k-1}}(x) - \widetilde{\mathscr{V}_{k-2}}(x), \quad \text{for all} \quad k \geq 2, \\ \widetilde{\mathscr{V}_0}(x) = 1, \quad \text{and} \quad \widetilde{\mathscr{V}_1}(x) = 4x - 3, \\ \widetilde{\mathscr{V}_k}(0) = (-1)^k(2k+1), \quad \text{and} \quad \widetilde{\mathscr{V}_k}(1) = 1, \quad \text{for all} \quad k \geq 0. \end{cases}$$

- The analytical form of shifted Chebyshev polynomials of the third kind of degree k in x is:

$$\widetilde{\mathscr{V}_k}(x) = \sum_{i=0}^{k}(-1)^i(2)^{2k-2i}\frac{(2k+1)\Gamma(2k-i+1)}{\Gamma(i+1)\Gamma(2k-2i+2)}x^{k-i}, \quad k \in \mathbb{Z}^+. \tag{1.32}$$

- The zeros of the polynomial $\widetilde{\mathscr{V}_k}(x)$ are of the form:

$$x_i = \frac{1}{2}\left(\cos\frac{\left(i-\frac{1}{2}\right)\pi}{k+\frac{1}{2}}+1\right), \quad i=1,2,\ldots,k. \tag{1.33}$$

- A function $u(x)$, which is square integrable in $[0,1]$, can be expressed in terms of shifted Chebyshev polynomials of the third kind as:

$$u(x) = \sum_{k=0}^{+\infty} \hat{u}_k \widetilde{\mathscr{V}_k}(x), \tag{1.34}$$

where for $k = 0, 1, 2, \ldots$

$$\hat{u}_k = \frac{2}{\pi}\int_0^1 u(x)\widetilde{\mathscr{V}_k}(x)x^{\frac{1}{2}}(1-x)^{-\frac{1}{2}}\mathrm{d}x. \tag{1.35}$$

For $x \in [-1,1]$ the coefficients $\hat{u}_k$ are given by:

$$\hat{u}_k = \frac{1}{\pi}\int_{-1}^1 u\left(\frac{x+1}{2}\right)\mathscr{V}_k(x)(1+x)^{\frac{1}{2}}(1-x)^{-\frac{1}{2}}\mathrm{d}x. \tag{1.36}$$

1.4 Gauss type quadratures

To gain more efficiency in calculating integrals when applying numerical methods, different types of numerical quadratures where developed. In this section, we discuss Gauss type quadratures, which are the most popular and precise since they have close links with orthogonal polynomials, and their exactitude is with the highest degree, which is less or equal to $2N+1$.
First, we introduce the Gauss integration formula and for a more general approach, we also introduce the Gauss-Lobatto integration formula, which will be used in the subsequent part of this thesis. The cases of Legendre polynomials and Chebyshev polynomials are also discussed.

1.4.1 Gauss integration

Theorem 1.1 *Let's $x_0 < x_1 < \cdots < x_N$ be the roots of the $(N+1)$-th orthogonal polynomial f_{N+1} and let $w_0, \ldots, w_N$ be the solution of*

$$\sum_{j=0}^{N}(x_j)^k w_j = \int_{-1}^1 x^k w(x)\mathrm{d}x,\ 0 \le k \le N.$$

Then $w_j > 0$ for $j = 0, \ldots, N$ and

$$\sum_{j=0}^{N} f(x_j) w_j = \int_{-1}^{1} f(x) w(x) \mathrm{d}x, \ \forall f \in \mathbb{P}_{2N+1}, \tag{1.37}$$

where w_j are called weights.
It should be noted that it is impossible to find x_j, w_j for $j = 0, \ldots, N$ such that the last formula is exact for all polynomials $f \in \mathbb{P}_{2N+2}$.

When using this type of quadrature, especially in collocation methods for differential equations, one needs to take into account the boundary conditions that are generally imposed at one or both end points. For this reason, the Gauss integration formula is generalised to include these points. We discuss here the Gauss-Radau formula which includes one hand side of the interval, and the Gauss-Lobatto formula, which takes both left and right hand sides of the interval. We choose here to focus on the latter since it will be used in the following chapters.

1.4.2 Gauss-Lobatto integration

Theorem 1.2 *Consider the following polynomial:*

$$g(x) = f_{N+1}(x) + a f_N(x) + b f_{N-1}(x), \tag{1.38}$$

where a and b are chosen so that $g(-1) = g(1) = 0$. Let $-1 = x_0 < x_1 < \cdots < x_N = 1$ be the $N+1$ roots of the (1.38), and let $w_0, \ldots, w_N$ be defined in Theorem 1.1. Then,

$$\sum_{j=0}^{N} f(x_j) w_j = \int_{-1}^{1} f(x) w(x) \mathrm{d}x, \ \forall f \in \mathbb{P}_{2N-1}. \tag{1.39}$$

To be precise, the corresponding nodes and weights of quadrature for Legendre and Chebyshev polynomials are cited hereafter. For Legendre polynomials, explicit formulas of the nodes are not known, necessitating numerical computation. However, explicit formulas for both the nodes and weights of Chebyshev polynomials are available.

- Gauss-Legendre quadrature

$$\begin{cases} x_j \text{ are zeros of } \mathscr{L}_{N+1}(x), \\ w_j = \dfrac{2}{(1-x_j^2)[\mathscr{L}'_{N+1}(x_j)]^2}, \ j = 0, \ldots, N. \end{cases} \tag{1.40}$$

- Legendre Gauss-Lobatto quadrature

$$\begin{cases} x_0 = -1, \ x_N = 1, \ x_j \text{ are zeros of } \mathscr{L}'_N(x), \\ w_j = \dfrac{2}{N(N+1)[\mathscr{L}_N(x_j)]^2}, \ j = 0, \ldots, N. \end{cases} \tag{1.41}$$

- Chebyshev Gauss quadrature

$$\begin{cases} x_j = \cos \dfrac{(2j+1)\pi}{2N+2}, \\ w_j = \dfrac{\pi}{N+1}, \ j = 0, \ldots, N. \end{cases} \tag{1.42}$$

- Chebyshev Gauss-Lobatto quadrature

$$\begin{cases} x_j = \cos \dfrac{\pi j}{N}, \\ w_j = \begin{cases} \dfrac{\pi}{2N}, \ j = 0, N. \\ \dfrac{\pi}{N}, \ j = 1, \ldots, N-1. \end{cases} \end{cases} \tag{1.43}$$

1.5 Numerical application of orthogonal polynomials

Orthogonal polynomials find numerous applications, with the numerical applications being the most commonly used in mathematics, science and engineering. One significant application is in approximating functions, where a given function can be written as a linear combination of orthogonal polynomials. Additionally in numerical integration, especially in the Gaussian quadrature, nodes and weights derived from orthogonal polynomials are well-known for the high accuracy in approximating integrals. Another application consists in curve fitting and regression analysis where orthogonal polynomials are used to find the best polynomial that

models a set of points. Furthermore, these polynomials play a crucial role in solving differential equations, eigenvalues problems, and setting error analysis are also widely used.
To demonstrate the broad application of orthogonal polynomials, some numerical investigations are presented in this section.

Example 1.1 ***Approximation of functions and derivatives***
To demonstrate the efficiency of orthogonal polynomials and their roots in approximating functions, we consider the example of the function $u(x) = \dfrac{1}{1+x^2}$ *in* $[-1, 1]$. *Starting by expressing the Chebyshev expansion serie of* $u(x)$ *using the Chebyshev polynomials of the first kind,*

$$u(x) = \sum_{k=0}^{\infty} \hat{u}_k T_k(x), \tag{1.44}$$

A Natural approximation of $u(x)$ *can be obtained using the first* $N+1$ *terms of this sum:*

$$u_N(x) = \sum_{k=0}^{N} \hat{u}_k T_k(x).$$

To determine the expansion coefficients $\{\hat{u}_k\}$, *we utilize the Chebyshev Gauss points defined in* (1.42)*:*

$$u_N(x_j) = \sum_{k=0}^{N} \hat{u}_k T_k(x_j),\ j = 0, \ldots, N. \tag{1.45}$$

To highlight the significance of using such points, Table 1.1 *provides the results of the maximum absolute error* $\mathscr{E}_{max}$ *obtained with different values of* N *in two distinct cases:*

- *Case 1: When using the Chebyshev points as a subdivision of* $[-1, 1]$ *in* (1.45).
- *Case 2: When using equidistant subdivision (homogeneous discretization) of the interval* $[-1, 1]$.

Where

$$\mathscr{E}_{max} = \max_{0 \leq j \leq N} |u_N(x_j) - u(x_j)|.$$

Table 1.1: Maximum absolute error values $\mathscr{E}_{max}$ when approximating $u(x) = \frac{1}{1+x^2}$ using (1.45)

N	$\mathscr{E}_{max}$ (case 1)	$\mathscr{E}_{max}$ (case 2)
4	1.1102e − 16	0
8	1.1102e − 16	5.5511e − 16
16	2.2204e − 16	2.0539e − 14
32	5.5511e − 16	8.6435e − 10
64	7.7715e − 16	1.2766e + 01
128	4.4408e − 16	3.0765e + 00
256	6.6613e − 16	2.4847e + 01
512	2.1094e − 15	8.1179e + 01

The advantage of using the Chebyshev points instead of equidistant subdivision lies in achieving stability. The values of $\mathscr{E}_{max}$ are of the same order regardless of the value of N, reflecting stability.
This behaviour is also observed when approximating the function $u(x) = \sin(x)$ in $[-1, 1]$ using the Chebyshev expansion series. The error remains at the same order of 10^{-16} for all the values of N when the Chebyshev points are used. In contrast, for $N = 64$, the approximate solution diverges when using an equidistant subdivision.

Table 1.2: Maximum absolute error values $\mathscr{E}_{max}$ when approximating $u(x) = \sin(x)$ using (1.45)

N	$\mathscr{E}_{max}$ (case 1)	$\mathscr{E}_{max}$ (case 2)
4	1.1102e − 16	3.3306e − 16
8	2.2204e − 16	8.8817e − 16
16	4.4408e − 16	1.5343e − 13
32	3.3306e − 16	1.6117e − 09
64	3.3306e − 16	2.0333e + 01
128	7.7715e − 16	5.8426e + 00
256	1.2212e − 15	6.0390e + 01
512	1.9984e − 15	2.4772e + 02

Now, in order to approximate the derivative of $u(x) = \sin(x)$ in $[-1, 1]$, starting

from the Chebyshev expansion serie of $u(x)$ *given in* (1.45)*, we can express it as:*

$$u'_N(x_j) = \sum_{k=0}^{N} \hat{u}_k T'_k(x_j),$$

This formula can be simplified to the following matrix expression:

$$U^{(1)} = \boldsymbol{D}^{(1)} U, \tag{1.46}$$

where $U^{(1)} = [u'_N(x_0), \ldots, u'_N(x_N)]^{\mathrm{T}}$, $U = [u_N(x_0), \ldots, u_N(x_N)]^{\mathrm{T}}$, *and* $\boldsymbol{D}^{(1)}$ *is an* $(N+1) \times (N+1)$ *matrix known as the differentiation matrix, with its elements given by:*

$$D^{(1)}_{j,k} = T'_k(x_j),\ 0 \leq j, k \leq N,$$

or in an explicit formula as:

$$D^{(1)}_{0,0} = \frac{2N^2+1}{6},\ D^{(1)}_{N,N} = -\frac{2N^2+1}{6},$$

$$D^{(1)}_{j,k} = \begin{cases} -\dfrac{x_j}{2(1-x_j^2)},\ j = k \neq 0, N \\ \dfrac{c_j}{c_k}\dfrac{1}{x_j - x_k},\ j \neq k. \end{cases} \tag{1.47}$$

The same formula as (1.46) *can be generalised for a derivative of order* p *where the matrix* $\boldsymbol{D}^{(p)}$ *is formulated as* $\boldsymbol{D}^{(p)} = (\boldsymbol{D}^{(1)})^p$*. For the special case of the second derivative, the approximation can be obtained using the matrix formula:*

$$U^{(2)} = \boldsymbol{D}^{(2)} U, \tag{1.48}$$

The results of approximating the first and second derivatives of $u(x) = sin(x)$ *are collected in* Table 1.3*. The maximum absolute error* $\mathscr{E}_{max}$ *is calculated for both the first and second derivatives using* (1.46) *and* (1.48) *respectively.*

Table 1.3: Maximum absolute error values when approximating the derivatives of $u(x) = \sin(x)$. $\mathscr{E}_{max}^{(1)}$ for the first derivative using (1.46) and $\mathscr{E}_{max}^{(2)}$ for the second derivative using (1.48) where $\mathbf{D}^{(2)} = (\mathbf{D}^{(1)})^2$

N	$\mathscr{E}_{max}^{(1)}$	$\mathscr{E}_{max}^{(2)}$
4	7.8488e − 03	8.5581e − 02
8	3.3365e − 07	1.4335e − 05
16	8.7485e − 14	9.7534e − 12
32	4.9152e − 12	2.0815e − 09
64	1.9982e − 11	4.2776e − 08
128	5.4066e − 10	3.9686e − 06
256	1.1682e − 08	3.4141e − 04
512	1.5016e − 07	1.5013e − 02

It's worth mentioning that when using a numerical method, the implementation of a mathematical formula in a programming language is of great importance. An accumulation of the error calculated for a given method can be observed to increase. One can justify this phenomenon by the considering roundoff errors, as the precision on our computers is limited. Therefore, the growth of error values becomes noticeable. To reduce the error accumulation, different techniques concerning the way of writing mathematical formulas are developed. This is especially crucial for the matrix calculations, as they are prone to significant errors.

Example 1.2 ***Approximation of integrals***

As mentioned earlier, orthogonal polynomials play a crucial role role in calculating integrals numerically. The Gaussian type quadrature relies basically on the values of the function to be integrated at the zeros of orthogonal polynomials to provide an estimation of the integral. Another technique that also utilizes orthogonal polynomials is known as the Clenshaw-Curtis type. The fundamental idea is to consider the interpolating polynomial of degree N of the function and then integrate it, with the help of some important properties of orthogonal polynomials.

In the following, we provide a brief description of the technique using the Cheby-

shev polynomials of the first kind as an illustrative example.
The goal is to determine an approximate value of the integral:

$$\mathcal{I} = \int_{-1}^{1} w(x) f(x)\, \mathrm{d}x.$$

Using the interpolating polynomial of degree N, denoted as $\mathscr{I}_N f$, which interpolates the function f at the zeros of $T_{N+1}(x)$ instead of f in the formula of the integral provides a natural approximation of the integral:

$$\mathcal{I} \simeq \mathcal{I}_N = \int_{-1}^{1} w(x) \mathscr{I}_N f(x)\, \mathrm{d}x;$$

where the interpolating polynomial of f using the Chebyshev polynomials of the first kind is given by:

$$\mathscr{I}_N f(x) = \sum_{j=0}^{N} \mu_j T_j(x).$$

Then

$$\mathcal{I}_N = \sum_{j=0}^{N} \mu_j \int_{-1}^{1} w(x) T_j(x)\, \mathrm{d}x = \sum_{j=0}^{N} \mu_j \rho_j, \tag{1.49}$$

where $\rho_j = \int_{-1}^{1} w(x) T_j(x)\, \mathrm{d}x$. Now, in order to find an explicit formula to evaluate the value of $\mathcal{I}_N$, we investigate the properties of Chebyshev polynomials. Using the discrete orthogonality formula of Chebyshev polynomials, which is a natural extension of the continuous orthogonality relationship, we replace the integral with the summation in the Chebyshev points as follows:

$$\begin{aligned} \alpha_{ij} &= \sum_{k=1}^{N+1} T_i(x_k) T_j(x_k) = 0,\ i \neq j,\ i, j \leq N. \\ \alpha_{ii} &= \begin{cases} (N+1),\ i = 0, \\ \dfrac{1}{2}(N+1),\ i \neq 0. \end{cases} \end{aligned} \tag{1.50}$$

leads to

$$\begin{aligned} \sum_{k=1}^{N+1} f(x_k) T_i(x_k) &= \sum_{k=1}^{N+1} \mathscr{I}_N f(x_k) T_i(x_k) \\ &= \sum_{j=0}^{N} \mu_j \sum_{k=1}^{N+1} T_i(x_k) T_j(x_k) = \mu_i \alpha_{ii}. \end{aligned}$$

Then,

$$\mu_i = \frac{1}{\alpha_{ii}} \sum_{k=1}^{N+1} f(x_k) T_i(x_k).$$

By replacing the last formula in (1.49)*, we obtain*

$$\mathcal{I}_N = \sum_{k=1}^{N+1} \omega_k f(x_k) \tag{1.51}$$

where

$$\omega_k = \sum_{j=0}^{N} \frac{\rho_j}{\alpha_{jj}} T_j(x_k) = \sum_{j=0}^{N} \frac{2\rho_j}{N+1} T_j(x_k).$$

Then, $\mathcal{I}_N$ *is determined by calculating the integrals in the formula of* ρ_j*.*
For the specific choice of the weight function corresponding to the Chebyshev polynomials of the first kind $w(x) = (1-x^2)^{-1/2}$*, we obtain*

$$\rho_j = \int_{-1}^{1} (1-x^2)^{-1/2} T_j(x)\, \mathrm{d}x = \int_0^{\pi} \cos(j\theta)\, \mathrm{d}\theta = \begin{cases} \pi, & j = 0, \\ 0, & j > 0, \end{cases}$$

so that

$$\omega_k = \frac{\pi}{N+1},$$

Hence,

$$\int_{-1}^{1} (1-x^2)^{-1/2} f(x)\, \mathrm{d}x \simeq \mathcal{I}_N = \frac{\pi}{N+1} \sum_{k=1}^{N+1} f(x_k),$$

which corresponds exactly to the Gauss-Chebyshev quadrature formula mentioned above.

Chapter 2

Advection-diffusion equation

Chapter 2

Advection-diffusion equation

In this chapter, we study the advection-diffusion equation in two different approaches. The first one aims to develop a numerical approximation for the solution of the advection-diffusion equation with constant and variable coefficients. We propose a numerical solution for the equation associated with Robin's mixed boundary conditions perturbed with a small parameter ε. The approximation is based on a couple of methods: A spectral method of Galerkin type with a basis composed of Legendre-polynomials and a Gauss quadrature of type Gauss-Lobatto applied for integral calculations with stability and convergence analysis. In addition, a Crank-Nicolson scheme is used for the temporal solution as a finite difference method. Several numerical examples are discussed to show the efficiency of the proposed numerical method, especially when ε tends to zero, so that we obtain the exact solution of the classic problem with homogeneous Dirichlet boundary conditions. The numerical convergence is well presented in different examples. Therefore, we build an efficient numerical method for different types of partial differential equations with different boundary conditions.
The second approach is based on using a spectral technique for both temporal and spatial variables. We propose first to write the integral equation corresponding to the advection-diffusion equation using the initial condition of the problem. Then, a suitable combination of orthogonal polynomials is selected to verify the boundary conditions and apply the Galerkin method. This procedure leads to write the expansion coefficients of the approximate solution in a matrix form and then

compressing it into a one-dimensional vector. The obtained system is re-adapted using the Kronecker product and solved using a Gauss elimination method. The numerical examples proposed at the end of the section, show the efficiency and high applicability of the suggested technique.

This chapter is divided into two main sections as follows:
In the first part, we start by delineating the problem under study and providing some preliminaries in Section 2.1.1. Subsequently, in Section 2.1.2 we proceed for the weak formulation of the problem and outline the proposed method by detailing the primary steps of spatial and temporal descritization in Section 2.1.3 . Following that, in Section 2.1.4, stability and convergence results are established. In Section 2.1.5, several numerical examples are presented and discussed to affirm the reliability of the described method.
In the second part, we start by introducing the studied problem in Section 2.2.1. The details of proposed technique are described in Section 2.2.2, and finally the numerical simulation is provided via different examples in Section 2.2.3.

2.1 First approach

The obtained results are the subject of an article entitled "Efficient Spectral Legendre Galerkin Approach for the Advection Diffusion Equation with Constant and Variable Coefficients under Mixed Robin Boundary Conditions" published in *Advances in the Theory of Nonlinear Analysis and its Application*, **7**, 133–147, 2023.

2.1.1 Description of the problem and preliminaries

In this part, we examine a model of advection-diffusion equation represented as

$$\frac{\partial u}{\partial t}(t,x) + a(x)\frac{\partial u}{\partial x}(t,x) - b(x)\frac{\partial^2 u}{\partial x^2}(t,x) = f(t,x), \tag{2.1}$$

This model is coupled with initial and the boundary conditions of Robin type,

perturbed with a small parameter $\varepsilon > 0$, given by

$$\begin{aligned} &u(0,x) = g(x), \\ &u(t,-1) - \varepsilon \frac{\partial u}{\partial x}(t,-1) = 0, \\ &u(t,1) + \varepsilon \frac{\partial u}{\partial x}(t,1) = 0; \end{aligned} \tag{2.2}$$

where

- $u(t,x)$ is the unknown function,
- $x \in [-1,1]$, $t > 0$ are the proposed variables,
- The coefficients of advection and diffusion are $a(x) \geq 0$ and $b(x) > 0$, respectively, defined in $\mathscr{C}^1([-1,1])$, taking the polynomial form.
- $f \in \mathscr{C}([0,1],[-1,1])$ and $g \in \mathscr{C}([-1,1])$ are given functions.

We define $L^2(I)$ as the space of measurable function v on I such that $\|v\| < +\infty$. The scalar product and the L^2 norm are respectively defined by

$$\langle u, v \rangle = (u,v)_{L^2} = \int_I u(x)v(x)\,\mathrm{d}x\ ; \quad \|v\|_{L^2}^2 = (v,v)_{L^2}.$$

For every positive m, the Sobolev space is defined as:

$$H^m(I) = \left\{ v \in L^2(I) :\ 0 \leq k \leq m,\ \frac{\mathrm{d}^k v}{\mathrm{d}x^k} \in L^2(I) \right\},$$

where the standard semi-norm and norm are given respectively by:

$$|v|_{H^m(I)} = \left\| \frac{\mathrm{d}^m v}{\mathrm{d}x^m} \right\|_{L^2(I)}\ ; \quad \|v\|_{H^m(I)} = \left(\sum_{k=0}^{m} \left\| \frac{\mathrm{d}^k v}{\mathrm{d}x^k} \right\|_{L^2(I)}^2 \right)^{1/2}.$$

2.1.2 Weak formulation of the problem

We consider the problem (2.1)−(2.2).
Starting by multiplying the equation (2.1) by a function v that depends only on x, and integrating by parts, we obtain

$$\int_{-1}^{1} \frac{\partial u}{\partial t}(t,x)v(x)\,\mathrm{d}x + \int_{-1}^{1} b(x)\frac{\partial u}{\partial x}(t,x)v'(x)\,\mathrm{d}x + \int_{-1}^{1} (a(x) + b'(x))\ \frac{\partial u}{\partial x}(t,x)v(x)\,\mathrm{d}x$$

$$= \int_{-1}^{1} f(t,x)v(x)\,\mathrm{d}x + \left[b(x)\frac{\partial u}{\partial x}(x)v(x)\right]_{-1}^{1}. \tag{2.3}$$

The boundary conditions give

$$\frac{\partial u}{\partial x}(t,-1) = \frac{u(t,-1)}{\varepsilon}, \qquad \frac{\partial u}{\partial x}(t,1) = -\frac{u(t,1)}{\varepsilon}.$$

Hence the weak formulation of the problem (2.1)−(2.2) is

$$\begin{aligned} &\text{Find } \; u(t) \in H^1(I) \text{ such that} \\ &\frac{\mathrm{d}}{\mathrm{d}t}\langle u(t), v\rangle + \xi(u(t), v) = \langle f(t), v\rangle \end{aligned} \tag{2.4}$$

with an initial condition $u(0,x) = g(x)$, where

$$\begin{aligned} \xi(u(t), v) = &\int_{-1}^{1} b(x)\frac{\partial u}{\partial x}(t,x)v'(x)\,\mathrm{d}x + \int_{-1}^{1}(a(x) + b'(x))\frac{\partial u}{\partial x}(t,x)v(x)\,\mathrm{d}x \\ &+ \frac{1}{\varepsilon}\left(b(1)u(t,1)v(1) + b(-1)u(t,-1)v(-1)\right). \end{aligned} \tag{2.5}$$

Theorem 2.1 *Let $T > 0$ be a final time and let $g \in L^2(I)$ be the initial data. The following problem, with the bilinear form $\xi(u(t), v)$ defined in* (2.5)

$$\begin{cases} \dfrac{\mathrm{d}}{\mathrm{d}t}\langle u(t), v\rangle + \xi(u(t), v) = \langle f(t), v\rangle, \quad \forall v \in H^1(I), \quad 0 < t < T, \\ \quad u(t=0) = g(x), \end{cases} \tag{2.6}$$

has a unique solution $u \in L^2(]0,T[; H^1(I)) \cap \mathscr{C}([0,T]; L^2(I))$.

Proof 2.1 *The idea of this proof is in [3].*
It is clear that $\xi(\cdot,\cdot)$ is a symmetric bilinear form. To ensure the existence and the uniqueness of the solution, we need to prove continuity and coercivity.
To establish continuity, we employ the Cauchy-Schwartz inequality and the fact that

$$|\, u(\pm 1)\,| \leq \sup |\, u(x)\,| \; = \|u\|_{L^\infty(I)}, \quad \forall x \in I.$$

By denoting

- $A_+ = \max a(x) \geq 0$,
- $B_+ = \max b(x) > 0$, $B'_+ = \max |b'(x)|$.

One can write

$$|\xi(u(t),v)| \leq \int_{-1}^{1} B_+ \left|\frac{\partial u}{\partial x}(t,x)v'(x)\right| \,\mathrm{d}x + \int_{-1}^{1} (A_+ + B'_+) \left|\frac{\partial u}{\partial x}(t,x)v(x)\right| \,\mathrm{d}x + \frac{b(1)+b(-1)}{\varepsilon} \|u(t)\|_\infty \ \|v\|_\infty.$$

Which leads to

$$|\xi(u(t),v)| \leq \left\|\frac{\partial u}{\partial x}(t)\right\|_{L^2(I)} \|v'\|_{L^2(I)} + (A_+ + B'_+) \left\|\frac{\partial u}{\partial x}(t)\right\|_{L^2(I)} \|v\|_{L^2(I)} + \frac{2B_+}{\varepsilon} \|u(t)\|_\infty \ \|v\|_\infty.$$

So, we obtain

$$\exists\, \delta > 0, \quad \forall\, u(t), v \in H^1(I), \quad |\xi(u(t),v)| \ \leq \delta \ \|u(t)\|_{H^1(I)} \ \|v\|_{H^1(I)},$$

such that $\delta = (1+\frac{2}{\varepsilon})B_+ + A_+ + B'_+$. *Hence, the continuity of* $\xi(\cdot,\cdot)$.

For the weak coercivity, by denoting

- $A_- = \min a(x) \geq 0$,
- $B_- = \min b(x) > 0,\ B'_- = \min |b'(x)|$

We have

$$\xi(u(t),u(t)) + \frac{A_-}{2}\|u\|^2_{L^2(I)} \geq B_- \left\|\frac{\partial u}{\partial x}\right\|^2_{L^2(I)} + \frac{B'_-}{2}(u^2(1) - u^2(-1)).$$

So, we obtain the existence of $M = \min(B_-, 1)$ *and* $\eta = \left(\frac{A_- + B'_-}{2} + 1\right)$, *where for all* $x \in I$ *we have*

$$\xi\left(u(t),u(t)\right) + \eta \ \|u(t)\|^2_{L^2(I)} \geq M \ \|u(t)\|^2_{H^1(I)}, \quad \forall u(t) \in H^1(I).$$

Hence, the existence and the uniqueness of the solution of the problem (2.6) *are proved.*

2.1.3 Construction of numerical approximation

The construction of the numerical approach is based on coupling two different methods. We begin with a spectral approximation using a Galerkin method for the spatial variable x, based on a special basis functions formed with Legendre polynomials. This helps us to form a simple algebraic system depending only on the temporal variable t, which we solve using a Crank-Nicolson scheme.

Spatial discretization

We define $V_N \subset H^1(I)$ as

$$V_N = \{v \in \mathbb{P}_N \ \textit{such that} \quad v(-1) - \varepsilon v'(-1) = 0 \quad \textit{and} \quad v(1) + \varepsilon v'(1) = 0\}.$$

The Legendre Galerkin scheme for (2.6) is

$$\begin{aligned} &\text{Find } \ u_N(t) \in V_N, \ \text{ such that} \\ &\frac{\mathrm{d}}{\mathrm{d}t}\langle u_N(t), v_N\rangle + \xi(u_N(t), v_N) = \langle f(t), v_N\rangle, \quad \forall\ v_N \in V_N. \end{aligned} \tag{2.7}$$

Where $u_N(t,x)$ denotes the approximate solution defined as

$$u_N(t,x) = \sum_{k=0}^{N} \hat{u}_k(t)\ \phi_k(x), \tag{2.8}$$

where $u_k(t)$ denotes the unknown coefficients, and $\phi_k(x)$ denotes the chosen spectral basis.
We choose as a basis of V_n a family of polynomials constructed from orthogonal Legendre polynomials defined by (see [80, 81])

$$\phi_k(x) = \gamma_k\ (\mathscr{L}_k(x) + \alpha_k\ \mathscr{L}_{k+1}(x) + \beta_k\ \mathscr{L}_{k+2}(x)), \qquad k = 0, \ldots, N-2, \tag{2.9}$$

where α_k, β_k and γ_k are coefficients determined such that

- $\{\phi_k(x)\}_k$ verify the boundary conditions of the problem (2.2),
- $\|\phi_k(x)\| = 1$.

By a simple calculation and using the properties of Legendre polynomials, we obtain for $\varepsilon > 0$ and $k = 0, \ldots, N-2$

$$\alpha_k = 0, \quad \beta_k = -\frac{1 + \varepsilon k(k+1)/2}{1 + \varepsilon(k+2)(k+3)/2}, \quad \gamma_k = \left(\frac{2}{2k+1} + \beta_k^2 \frac{2}{2k+5}\right)^{-1/2}. \tag{2.10}$$

Then the approximate solution can be written using (2.9) in the form

$$u_N(t,x) = \sum_{k=0}^{N-2} \hat{u}_k(t)\ \phi_k(x). \tag{2.11}$$

By substituting (2.11) in (2.7) and taking the test functions as the same basis functions, we obtain the following scheme for all $j = 0, \ldots, N-2$

$$\frac{\mathrm{d}}{\mathrm{d}t}\sum_{k=0}^{N-2}\hat{u}_k(t)\,\langle\phi_k(x),\phi_j(x)\rangle + \sum_{k=0}^{N-2}\hat{u}_k(t)\,\xi(\phi_k(x),\phi_j(x)) = \langle f(t,x),\phi_j(x)\rangle, \quad (2.12)$$

such that

$$\langle\phi_k(x),\phi_j(x)\rangle = \int_{-1}^{1}\phi_k(x)\,\phi_j(x)\,\mathrm{d}x, \quad (2.13)$$

$$\begin{aligned}\xi(\phi_k(x),\phi_j(x)) = &\int_{-1}^{1} b(x)\,\phi_k'(x)\,\phi_j'(x)\,\mathrm{d}x + \int_{-1}^{1}(a(x)+b'(x))\,\phi_k'(x)\,\phi_j(x)\,\mathrm{d}x \\ &+ \frac{1}{\varepsilon}\left(b(1)\,\psi_k(1)\,\phi_j(1) + b(-1)\,\phi_k(-1)\,\phi_j(-1)\right), \end{aligned} \quad (2.14)$$

$$\langle f(t,x),\phi_j(x)\rangle = \int_{-1}^{1} f(t,x)\,\phi_j(x)\,\mathrm{d}x. \quad (2.15)$$

To achieve optimal results from spectral method and ensure spectral accuracy, especially when calculating integrals, we employ a Gauss-Quadrature method using Legendre-Gauss-Lobatto nodes (LGL nodes) and their corresponding weights. Due to their high accuracy, Gauss formulas play a fundamental role in the theoretical analysis of spectral methods. The capability of integrating polynomials by solely knowing their values at M points is of significant importance and will be extensively utilized. In addition, the inclusion of points $x = -1$ and $x = 1$ in the nodes proves crucial for enforcing boundary conditions [29, 73, 16]. This method is characterized by the following formula for p polynomial of N degree, where η_i represents the LGL nodes and w_i represents the corresponding weights

$$\int_{-1}^{1} pw\,\mathrm{d}x = \sum_{i=0}^{N} p(\eta_i^{(N)})w_i^{(N)}.$$

Let us denote $\mathbf{A}$ and $\mathbf{B}$ as $(N-1)\times(N-1)$ matrices formulated using (2.13)−(2.14)

$$\mathbf{A}_{k,j} = \left[\langle\phi_k,\phi_j\rangle\right]_{0\le k,\,j\le N-2}, \quad \mathbf{B}_{k,j} = \left[\xi(\phi_k,\phi_j)\right]_{0\le k,\,j\le N-2},$$

and using (2.15), we define $\mathbf{C}$ as a $(n-1)$ vector such that

$$\mathbf{C}(t) = (C_0(t),\ldots,C_{n-2}(t))^{\mathrm{T}} \text{ where } \quad C_j(t) = \langle f(t,x),\ \phi_j\rangle \quad \text{for } j = 0,\ldots,N-2.$$

By denoting the vector of the unknown coefficients

$$U(t) = (\hat{u}_0(t), \hat{u}_1(t), \ldots, \hat{u}_{N-2}(t))^{\mathrm{T}}$$

we can write (2.12) in a matrix form (2.16)

$$\frac{\mathrm{d}}{\mathrm{d}t}\mathbf{A}U(t) + \mathbf{B}U(t) = \mathbf{C}(t). \tag{2.16}$$

Joined with the initial condition from (2.2), we obtain a differential system that can be solved using different methods like finite differences methods, implicit/explicit Euler and Runge Kutta methods.

Time discretization

Now, to solve the differential system (2.16), we employ a finite differences method, specifically using a Crank-Nicolson scheme.
To implement this, we begin by subdividing the time interval $[0, T]$ into q subintervals $I_j = [t_m, t_{m+1}]$ of the same length $\Delta t = t_{m+1} - t_m$ for $m = 0, \ldots, q-1$ and $t_0 = 0$.
A discretization of spatial domain is also required. We use the LGL nodes in $[-1, 1]$ denoted by η_i.
Let $U_i^m = U(t_m, \eta_i)$ represent the solution of (2.16). Using the Crank-Nicolson scheme, we obtain

$$\left(\mathbf{A} + \frac{\Delta t}{2}\mathbf{B}\right) U_i^{m+1} = \left(\mathbf{A} - \frac{\Delta t}{2}\mathbf{B}\right) U_i^m + \frac{\Delta t}{2}\left(\mathbf{C}(t_m) + \mathbf{C}(t_{m+1})\right),$$
$$U_i^0 = g(\eta_i), \tag{2.17}$$

where $g(\eta_i)$ is the value of $g(x)$ at each node η_i of the discretization of $[-1, 1]$.

2.1.4 Stability and convergence analysis

In this section, we establish the stability and convergence results for the Legendre-Galerkin spectral method in order to achieve spectral accuracy. The theorems presented here are derived following the same approach as in chapter 6 from [15]. Throughout this discussion, we use $\mathcal{C}$ to represent a generic positive constant independent of N.

Theorem 2.2 *There exists a positive constant $\mathcal{C}$, independent of N, such that the solution u_N of (2.7) satisfies the following estimate*

$$\|u_N(t)\|^2_{L^2(I)} + K\int_0^t \|u_N(s)\|^2_{L^2(I)}\,\mathrm{d}s \leq \|u_N(0)\|^2_{L^2(I)} + \mathcal{C}\int_0^t \|f(s)\|^2_{L^2(I)}\,\mathrm{d}s. \quad (2.18)$$

Proof 2.2 *By setting $v_N = u_N$ in (2.7), we obtain*

$$\frac{1}{2}\frac{\mathrm{d}}{\mathrm{d}t}\|u_N(t)\|^2_{L^2(I)} + \xi(u_N(t), u_N(t)) = \langle f(t), u_N(t)\rangle. \quad (2.19)$$

Since $\xi(.,.)$ is only weakly coercive then there exists $K > 0$ such that

$$K|u|^2_{H^1(I)} \leq \xi(u,u),\ \forall u \in H^1(I) \quad (2.20)$$

where $|u|_{H^1(I)}$ is the semi norm on $H^1(I)$.
Using (2.20) in (2.19) we obtain

$$\frac{1}{2}\frac{\mathrm{d}}{\mathrm{d}t}\|u_N(t)\|^2_{L^2(I)} + K\|u_N(t)\|^2_{L^2(I)} \leq \|f(t)\|_{L^2(I)}\|u_N(t)\|_{L^2(I)}. \quad (2.21)$$

Now, employing the Young inequality, we derive

$$\frac{\mathrm{d}}{\mathrm{d}t}\|u_N(t)\|^2_{L^2(I)} + K\|u_N(t)\|^2_{L^2(I)} \leq \frac{1}{K}\|f(t)\|^2_{L^2(I)}. \quad (2.22)$$

Integrating the last estimate for $t \geq 0$, we obtain the desired estimate (2.18) which ensures the stability since $\frac{1}{K}$ is independent of N with $u_N(0) = g(x)$.

Moving to the convergence analysis, we first establish some definitions.
Let's define the error function between the solution $u_N(t)$ of the scheme (2.7) and the exact solution of (2.6) as

$$E(t) = R_N u(t) - u_N(t)$$

where R_N is the projection defined from $H^1(I) \longrightarrow V_N$ such that when $N \to \infty$, we have

$$\|u - R_N u\|_{H^1(I)} \to 0 \quad \textit{for all} \quad u \in H^1(I). \quad (2.23)$$

Let $u \in L^2(I)$, and we define the norm of u in the dual space of $H^1(I)$ denoted $(H^1(I))^*$ by

$$\|u\|_{(H^1(I))^*} = \sup_{\substack{v\in H^1(I)\\ v\neq 0}} \frac{\langle u, v\rangle}{\|v\|}.$$

Additionally, we have

$$\|u\|_{(H^1(I))^*} \leq \mathcal{C}\|u\|_{L^2(I)}.$$

Theorem 2.3 *Let $u(t)$ be the exact solution of (2.6) and $u_N(t)$ the solution of (2.7). The following estimate holds*

$$\begin{aligned}&\|E(t)\|^2 + K\int_0^t |E(s)|^2_{H^1(I)}\,\mathrm{d}s \leq \\ &\|E(0)\|^2 + \mathcal{C}\left(\int_0^t \left\|\frac{\partial u}{\partial t}(s) - R_N\frac{\partial u}{\partial t}(s)\right\|_{(H^1(I))^*}\mathrm{d}s + \int_0^t \|(u-R_Nu)(s)\|_{H^1(I)}\mathrm{d}s\right),\end{aligned} \tag{2.24}$$

where $\mathcal{C}$ is a constant independent of N.

Proof 2.3 *$E(t)$ satisfies the following estimate using the weak corecivity of $\xi(.,.)$*

$$\frac{1}{2}\frac{\mathrm{d}}{\mathrm{d}t}\|E(t)\|^2 + K\,|E(t)|^2_{H^1(I)} \leq \left|\langle\frac{\partial u}{\partial t} - R_N\frac{\partial u}{\partial t}, E(t)\rangle + \xi(u-R_Nu, E(t))\right| \tag{2.25}$$

Using the above definitions and the continuity of the form $\xi(.,.)$, we obtain the existence of a constant $\mathcal{C}$ independent of N, such that

$$\begin{aligned}&\left|\langle\frac{\partial u}{\partial t} - R_N\frac{\partial u}{\partial t}, E(t)\rangle + \xi(u-R_Nu, E(t))\right| \\ &\leq \\ &\mathcal{C}\,\|E(t)\|_{H^1(I)}\left(\left\|\frac{\partial u}{\partial t} - R_N\frac{\partial u}{\partial t}\right\|_{(H^1(I))^*} + \|u-R_Nu\|_{H^1(I)}\right)\end{aligned} \tag{2.26}$$

By replacing this result in (2.25), an error bound is estimated through integration for all $t \geq 0$. We conclude the convergence of the approximate solution $u_N(t,x)$ to the exact solution $u(t,x)$.

2.1.5 Numerical results

To assess the performance of the described spectral method, we present the following examples, involving the numerical solution of the problem (2.1)−(2.2). The numerical results confirm the efficiency of the method through the calculation of

various error norms. Another approach to validate the reliability of the method is to compare the obtained results of the approximate solution with the the analytical solution of the problem, considering boundary conditions of the Dirichlet type. To demonstrate the efficiency of the proposed method, we examine hereafter two methods of presenting the numerical results

- Since the problem (2.1) is formulated with Robin boundary conditions (2.2) perturbed with a parameter ε, the exact solution in this case is unknown. We calculate the approximate error for a fixed value of ε ($\varepsilon \neq 0$) using the formula

$$ERROR = \|u_N - u_{N+2}\|_\infty \quad N = 2, 4, 6, \ldots \tag{2.27}$$

- Another way to affirm the reliability of the method is by comparing the obtained results of the approximate solution as ε tends to 0 with the analytical solution of the problem under Dirichlet boundary conditions. In this context, different error values are calculated.
  We define the absolute error by

$$\mathscr{E}(t,x) = \mid u_{exact}(t,x) - u_N(t,x) \mid, \tag{2.28}$$

  The maximum absolute error by

$$\mathscr{E}_{max} = \|u_{exact} - u_N\|_\infty = \max_i |(u_{exact})_i - (u_N)_i|, \qquad i = 1, 2, \ldots, N_x, \tag{2.29}$$

  The square error norm by

$$\mathscr{E}_2 = \|u_{exact} - u_N\|_2 = \left[\Delta x \sum_{i=1}^{N_x} |(u_{exact})_i - (u_N)_i|^2\right]^{1/2} \tag{2.30}$$

  where N_x is the number of interval subdivisions, and Δx is the appropriate step,
  and the relative error is given by

$$\mathscr{E}_{re} = \frac{\|u_{exact} - u_N\|_2}{\|u_{exact}\|_2}. \tag{2.31}$$

The figures are obtained for $N_x = 20$ subdivisions using the Legendre-Gauss-Lobatto nodes in the domain $[-1, 1]$, and 100 subdivision of the temporal domain.

Example 2.1 *We consider the equation* (2.1) *with constant coefficients* $a(x) = 0.01$, $b(x) = 1$, *and a final time* $T = 1$. *The initial condition is given by*

$$u(0, x) = \cos(\frac{\pi}{2}x),$$

and the term $f(t, x)$ *is calculated so that the exact solution under homogeneous Dirichlet boundary conditions, is*

$$u(t, x) = \exp(-t)\cos(\frac{\pi}{2}x).$$

Discussion: Figure 2.1 and Figure 2.2 illustrate the convergence of the approximate solution to the exact solution at different values of ε, specifically $\varepsilon = 0.2,\ 0.1,\ 0.02,\ 0.01,\ 0.001$. When ε tends to zero, the approximate solution approaches the exact one from Dirichlet boundary conditions.
The variations of the error of the approximate solution ($ERROR$) are depicted in Figure 2.3. It is observed that the error of the approximate solution decreases as N increases.
In Figure 2.4, we compare the exact solution of the problem with homogeneous Dirichlet boundary conditions to the approximative solution obtained using the approximative method when $\varepsilon = 10^{-8}$ and $N = 10$.

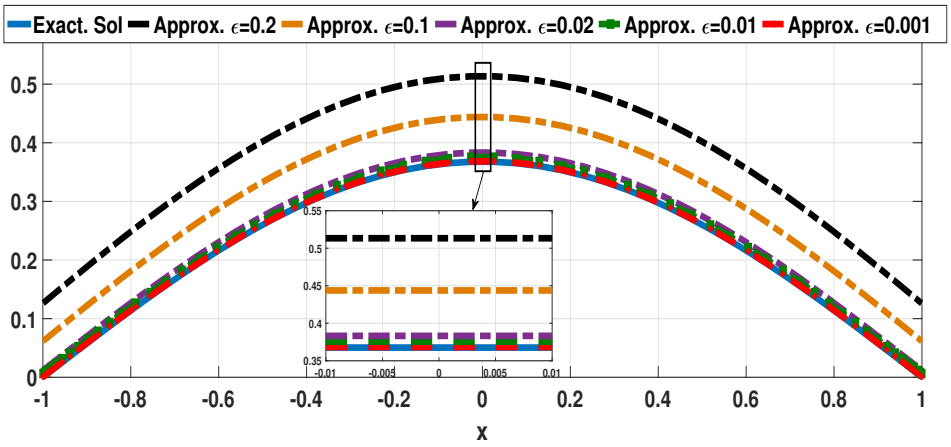

Figure 2.1: The behavior of the approximate solution when ε tends to 0 at $N = 10$ for fixed $t = 1$ for Example 2.1

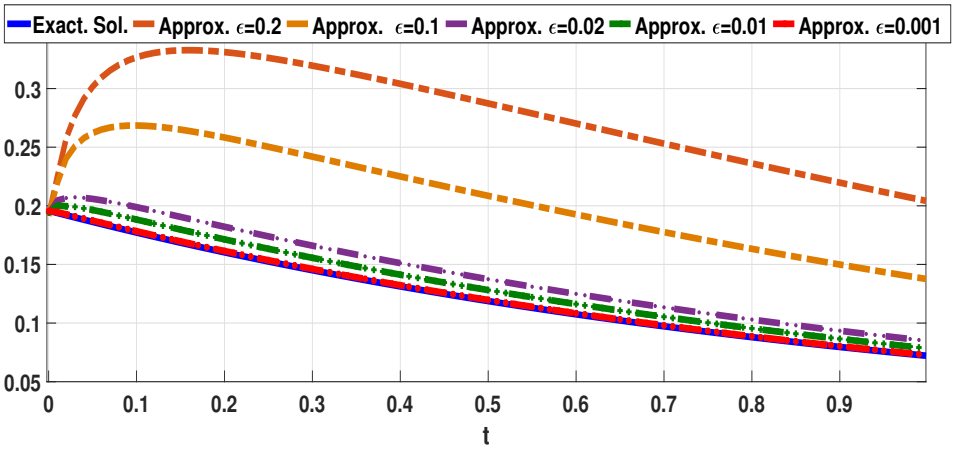

Figure 2.2: The behavior of the approximate solution when ε tends to 0 at $N = 10$ for fixed $x = -0.874$ for Example 2.1

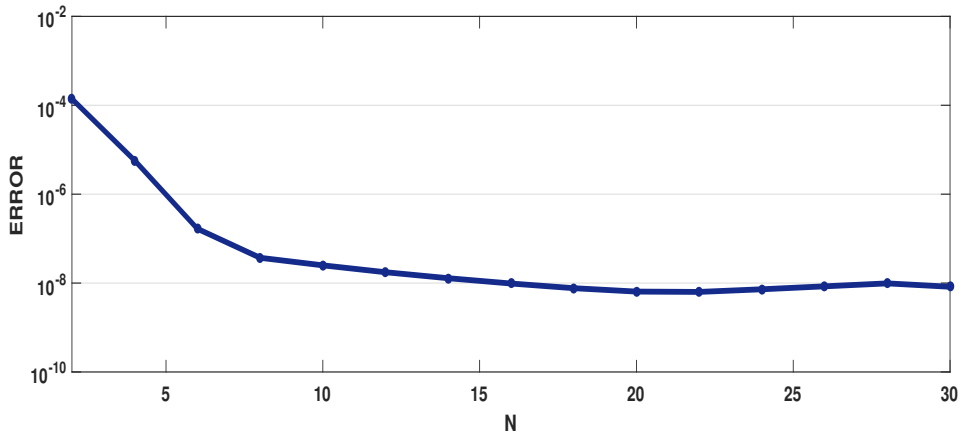

Figure 2.3: Logarithmic approximation error as a function of N at $\varepsilon = 10^{-8}$ for Example 2.1

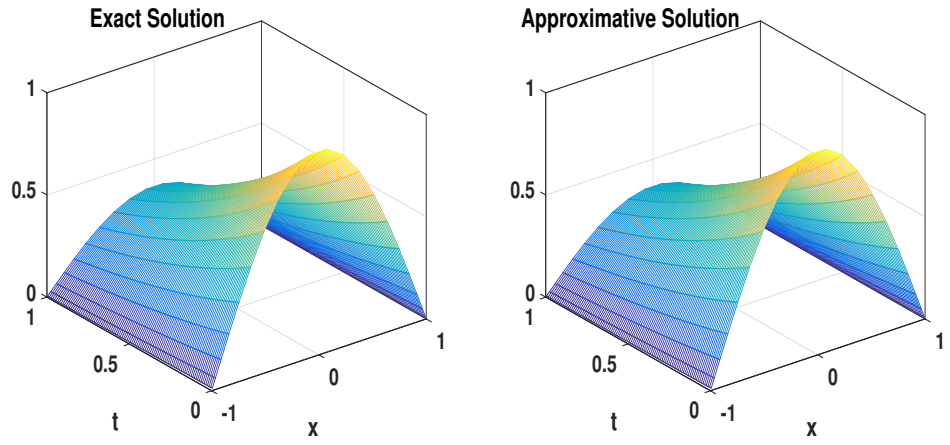

Figure 2.4: Representation of the exact solution for the problem with Dirichlet boundary conditions and the approximate solution at $N = 8$ and $\varepsilon = 10^{-8}$ for Example 2.1

Example 2.2 *We assume that in* (2.1) $a(x) = 0$, $b(x) = 1$, $T = 1$. *The initial condition is given by*

$$u(0, x) = cos(\frac{\pi}{2}x),$$

and the term $f(t, x)$ *is set to be* 0. *In this case, the exact solution under homogeneous Dirichlet boundary conditions is given by*

$$u(t, x) = \cos\left(\frac{\pi}{2}x\right) \exp\left(-\frac{b(x)\pi^2}{4}t\right).$$

Discussion: Figure 2.5 displays the exact and the obtained approximate solutions for various values of N. The plot illustrates the convergence of the approximation for different N, where $N = 6, 8, 10$ and $\varepsilon = 10^{-2}, 10^{-3}, 10^{-4}$ at $x = 0.227$ and $t = 1$. In each case, an error value is provided, calculated using the appropriate ε and N. The obtained results demonstrate the convergence of the approximate solution when ε tends to 0, aligning with the exact solution under Dirichlet boundary conditions.

Table 2.1 provides the square error norm $\mathscr{E}_2$ calculated for different values of N.

Table 2.1: Error values as a function of N for $\varepsilon = 10^{-8}$ for Example 2.2.

N	$\mathscr{E}_2$
4	6.46185e − 05
8	8.93058e − 06
12	8.93059e − 06
16	8.92040e − 06
20	8.86360e − 06

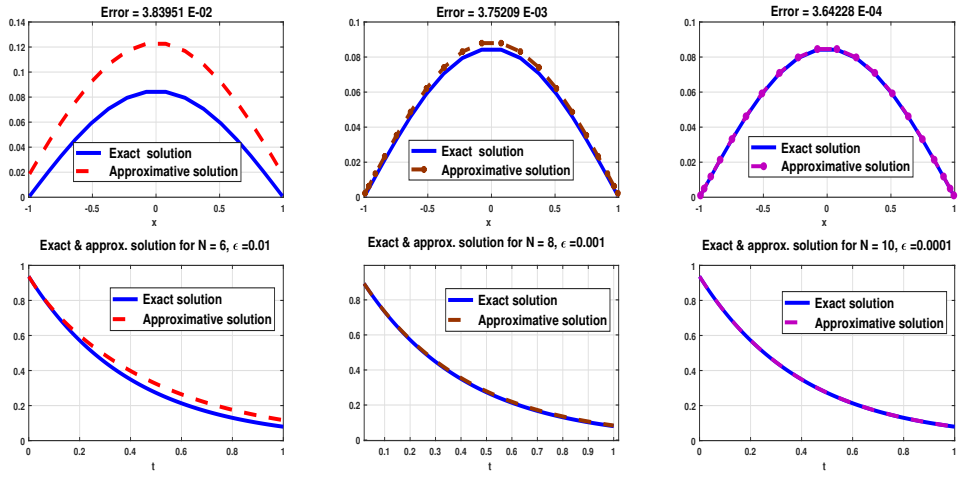

Figure 2.5: The behavior of exact and approximate solution for different N and ε with the appropriate $\mathscr{E}_2$ for fixed $T = 1$ (up) and fixed $x = 0.227$ (down) for Example 2.2

Example 2.3 *Let's consider the problem with* $a(x) = 0.09$, $b(x) = 2$,*and the final time* $T = 1$. *The initial condition is* $u(0, x) = 0$ *and the term* $f(t, x)$ *is calculated so that the exact solution, under homogeneous Dirichlet boundary conditions, is given by*

$$u(t, x) = t^2 \cos(x\frac{\pi}{2}).$$

Discussion: Figure 2.7 depicts the convergence of the approximate solution with decreasing ε down to $\varepsilon = 0.001$. When ε takes the values 0.08, 0.05, 0.025, 0.001,

the curve of the approximation for a fixed x or a fixed t approaches the curve of the exact solution under the Dirichlet boundary conditions. This convergence trend is reflected in Table 2.2, where the error is calculated for different values of N. Notably, for $\varepsilon = 10^{-8}$, the numerical solution closely aligns with the exact solution. Table 2.3 introduces the $\mathscr{E}_{re}$ at $N = 4,\ 8$, and 10 with different LGL nodes in $[-1, 1]$.

Table 2.2: Error values as a function of N for $\varepsilon = 10^{-8}$ for Example 2.3.

N	$\mathscr{E}_2$	N	$\mathscr{E}_2$
4	9.22208e − 04	14	8.74526e − 06
6	1.36494e − 04	16	6.03520e − 06
8	5.11646e − 05	20	2.77529e − 06
10	2.46797e − 05	24	1.68477e − 06
12	1.39021e − 05	30	8.29894e − 07

Table 2.3: Relative error $\mathscr{E}_{re}$ for different N when $\varepsilon = 10^{-8}$ for Example 2.3.

x	$N = 4$	$N = 8$	$N = 10$
−0.944	7.51812e − 03	6.43507e − 04	3.26354e − 04
−0.755	1.14864e − 03	2.38689e − 05	4.65406e − 05
−0.458	2.60600e − 04	3.26515e − 06	3.28677e − 05
−0.095	9.29549e − 04	3.15130e − 05	1.86307e − 05
0.281	4.41661e − 04	5.66697e − 05	1.39810e − 05
0.617	2.32730e − 03	6.63974e − 05	2.60646e − 05
0.865	8.60915e − 04	2.34344e − 04	4.61786e − 06

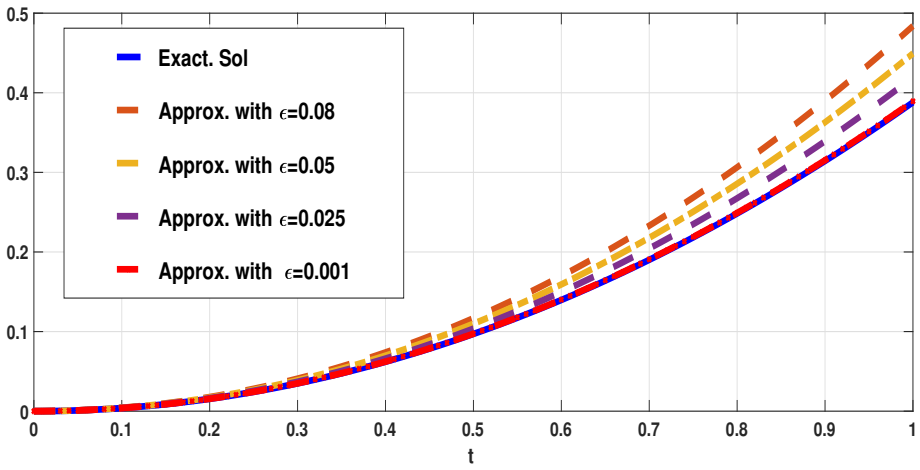

Figure 2.6: The exact solution compared to the approximate solution for different ε with $N = 10$, for fixed $x = -0.281$ for Example 2.3

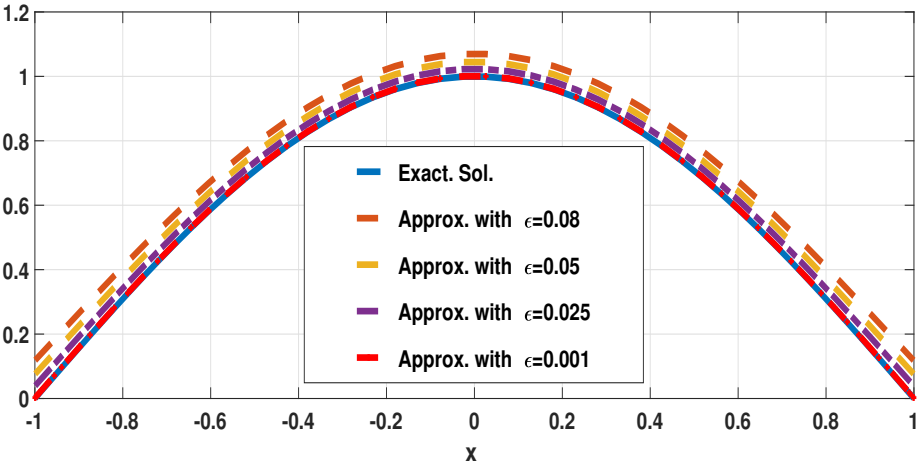

Figure 2.7: The exact solution compared to the approximate solution for different ε with $N = 10$, for fixed $T = 1$ for Example 2.3

Example 2.4 *Let's consider the equation* (2.1) *with variable coefficients* $a(x) = 0$ *and* $b(x) = 1 - x^2$, *a final time* $T = 1$, *and the initial condition given by*

$$u(0, x) = x \cos(x\frac{\pi}{2})$$

The term $f(t,x)$ is calculated so that the exact solution under homogeneous Dirichlet boundary conditions is given by

$$u(t,x) = x\exp(t)\cos(x\frac{\pi}{2}).$$

Discussion: Table 2.4 presents the $\mathscr{E}_{max}$ and $\mathscr{E}_2$ for decreasing ε from 10^{-1} to 10^{-10} when $N = 10$. Table 2.5 exposes the relative error calculated at different nodes when $N = 4,\ 8$ and 12, the results, obtained when $\varepsilon = 10^{-8}$, demonstrates the convergence of the approximation to the exact solution of the problem with Dirichlet boundary conditions as ε approaches 0.

Table 2.4: Error values for different ε at $N = 10$ for Example 2.4.

ε	$\mathscr{E}_2$	$\mathscr{E}_{max}$
10^{-1}	9.05505e − 01	1.03184e + 00
10^{-2}	2.91516e − 01	3.25393e − 01
10^{-3}	3.62864e − 02	4.05446e − 02
10^{-4}	3.73871e − 03	4.17051e − 03
10^{-5}	3.75677e − 04	4.18251e − 04
10^{-6}	3.81611e − 05	4.18316e − 05
10^{-7}	4.45936e − 06	4.17778e − 06
10^{-8}	1.28603e − 06	1.28416e − 06
10^{-10}	1.02004e − 06	1.11888e − 06

Table 2.5: Relative error values $\mathscr{E}_{re}$ for different N when $\varepsilon = 10^{-8}$ for Example 2.4.

x	$N = 4$	$N = 8$	$N = 12$
−0.912	1.46648e − 01	4.52127e − 05	2.29492e − 06
−0.510	1.51450e − 03	1.44248e − 05	1.33381e − 06
0.076	5.97860e − 02	2.44510e − 05	1.22646e − 06
0.227	4.95987e − 02	9.91097e − 06	1.24621e − 06
0.746	7.19953e − 02	2.44251e − 06	1.55148e − 06

Example 2.5 *Let's consider the equation with* $a(x) = 1 - x^2$, $b(x) = 2$, $T = 1$. *The initial condition is given by*

$$u(0, x) = (1 - x^2) \sin\left(x\frac{\pi}{2}\right).$$

The term $f(t, x)$ *is obtained so that the exact solution for the problem with Dirichlet boundary conditions is given by*

$$u(t, x) = \exp\left(\frac{-\pi^2}{4}t\right)(1 - x^2) \sin\left(x\frac{\pi}{2}\right).$$

Discussion: Figure 2.8 is generated using various decreasing values of ε. It is evident that as ε tends to 0, the obtained approximation is closely aligns with the exact solution for the problem with Dirichlet boundary conditions.
Table 2.6 displays the error calculated at different values of ε. It is observed that with increasing N, the approximate solution becomes more accurate when compared to the exact one. This approach investigates the numerical convergence of the obtained approximate solution at the Dirichlet boundary conditions when ε tends to 0.
Figure 2.9 illustrates the exact solution of the Dirichlet boundary conditions problem alongside the approximate solution obtained using the proposed numerical method. Additionally, the absolute error is depicted. Even with a new step of discretization for the temporal domain $\Delta t = 0.001$, the results of convergence remain consistent.

Table 2.6: Error values for different values of N when $\varepsilon = 10^{-8}$.

N	$\mathscr{E}_2$	$\mathscr{E}_{max}$
4	3.86296e − 03	4.19989e − 03
6	3.98687e − 04	4.56514e − 04
8	1.26445e − 04	1.50269e − 04
10	6.06861e − 05	7.60106e − 05
12	3.39352e − 05	3.93346e − 05
14	2.12362e − 05	2.51413e − 05
16	1.45927e − 05	1.74079e − 05
20	6.52682e − 06	7.32607e − 06

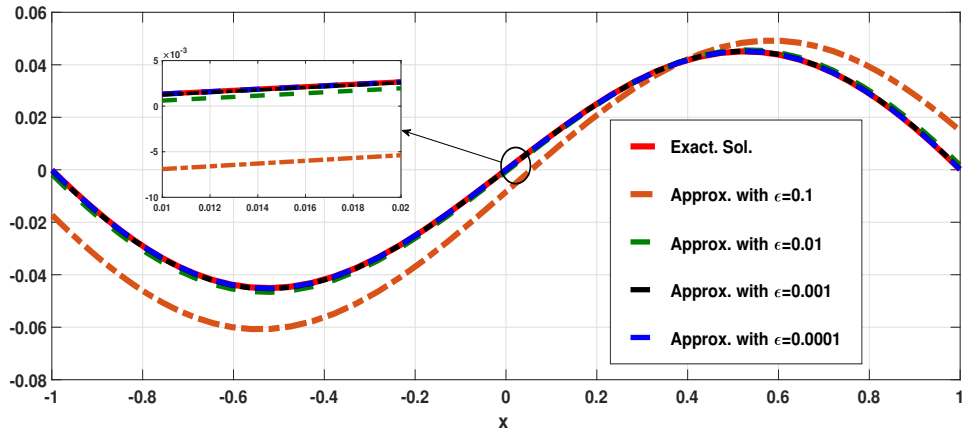

Figure 2.8: Exact and approximate solutions for different ε at $N = 10$ and $t = 1$ for Example 2.5

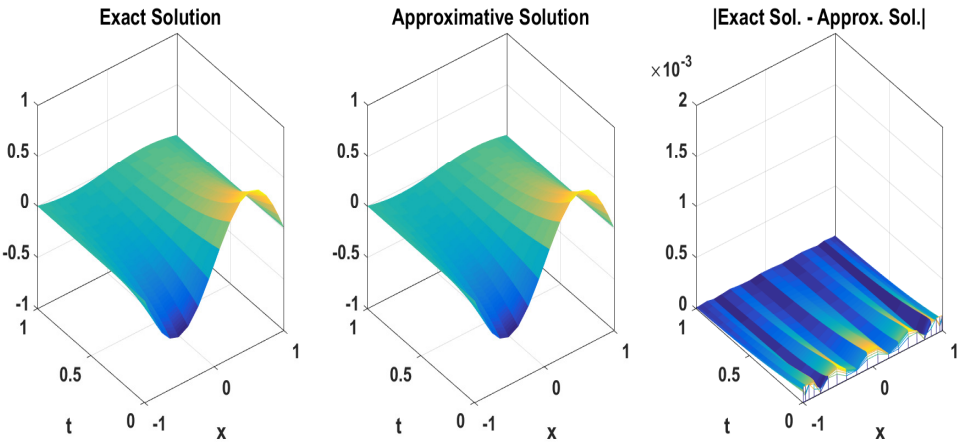

Figure 2.9: Representation of the exact solution of Dirichlet boundary conditions problem, the approximate solution obtained using the described method and the absolute error for $N = 16$, $\varepsilon = 10^{-8}$ and $\Delta t = 0.001$ for Example 2.5

2.1.6 Concluding remarks

In this study, the advantages of Legendre polynomials, along with their important properties and Gauss quadratures, are utilized to construct an approximation

of the advection-diffusion solution. The proposed numerical approach is outlined in two steps: initially, the basis used in Galerkin approximation is defined, and the type of Gauss quadrature employed for precise integral calculations is specified. Subsequently, a Crank-Nicolson scheme is developed to solve the resulting system based on the time variable. The stability and the convergence analysis of the method are rigorously analyzed, providing estimates based on initial values for stability and an error bound that characterizes the convergence. Several examples covering different cases are presented with various types of results to demonstrate the numerical convergence of the approximate solution to the exact one under Dirichlet boundary conditions as ε tends to zero. The obtained results are introduced and interpreted in different error types (the $\mathscr{E}_{re}$, $\mathscr{E}_2$ and $\mathscr{E}_{max}$). The findings suggest that the introduced method is efficient and applicable to solving many time-dependent problems involving different partial differential equations with different types of boundary conditions. The proposed approach exhibits spectral accuracy, enabling high precision in the approximation which has been illustrated by several numerical examples.

2.2 Second approach

A part of the obtained results was the subject of an international communication entitled "A Highly Accurate Numerical Method Using Compact Combination Basis and Kronecker Product to Solve Partial Differential Equations" in the *International Conference on Contemporary Mathematics and its Applications (ICCMA 2023) 26-27 November 2023, Mila- Algeria.*

2.2.1 Description of the problem

We consider the following one-dimensional advection-diffusion equation

$$\frac{\partial u}{\partial t}(t,x) = \alpha \frac{\partial^2 u}{\partial x^2}(t,x) + \beta \frac{\partial u}{\partial x}(t,x) + f(t,x); \tag{2.32}$$

coupled with the following boundary conditions of Dirichlet type and the initial condition

$$u(t,0) = h_0(t),\ u(t,1) = h_1(t), \quad u(0,x) = g(x). \tag{2.33}$$

where

- $u(t,x)$ is the unknown function,
- $t, x \in [0,1]$ are the proposed variables,
- The coefficients of advection and diffusion are $\alpha > 0$ and $\beta \geq 0$, respectively.
- $f \in \mathscr{C}([0,1],[0,1])$, $h_0, h_1 \in \mathscr{C}([0,1])$, and $g \in \mathscr{C}([0,1])$ are given functions.

2.2.2 Shifted Legendre Galerkin method

Starting by writting the corresponding integral equation to the advection-diffusion equation by integrating (2.32) with respect to the temporal variable t and taking into consideration the initial condition in (2.33). The studied problem becomes

$$\begin{aligned} &u(t,x) - \alpha \int_0^t \frac{\partial^2 u}{\partial x^2}(z,x)\,\mathrm{d}z - \beta \int_0^t \frac{\partial u}{\partial x}(z,x)\,\mathrm{d}z = \int_0^t f(z,x)\mathrm{d}z + g(x), \\ &u(t,0) = h_0(t),\ u(t,1) = h_1(t),\ t \geq 0. \end{aligned} \tag{2.34}$$

For the case of non-homogeneous boundary conditions, where $h_0(t), h_1(t) \neq 0$, we introduce the following transformation which consists on transforming the non-homogeneous boundary conditions into homogeneous ones

$$v(t,x) = u(t,x) - (1-x)\,h_0(t) - x\,h_1(t).$$

The problem (2.34) becomes

$$\begin{aligned} &v(t,x) - \alpha \int_0^t \frac{\partial^2 v}{\partial x^2}(z,x)\,\mathrm{d}z - \beta \int_0^t \frac{\partial v}{\partial x}(z,x)\,\mathrm{d}z = f_1(t,x), \\ &v(t,0) = 0,\ v(t,1) = 0,\ t \geq 0. \end{aligned} \tag{2.35}$$

where

$$f_1(t,x) = \int_0^t f(z,x),\mathrm{d}z + g(x) + \beta \int_0^t (h_1(z) - h_0(z))\,\mathrm{d}z - (1-x)h_0(t) - xh_1(t).$$

Hereafter, we consider the case of homogeneous boundary conditions in (2.34). We choose at this stage to use a spectral approach for both spatial and temporal

discretizations.
We define

$$S_N = span\{\widetilde{\mathscr{L}_i}(x)\widetilde{\mathscr{L}_j}(t),\, i,j = 0,1,\ldots,N\}$$

where $\widetilde{\mathscr{L}_i}(x)$ denotes the shifted Legendre polynomial of degree i on x.
And

$$P_N = \{z \in S_N :\, z(0,t) = z(1,t) = 0,\, 0 < t \leq 1\}$$

The spectral scheme is to find $u_N(t,x) \in P_N$ such that $\forall\, v(t,x) \in P_N$

$$\begin{aligned}\langle u_N(t,x) - \alpha \int_0^t \frac{\partial^2 u_N}{\partial x^2}(z,x)\,\mathrm{d}z - \beta \int_0^t \frac{\partial u_N}{\partial x}(z,x)\,\mathrm{d}z,\, v(t,x)\rangle \\ = \langle \int_0^t f(z,x)\,\mathrm{d}z + g(x), v(t,x)\rangle, \qquad (2.36)\end{aligned}$$

where $\langle u,v\rangle$ designed the scalar product in $L^2((0,1)\times(0,1])$.

To apply The spectral Galerkin method, we need to select suitable basis functions: a compact combination of different degrees of Legendre polynomials is applied for the spatial resolution. We consider the following type of basis functions

$$\begin{aligned}\phi_i(x) &= \widetilde{\mathscr{L}_i}(x) - \widetilde{\mathscr{L}_{i+2}}(x), \\ \psi_j(t) &= \widetilde{\mathscr{L}_j}(t), \qquad (2.37)\end{aligned}$$

One can define the space $P_N = span\{\phi_i(x)\psi_j(t), i,j = 0,\ldots,N\}$ in which the approximate solution is given by

$$u_N(t,x) = \sum_{i=0}^{N}\sum_{j=0}^{N} \hat{u}_{i,j}\,\phi_i(x)\psi_j(t), \qquad (2.38)$$

By choosing the test functions as $\phi_n(x)\psi_m(t)$, for $0 \leq n,m \leq N$, the spectral scheme can be written as

$$\begin{aligned}\langle u_N(t,x)\,,\, \phi_n(x)\psi_m(t)\rangle - \alpha\langle \int_0^t \frac{\partial^2 u_N}{\partial x^2}(z,x)\,\mathrm{d}z\,,\, \phi_n(x)\psi_m(t)\rangle \\ - \beta\langle \int_0^t \frac{\partial u_N}{\partial x}(z,x)\,\mathrm{d}z\,,\, \phi_n(x)\psi_m(t)\rangle \\ = \langle \int_0^t f(z,x)\,\mathrm{d}z + g(x), \phi_n(x)\psi_m(t)\rangle. \qquad (2.39)\end{aligned}$$

Then, each item in the left hand side of (2.39) can be simplified and expressed in a matrix form

$$\begin{aligned}\langle u_N(t,x)\,,\,\phi_n(x)\psi_m(t)\rangle &= \left\langle \sum_{i=0}^{N}\sum_{j=0}^{N} \hat{u}_{i,j}\phi_i(x)\psi_j(t), \phi_n(x)\psi_m(t) \right\rangle \\ &= \sum_{i=0}^{N}\sum_{j=0}^{N} \hat{u}_{i,j}\ \langle\phi_i(x),\phi_n(x)\rangle\,\langle\psi_j(t),\psi_m(t)\rangle, \\ &= \mathbf{A}\mathbf{U}\mathbf{B}^{\mathrm{T}}. \end{aligned} \tag{2.40}$$

where $\mathbf{U}$ is the matrix of the unknown spectral expansion coefficients of the unsolved quantity $u(t,x)$ under the proposed numerical technique, given by

$$\mathbf{U} = \begin{pmatrix} \hat{u}_{0,0} & \hat{u}_{0,1} & \dots & \hat{u}_{0,N} \\ \hat{u}_{1,0} & \hat{u}_{1,1} & \dots & \hat{u}_{1,N} \\ \vdots & \vdots & \ddots & \vdots \\ \hat{u}_{N,0} & \hat{u}_{N,1} & \dots & \hat{u}_{N,N} \end{pmatrix} \tag{2.41}$$

and

$$\mathbf{A} = [\langle\phi_i(x),\phi_n(x)\rangle]_{0\le i,n\le N}\,, \quad \mathbf{B} = [\langle\psi_j(t),\psi_m(t)\rangle]_{0\le j,m\le N}\,.$$

Similarly,

$$\begin{aligned}&\langle \int_0^t \frac{\partial^2 u_N}{\partial x^2}(z,x)\,\mathrm{d}z\,,\,\phi_n(x)\psi_m(t)\rangle \\ &\qquad = \left\langle \int_0^t \frac{\partial^2}{\partial x^2}\left(\sum_{i=0}^{N}\sum_{j=0}^{N}\hat{u}_{i,j}\,\phi_i(x)\psi_j(z)\right)\mathrm{d}z, \phi_n(x)\psi_m(t)\right\rangle, \\ &\qquad = \sum_{i=0}^{N}\sum_{j=0}^{N}\hat{u}_{i,j}\,\langle\phi_i''(x),\phi_n(x)\rangle\ \left\langle\int_0^t \psi_j(z))\,\mathrm{d}z, \psi_m(t)\right\rangle, \\ &\qquad = \mathbf{A}_{xx}\mathbf{U}\mathbf{B}_t^{\mathrm{T}}, \end{aligned} \tag{2.42}$$

where

$$\mathbf{A}_{xx} = [\langle\phi_i''(x),\phi_n(x)\rangle]_{0\le i,n\le N}\,, \quad \mathbf{B}_t = \left[\langle\int_0^t \psi_j(z))\mathrm{d}z, \psi_m(t)\rangle\right]_{0\le j,m\le N}.$$

Also,

$$\langle \int_0^t \frac{\partial u_N}{\partial x}(z,x)\,\mathrm{d}z\,,\,\phi_n(x)\psi_m(t)\rangle$$

$$= \left\langle \int_0^t \frac{\partial}{\partial x} \left(\sum_{i=0}^{N} \sum_{j=0}^{N} \hat{u}_{i,j}\, \phi_i(x)\psi_j(z)) \right) \mathrm{d}z, \phi_n(x)\psi_m(t) \right\rangle,$$

$$= \sum_{i=0}^{N} \sum_{j=0}^{N} \hat{u}_{i,j}\, \langle \phi_i'(x), \phi_n(x) \rangle \left\langle \int_0^t \psi_j(z))\, \mathrm{d}z, \psi_m(t) \right\rangle,$$

$$= \mathbf{A}_x \mathbf{U} \mathbf{B}_t^{\mathrm{T}}, \tag{2.43}$$

where

$$\mathbf{A}_x = [\langle \phi_i'(x), \phi_n(x) \rangle]_{0 \le i,n \le N}.$$

For the right-hand side of (2.39), one can calculate it directly using

$$\langle \int_0^t f(z,x)\, \mathrm{d}z + g(x), \phi_n(x)\psi_m(t) \rangle = F, \tag{2.44}$$

where

$$F = \left[\langle \int_0^t f(z,x)\, \mathrm{d}z + g(x), \phi_n(x)\psi_m(t) \rangle \right]_{0 \le n,m \le N}.$$

Collecting the precedent formulas, the obtained system can be written in the matrix form

$$\mathbf{A}\mathbf{U}\mathbf{B}^{\mathrm{T}} - \alpha\, \mathbf{A}_{xx}\mathbf{U}\mathbf{B}_t^{\mathrm{T}} - \beta \mathbf{A}_x \mathbf{U}\mathbf{B}_t^{\mathrm{T}} = F. \tag{2.45}$$

The system (2.45) can be reformulated using the Kronecker product as follows

$$(\mathbf{B} \otimes \mathbf{A} - \alpha\, \mathbf{B}_t \otimes \mathbf{A}_{xx} - \beta\, \mathbf{B}_t \otimes \mathbf{A}_x)\overline{\mathbf{U}} = \overline{F}, \tag{2.46}$$

where $\mathbf{U}$ and F are compressed into the one-dimentional vectors by columns $\overline{\mathbf{U}}$ and $\overline{F}$ in the following form

$$\overline{\mathbf{U}} = [\hat{u}_{0,0}, \hat{u}_{1,0}, \ldots, \hat{u}_{N,0}, \ldots, \hat{u}_{0,N}, \ldots, \hat{u}_{N,N}]^{\mathrm{T}}.$$

Remark 2.1 *The Kronecker product of the $(n \times m)$ matrix $\boldsymbol{A} = (a_{i,j})_{1 \le i \le n, 1 \le j \le m}$ and the $(p \times q)$ matrix $\boldsymbol{B} = (b_{i,j})_{1 \le i \le p, 1 \le j \le q}$ is denoted by $\boldsymbol{A} \otimes \boldsymbol{B}$, which is the $np \times mq$ matrix of the form*

$$\boldsymbol{A} \otimes \boldsymbol{B} = \begin{pmatrix} a_{1,1}\boldsymbol{B} & a_{1,2}\boldsymbol{B} & \ldots & a_{1,m}\boldsymbol{B} \\ a_{2,1}\boldsymbol{B} & a_{2,2}\boldsymbol{B} & \ldots & a_{2,m}\boldsymbol{B} \\ \vdots & \vdots & \ddots & \vdots \\ a_{n,1}\boldsymbol{B} & a_{n,2}\boldsymbol{B} & \ldots & a_{n,m}\boldsymbol{B} \end{pmatrix}$$

The final system is a linear system of equations for $\overline{\mathbf{U}}$ that can be solved using a Gauss elimination method to obtain the expansion coefficients $\overline{\mathbf{U}}$ of $u_N(t,x)$. Then, by making use of (2.38), we can obtain the desired approximation.

2.2.3 Numerical results

To demonstrate the efficiency of the proposed method, we present here some numerical examples and discuss the obtained results. Different types of error norms are calculated using the formulas (2.28)−(2.31).

Example 2.6 *Let's consider the heat equation (the case of* (2.32) *with* $\beta = 0$*), with the following initial condition*

$$u(0,x) = \sin(\pi x).$$

The exact solution for the problem is given by

$$u(t,x) = \exp(-t)\sin(\pi x),$$

and the boundary conditions can be obtained from the exact solution.

Discussion: Table 2.7 presents the values of $\mathscr{E}_{max}$ calculated in different moments from $[0,1]$ for different values of N. Figure 2.10 depicts the global behaviour of the exact solution, the approximate solution and the respective absolute error when $N = 16$. The obtained results mark the great order in error values achieving 10^{-16}, confirming the high accuracy of the proposed technique.

Table 2.7: $\mathscr{E}_{max}$ values for different N calculated for different times for Example 2.6.

t	$N = 8$	$N = 12$	$N = 16$
0.1	3.0206e − 10	2.8865e − 15	1.2212e − 15
0.3	2.4035e − 10	2.3314e − 15	9.8532e − 15
0.5	1.9377e − 10	1.9984e − 15	8.1878e − 16
0.7	1.6966e − 10	1.6653e − 15	6.6613e − 16
0.9	1.3603e − 10	1.1657e − 15	5.4123e − 16

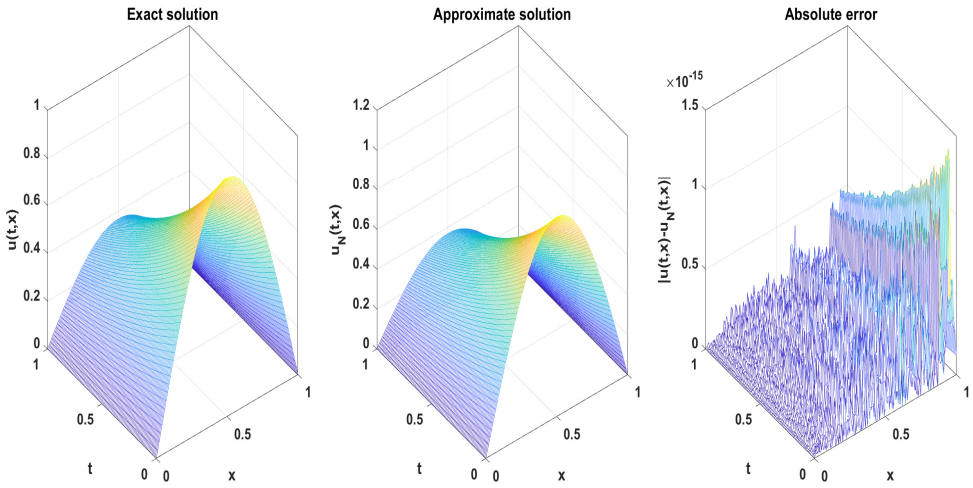

Figure 2.10: Exact and approximate solutions with the respective absolute error obtained for $N = 16$ for Example 2.6.

Example 2.7 *Another heat equation is considered with the following initial condition* $u(0, x) = 0$. *The exact solution for the problem is given by*

$$u(t, x) = t^2 \sin(x),$$

and the boundary conditions can be obtained from the exact solution.

Discussion: Table 2.8 displays the values of $\mathscr{E}_{max}$ calculated for increasing values of N in different instants. Figure 2.11 shows the 3D plot of the exact solution, the approximate solution and the respective absolute error when $N = 16$. The results confirm the high accuracy achieved while approximating the exact solution by using small values of N.

Table 2.8: $\mathscr{E}_{max}$ values for different N calculated for $t = 0.2$, $t = 0.5$ and $t = 1$ for Example 2.7.

N	$t = 0.2$	$t = 0.5$	$t = 1$
2	8.0295e − 07	5.2133e − 06	2.1135e − 05
4	1.2252e − 09	7.7715e − 09	3.1247e − 08
6	1.0653e − 12	6.7109e − 12	2.6915e − 11
8	6.0715e − 16	3.7886e − 15	1.5154e − 14
10	1.3877e − 17	2.7755e − 17	1.1102e − 16

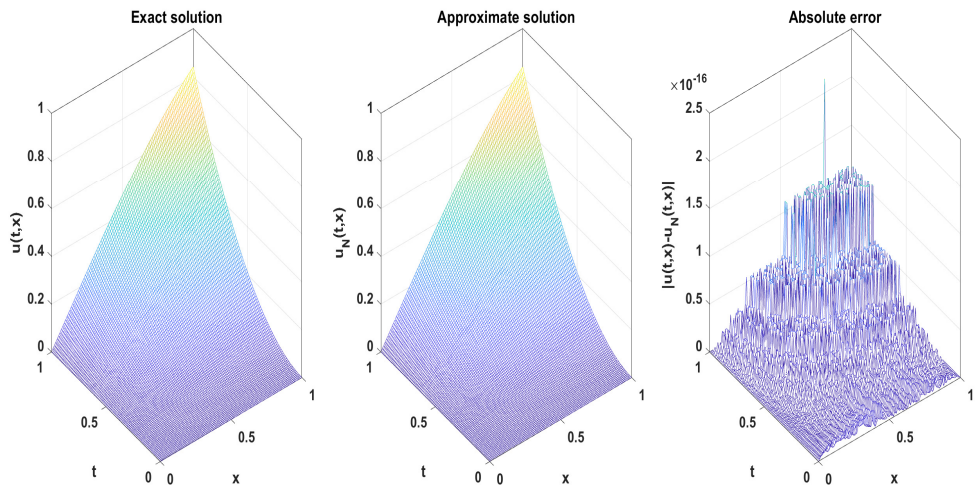

Figure 2.11: Exact and approximate solutions with the respective absolute error obtained for $N = 14$ for Example 2.7.

Example 2.8 *We consider the advection-diffusion equation* (2.32) *with* $\alpha = 0.1$ *and* $\beta = 1$*, and the following initial condition*

$$u(0,x) = \exp(5x)\left[\cos(\frac{\pi}{2}x) + \frac{1}{4}\sin(\frac{\pi}{2}x)\right].$$

The exact solution for the problem is given by

$$u(t,x) = \exp(5(x - t/2))\exp\left(-\frac{\pi^2}{40}t\right)\left[\cos(\frac{\pi}{2}x) + \frac{1}{4}\sin(\frac{\pi}{2}x)\right].$$

The boundary conditions can be obtained directly from the exact solution.

Discussion: Table 2.9 displays the values of the maximum absolute error $\mathscr{E}_{max}$ calculated in different times from $[0,1]$ using increasing values of N. The table shows clearly the decreasing values of the error in an homogeneous way every where in $[0,1]$. This behaviour is also expressed in Figure 2.12, where the plots of the approximate solution and the exact solution are identical. Finally, in Figure 2.13, the physical behaviour of the exact solution, approximate solution and the absolute error is presented in 3D. The results show great accuracy while approximating the exact solution using the proposed technique with an order of the absolute error reaching 10^{-10}.

Table 2.9: $\mathscr{E}_{max}$ values for different N calculated for different times for Example 2.8.

t	$N = 4$	$N = 8$	$N = 12$
0.1	4.3255e − 02	1.1060e − 05	5.8879e − 10
0.2	3.6044e − 02	8.1656e − 06	4.5787e − 10
0.3	3.3736e − 02	6.4417e − 06	3.4294e − 10
0.4	2.5662e − 02	5.0082e − 06	2.6536e − 10
0.5	1.5332e − 02	3.5614e − 06	1.9536e − 10
0.6	1.3094e − 02	2.9694e − 06	1.5447e − 10
0.7	9.7458e − 02	2.3741e − 06	1.1458e − 10
0.8	1.3021e − 02	1.4681e − 06	9.1814e − 11
0.9	1.1064e − 02	1.4537e − 06	6.0396e − 11
1	1.1548e − 02	3.5496e − 06	2.0562e − 10

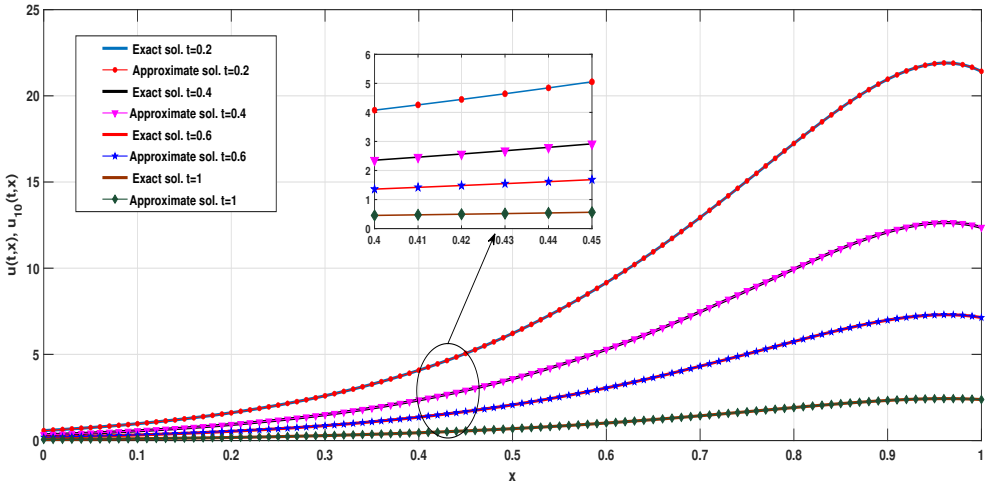

Figure 2.12: Exact and approximate solutions with the respective absolute error obtained for $N = 10$ for Example 2.8.

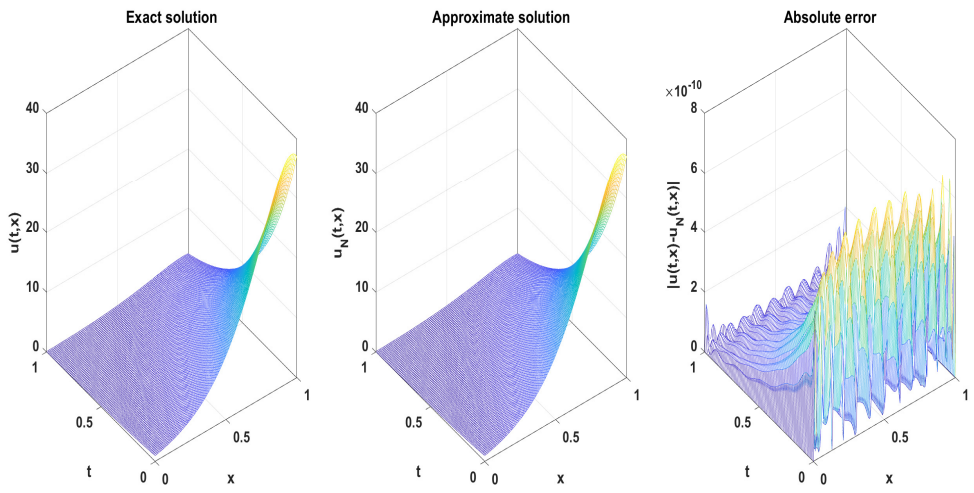

Figure 2.13: Exact and approximate solutions with the respective absolute error obtained for $N = 12$ for Example 2.8.

2.2.4 Concluding remarks

In this second approach, the advection diffusion equation is treated in a different way using the same idea of the first approach. It highlights, first, the transition between the partial differential equations and the integral equations. Then, by taking into account the boundary conditions, the compact combinations of orthogonal polynomials are investigated to approximate the exact solution using a Galerkin method. The obtained results show the efficiency and applicability of the proposed technique and the high accuracy it offers.

Chapter 3

Integral and integro-differential equations

Chapter 3

Integral and integro-differential equations

The presented results are the subject of an article entitled "Spectral Collocation Method for Handling Integral and Integrodifferential Equations of n-th Order via Certain Combinations of Shifted Legendre Polynomials" published in *Mathematical Problems in Engineering*, **2022**, 2022.

Hereafter, an accurate and efficient numerical method based on spectral collocation is presented to solve integral equations and integro-differential equations of n-th order. The method is developed using compact combinations of shifted Legendre polynomials as a spectral basis and shifted Legendre Gauss Lobatto nodes as collocation points to construct the appropriate algorithm that leads to simple systems easy to solve. The technique treats both types of equations: linear and nonlinear equations. The study aims to provide the relevant spectral basis by the use of compact combinations, allowing us to take advantage of shifted Legendre polynomials and to reduce the dimension of the space of approximation. The reliability of the proposed algorithms is proven via different examples of several cases, and the results are discussed to confirm the effectiveness of the spectral approach.

This chapter is structured as follows: we begin by describing the studied problem in Section 3.1. Making use of some formulas presented in the preliminaries

chapter, we describe the proposed method by characterizing the main steps of the method in Section 3.2. Next, we study separately the linear and the nonlinear cases and we apply the Gauss quadrature in each case. In Section 3.3, several numerical examples are presented and discussed to confirm the reliability of the described method.

3.1 Description of the problem

We are interested in using a shifted-Legendre collocation method to solve the integro-differential equation of n-th order (3.1)

$$a_0(x)u(x) + \sum_{i=1}^{n} a_i(x)u^{(i)}(x) = f(x) + \lambda \int_0^1 \mathscr{K}(x,t)\mathscr{F}(t,u(t))\,\mathrm{d}t, \tag{3.1}$$

joined to the initial conditions (3.2)

$$u^{(j)}(0) = 0, \qquad j = 0, \ldots, n-1, \tag{3.2}$$

where

- $u(x)$ is the unknown function,
- $u^{(i)}(x) = \dfrac{\mathrm{d}^i u(x)}{\mathrm{d}x^i}$ denotes the i-th derivative of $u(x)$,
- $\{a_i(x),\ i = 0, \ldots, n\}$ are given functions in $\mathscr{C}([0,1])$,
- $\mathscr{K}(x,t)$ is the known kernel, which is a continuous and square integrable function,
- $\mathscr{F}$ is a given function of $u(t)$, which can be linear ($\mathscr{F}(t,u(t)) = u(t)$) or nonlinear (the case of $\mathscr{F}(t,u(t)) = (u(t))^s,\ s \neq \{0,1\}$),
- λ is a given constant, and $f \in L^2([0,1])$ a known function.

The order of derivation n denotes the order of the integro-differential equation (3.1); when $a_i(x) = 0,\ (\forall x \in [0,1],\ \forall i = 1, \ldots, n)$, we derive the case of integral equations.

3.2 Shifted Legendre Galerkin method

We define S_N as

$$S_N = span\{\widetilde{\mathscr{L}_0}(x), \widetilde{\mathscr{L}_1}(x), \ldots, \widetilde{\mathscr{L}_N}(x)\}$$

where $\{\widetilde{\mathscr{L}_k}(x),\ k = 0, \ldots, N\}$ are the shifted Legendre polynomials defined on $[0, 1]$.

We set $V_N \subset S_N$, the subspace where the initial conditions (3.2) are verified

$$V_N = \{v \in S_N \ such\ that\ v^{(j)}(0) = 0\ for\ j = 0, \ldots, n-1\}$$

The spectral scheme to solve (3.1) is to find $u_N \in V_N$ such that for all $v \in V_N$

$$\begin{aligned} &\langle a_0(x)u_N(x), v(x)\rangle + \sum_{i=1}^{n}\langle a_i(x)u_N^{(i)}(x), v(x)\rangle \\ &= \\ &\langle f(x), v(x)\rangle + \lambda\langle \int_0^1 \mathscr{K}(x,t)\mathscr{F}(t, u_N(t))\ dt, v(x)\rangle \end{aligned} \tag{3.3}$$

where $\langle u, v\rangle = \int_0^1 u(x)v(x)\ \mathrm{d}x$ denotes the inner product in the space $L^2(0, 1)$.

When applying a spectral method, one considers the choice of an appropriate basis to ensure that the obtained system is as simple as possible. Therefore, we aim to use compact combinations of orthogonal polynomials as basis functions to enhance efficiency. Numerous studies have developed various combinations for different equations [24, 69, 91, 82, 14]. The selection of orthogonal polynomials as basis functions allows us to leverage their advantages, particularly as a Hilbert basis for $L^2(I)$. Moreover, opting for compact combinations of orthogonal polynomials, not only allows us to benefit from these orthogonal polynomials but also reduces the dimension of the space of approximation from $(N+1)$ to $(N-n+1)$.

3.2.1 The choice of basis functions

In this study, we opt for a spectral basis composed of shifted Legendre polynomials of the form

$$\phi_k(x) = \widetilde{\mathscr{L}_k}(x) + \sum_{i=1}^{n}\alpha_{ik}\widetilde{\mathscr{L}_{k+i}}(x), \qquad k = 0, \ldots, N-n. \tag{3.4}$$

The coefficients $\{\alpha_{ik}\}$ are calculated in such a way that $\phi_k(x)$ satisfies the initial conditions (3.2), indicating that

$$\phi_k^{(j)}(0) = 0, \quad j = 0, \ldots, n-1, \quad k = 0, \ldots, N-n$$

Therefore

$$\widetilde{\mathscr{L}}_k^{(j)}(0) + \sum_{i=1}^{n} \alpha_{ik}\, \widetilde{\mathscr{L}}_{k+i}^{(j)}(0) = 0, \quad j = 0, \ldots, n-1, \quad k = 0, \ldots, N-n. \tag{3.5}$$

Considering the significant properties of shifted Legendre polynomials, derived from those of Legendre polynomials (1.12)− (1.19), the basis coefficients are determined by the following system

$$\begin{cases} \displaystyle\sum_{i=1}^{n} (-1)^i \alpha_{ik} = -1, \qquad j = 0 \\ \displaystyle\sum_{i=1}^{n} \alpha_{ik} \left((-1)^i \prod_{m=0}^{j-1} (k+i-m)(k+i+m+1) \right) = -\prod_{m=0}^{j-1} (k-m)(k+m+1), \\ \qquad\qquad j = 1, \ldots, n-1. \end{cases} \tag{3.6}$$

Remark 3.1 *If $u^{(j)}(0) = c_j,\ c_j \neq 0$ for a certain $j \in \{0, \ldots, n-1\}$, we move to homogeneous initial conditions through a suitable change of variables.*

The determinant of system (3.6) being different from zero leads to the derivation of specific cases

- When $n = 1$, we have $\alpha_{1k} = 1$.
- When $n = 2$, the system (3.5) takes the form

$$\begin{cases} \widetilde{\mathscr{L}_k}(0) + \alpha_{1,k} \widetilde{\mathscr{L}_{k+1}}(0) + \alpha_{2,k} \widetilde{\mathscr{L}_{k+2}}(0) = 0, \\ \widetilde{\mathscr{L}_k^{(1)}}(0) + \alpha_{1,k} \widetilde{\mathscr{L}_{k+1}^{(1)}}(0) + \alpha_{2,k} \widetilde{\mathscr{L}_{k+2}^{(1)}}(0) = 0; \end{cases} \tag{3.7}$$

  which can be simplified using Legendre polynomials properties to

$$\begin{cases} (-1)^k + \alpha_{1,k}(-1)^{k+1} + \alpha_{2,k}(-1)^{k+2} = 0, \\ \dfrac{k(k+1)}{2}(-1)^{k+1} + \alpha_{1,k} \dfrac{(k+1)(k+2)}{2}(-1)^{k+2} \\ \qquad\qquad + \alpha_{2,k} \dfrac{(k+2)(k+3)}{2}(-1)^{k+3} = 0. \end{cases} \tag{3.8}$$

So, we obtain

$$\alpha_{1k} = \frac{2k+3}{k+2}, \quad \alpha_{2k} = \frac{k+1}{k+2}.$$

- When $n = 3$, the system (3.5) takes the form

$$\begin{cases} \widetilde{\mathscr{L}_k}(0) + \alpha_{1k}\widetilde{\mathscr{L}_{k+1}}(0) + \alpha_{2k}\widetilde{\mathscr{L}_{k+2}}(0) + \alpha_{3k}\widetilde{\mathscr{L}_{k+3}}(0) = 0, \\ \widetilde{\mathscr{L}_k^{(1)}}(0) + \alpha_{1k}\widetilde{\mathscr{L}_{k+1}^{(1)}}(0) + \alpha_{2k}\widetilde{\mathscr{L}_{k+2}^{(1)}}(0) + \alpha_{3k}\widetilde{\mathscr{L}_{k+3}}(0) = 0, \\ \widetilde{\mathscr{L}_k^{(2)}}(0) + \alpha_{1k}\widetilde{\mathscr{L}_{k+1}^{(2)}}(0) + \alpha_{2k}\widetilde{\mathscr{L}_{k+2}^{(2)}}(0) + \alpha_{3k}\widetilde{\mathscr{L}_{k+3}}(0) = 0. \end{cases} \tag{3.9}$$

Using (1.19), we obtain

$$\alpha_{1k} = \frac{3(2k+3)}{2k+5}, \quad \alpha_{2k} = \frac{3(k+1)}{k+3}, \quad \alpha_{3k} = \frac{(k+1)(2k+3)}{(k+3)(2k+5)}.$$

It is obvious that the set $\{\phi_k(x)\}$ is linearly independent, and $\dim(V_N) = N - n + 1$. Therefore, we have $V_N = span\{\phi_k(x), k = 0, \ldots, N-n\}$. Consequently, our approximation can be expressed in the following form

$$u_N(x) = \sum_{k=0}^{N-n} \hat{u}_k \phi_k(x).$$

3.2.2 Resolution of the system

The spectral scheme (3.3) becomes for $j = 0, \ldots, N-n$

$$\begin{aligned} &\langle a_0(x) \sum_{k=0}^{N-n} \hat{u}_k \phi_k(x), \phi_j(x)\rangle + \sum_{i=1}^{n} \langle a_i(x) \left(\sum_{k=0}^{N-n} \hat{u}_k \phi_k(x) \right)^{(i)}, \phi_j(x)\rangle \\ &= \\ &\langle f(x), \phi_j(x)\rangle + \lambda \langle \int_0^1 \mathscr{K}(x,t) \mathscr{F}\left(t, \sum_{k=0}^{N-n} \hat{u}_k \phi_k(t) \right) \mathrm{d}t, \phi_j(x)\rangle. \end{aligned} \tag{3.10}$$

With some simplifications (3.10) can be written in a final form as

$$\begin{aligned} &\sum_{k=0}^{N-n} \hat{u}_k \langle a_0(x)\phi_k(x), \phi_j(x)\rangle + \sum_{k=0}^{N-n} \hat{u}_k \sum_{i=1}^{n} \langle a_i(x)\phi_k^{(i)}(x), \phi_j(x)\rangle \\ &= \\ &\langle f(x), \phi_j(x)\rangle + \lambda \langle \int_0^1 \mathscr{K}(x,t) \mathscr{F}\left(t, \sum_{k=0}^{N-n} \hat{u}_k \phi_k(t) \right) \mathrm{d}t, \phi_j(x)\rangle. \end{aligned} \tag{3.11}$$

At this stage, we consider the two cases depending on the linearity/nonlinearity of $\mathscr{F}(t, u(t))$.

- **Linear case:**
  We assume that $\mathscr{F}(t, u(t)) = u(t)$. Then, (3.11) becomes for all $j = 0, \ldots, N-n$

$$\begin{aligned} &\sum_{k=0}^{N-n} \hat{u}_k \langle a_0(x)\phi_k(x), \phi_j(x)\rangle + \sum_{k=0}^{N-n} \hat{u}_k \sum_{i=1}^{n} \langle a_i(x)\phi_k^{(i)}(x), \phi_j(x)\rangle \\ &\qquad = \\ &\langle f(x), \phi_j(x)\rangle + \lambda \sum_{k=0}^{N-n} \hat{u}_k \langle \int_0^1 \mathscr{K}(x,t)\phi_k(t)\, \mathrm{d}t, \phi_j(x)\rangle. \end{aligned} \tag{3.12}$$

  By setting the following notations

$$\mathbf{f} = (f_0, f_1, \ldots, f_{N-n})^T, \qquad f_j = \langle f(x), \phi_j(x)\rangle;$$

$$\mathbf{U} = (\hat{u}_1, \hat{u}_2, \ldots, \hat{u}_{N-n})^T, \qquad u_N(x) = \sum_{k=0}^{N-n} \hat{u}_k \phi_k(x);$$

$$\mathbf{A}_0 = (a_{jk}^0)_{0\le j,k\le N-n}, \qquad a_{jk}^0 = \langle a_0(x)\phi_k(x), \phi_j(x)\rangle;$$

$$\mathbf{A}_{i,n} = (a_{jk}^{i,n})_{0\le j,k\le N-n}, \qquad a_{jk}^{i,n} = \langle a_i(x)\phi_k^{(i)}(x), \phi_j(x)\rangle;$$

$$\mathbf{M} = (m_{jk})_{0\le j,k\le N-n}, \qquad m_{jk} = \langle \int_0^1 \mathscr{K}(x,t)\phi_k(t)\, \mathrm{d}t, \phi_j(x)\rangle,$$

  the spectral scheme (3.12) is equivalent to the following linear system of matrix form

$$(\mathbf{A}_0 + \sum_{i=1}^{n} \mathbf{A}_{i,n} - \lambda \mathbf{M})\mathbf{U} = \mathbf{f}. \tag{3.13}$$

- **Nonlinear case:**
  By taking $\mathscr{F}(t, u(t))$ of a nonlinear form as $\mathscr{F}(t, u(t)) = (u(t))^s,\ s \neq \{0, 1\}$, then (3.11) becomes

$$\begin{aligned} &\sum_{k=0}^{N-n} \hat{u}_k \langle a_0(x)\phi_k(x), \phi_j(x)\rangle + \sum_{k=0}^{N-n} \hat{u}_k \sum_{i=1}^{n} \langle a_i(x)\phi_k^{(i)}(x), \phi_j(x)\rangle \\ &\qquad = \\ &\langle f(x), \phi_j(x)\rangle + \lambda \langle \int_0^1 \mathscr{K}(x,t) \left(\sum_{k=0}^{N-n} \hat{u}_k \phi_k(t) \right)^s \mathrm{d}t, \phi_j(x)\rangle; \end{aligned} \tag{3.14}$$

We define $\mathscr{G}$ as a vectorial function by

$$\mathscr{G} = (\mathscr{G}_0(\hat{u}_0, \ldots, \hat{u}_{N-n}), \mathscr{G}_1(\hat{u}_0, \ldots, \hat{u}_{N-n}), \ldots, \mathscr{G}_{N-n}(\hat{u}_0, \ldots, \hat{u}_{N-n}))^{\mathrm{T}}$$

where

$$\begin{aligned}\mathscr{G}_j(\hat{u}_0, \ldots, \hat{u}_{N-n}) = \sum_{k=0}^{N-n} \hat{u}_k \left(\langle a_0(x)\phi_k(x), \phi_j(x)\rangle + \sum_{i=1}^{n} \langle a_i(x)\phi_k^{(i)}(x), \phi_j(x)\rangle \right) \\ - \langle f(x), \phi_j(x)\rangle - \lambda \langle \int_0^1 \mathscr{K}(x,t) \left(\sum_{k=0}^{N-n} \hat{u}_k \phi_k(t) \right)^s \mathrm{d}t, \phi_j(x)\rangle.\end{aligned} \tag{3.15}$$

The Jacobian matrix of $\mathscr{G}$ is given by

$$\boldsymbol{J}_{\mathscr{G}}(\hat{u}_0, \ldots, \hat{u}_{N-n}) = (J_{jk}), \quad 0 \leq j, k \leq N-n$$

$$J_{jk} = \frac{\partial \mathscr{G}_j(\hat{u}_0, \ldots, \hat{u}_{N-n})}{\partial \hat{u}_k},$$

where

$$\begin{aligned}J_{jk} = \langle a_0(x)\phi_k(x), \phi_j(x)\rangle + \sum_{i=1}^{n} \langle a_i(x)\phi_k^{(i)}(x), \phi_j(x)\rangle \\ - \lambda \langle \int_0^1 \mathscr{K}(x,t) s\phi_k(t) \left(\sum_{k=0}^{N-n} \hat{u}_k \phi_k(t) \right)^{s-1} \mathrm{d}t, \phi_j(x)\rangle.\end{aligned} \tag{3.16}$$

3.2.3 Gauss-Lobatto quadrature

The coupling of the Galerkin method with numerical integration methods aims to preserve the advantages of both methods. Integrals appearing in the weak formulation of the problem are efficiently approximated by a quadrature formula. Hereafter, we denote the Legendre-Gauss-Lobatto nodes of $[-1, 1]$ by x_p with their respective weights w_p as defined in (1.41). When moving to $[0, 1]$ we can define the shifted Legendre-Gauss-Lobatto nodes (SLGL) with their respective weights as

$$\overline{x_p} = \frac{1}{2}(x_p + 1), \qquad \overline{w_p} = \frac{1}{2} w_p. \tag{3.17}$$

- **Linear case:**

  By utilizing Gauss-Lobatto integration (1.39) to evaluate the integrals appearing the formula (3.12) in the shifted Legendre-Gauss-Lobatto nodes (3.17), (3.12) becomes for all $j = 0, \ldots, N-n$

$$\sum_{k=0}^{N-n} \hat{u}_k \sum_{p=0}^{N_x} a_0(\overline{x_p})\phi_k(\overline{x_p})\phi_j(\overline{x_p})\overline{w_p} + \sum_{k=0}^{N-n} \hat{u}_k \sum_{i=1}^{n} \sum_{p=0}^{N_x} a_i(\overline{x_p})\phi_k^{(i)}(\overline{x_p})\phi_j(\overline{x_p})\overline{w_p}$$
$$=$$
$$\sum_{p=0}^{N_x} f(\overline{x_p})\phi_j(\overline{x_p})\overline{w_p} + \lambda \sum_{k=0}^{N-n} \hat{u}_k \sum_{p=0}^{N_x} \sum_{q=0}^{Nx} \mathscr{K}(\overline{x_p}, \overline{x_q})\phi_k(\overline{x_q})\phi_j(\overline{x_p})\overline{w_q}\ \overline{w_p}, \tag{3.18}$$

  which leads to matrix system (3.13), with

$$f_j = \sum_{p=0}^{N_x} f(\overline{x_p})\phi_j(\overline{x_p})\overline{w_p};$$

$$a_{jk}^0 = \sum_{p=0}^{N_x} a_0(\overline{x_p})\phi_k(\overline{x_p})\phi_j(\overline{x_p})\overline{w_p};$$

$$a_{jk}^{i,n} = \sum_{p=0}^{N_x} a_i(\overline{x_p})\phi_k^{(i)}(\overline{x_p})\phi_j(\overline{x_p})\overline{w_p};$$

$$m_{jk} = \sum_{p=0}^{N_x} \sum_{q=0}^{Nx} \mathscr{K}(\overline{x_p}, \overline{x_q})\phi_k(\overline{x_q})\phi_j(\overline{x_p})\overline{w_q}\ \overline{w_p}.$$

  To solve (3.13) in both cases, we proceed with the Gauss elimination method.

- **Nonlinear case:**

  The formula (3.15) becomes for all $j = 0, \ldots, N-n$

$$\begin{aligned}\mathscr{G}_j(\hat{u}_0, \ldots, \hat{u}_{N-n}) = &\sum_{k=0}^{N-n} \hat{u}_k \sum_{p=0}^{N_x} a_0(\overline{x_p})\phi_k(\overline{x_p})\phi_j(\overline{x_p})\overline{w_p} \\ &+ \sum_{k=0}^{N-n} \hat{u}_k \sum_{i=1}^{n} \sum_{p=0}^{N_x} a_i(\overline{x_p})\phi_k^{(i)}(\overline{x_p})\phi_j(\overline{x_p})\overline{w_p} - \sum_{p=0}^{N_x} f(\overline{x_p})\phi_j(\overline{x_p})\overline{w_p} \\ &- \lambda \sum_{p=0}^{N_x} \sum_{q=0}^{Nx} \mathscr{K}(\overline{x_p}, \overline{x_q}) \left(\sum_{k=0}^{N-n} \hat{u}_k \phi_k(\overline{x_q}) \right)^s \phi_j(\overline{x_p})\overline{w_q}\ \overline{w_p},\end{aligned} \tag{3.19}$$

and the Jacobian matrix of $\mathscr{G}$

$$\boldsymbol{J}_{\mathscr{G}}(\hat{u}_0,\ldots,\hat{u}_{N-n}) = (J_{jk}), \quad 0 \le j,k \le N-n$$

$$J_{jk} = \frac{\partial \mathscr{G}_j(\hat{u}_0,\ldots,\hat{u}_{N-n})}{\partial \hat{u}_k},$$

where

$$J_{jk} = \sum_{p=0}^{N_x} a_0(\overline{x_p})\phi_k(\overline{x_p})\phi_j(\overline{x_p})\overline{w_p} + \sum_{i=1}^{n}\sum_{p=0}^{N_x} a_i(\overline{x_p})\phi_k^{(i)}(\overline{x_p})\phi_j(\overline{x_p})\overline{w_p}$$
$$- \lambda \sum_{p=0}^{N_x}\sum_{q=0}^{N_x} \mathscr{K}(\overline{x_p},\overline{x_q})\, s\, \phi_k(\overline{x_q}) \left(\sum_{k=0}^{N-n} \hat{u}_k\phi_k(\overline{x_q})\right)^{s-1} \phi_j(\overline{x_p})\overline{w_q}\ \overline{w_p}, \tag{3.20}$$

Now, to solve (3.15)-(3.16) and (3.19)-(3.20) we use the following Newton algorithm:

- Initialisation: Let be $\epsilon > 0$, an initial vector

  $$U^0 = (\hat{u}_0^0, \hat{u}_1^0, \ldots, \hat{u}_{N-n}^0)$$

  and

  $$\mathscr{G}^0 = \Big(\mathscr{G}_0(\hat{u}_0^0,\ldots,\hat{u}_{N-n}^0), \mathscr{G}_1(\hat{u}_0^0,\ldots,\hat{u}_{N-n}^0), \ldots, \mathscr{G}_{N-n}(\hat{u}_0^0,\ldots,\hat{u}_{N-n}^0)\Big)^{\mathrm{T}}$$

- Iteration: Solve

  $$\boldsymbol{J}_{\mathscr{G}}(U^{m+1} - U^m) = -\mathscr{G}^m.$$

- Stop: If $\|U^{m+1} - U^m\| < \epsilon$, stop the iteration.

3.3 Numerical results

In this section, various examples are presented for discussion to illustrate the effectiveness of the described method. To compare the exact solution $u(x)$ with the approximate solution $u_N(x)$, we calculate the absolute error $\mathscr{E}$ (2.28), the maximum error norm $\mathscr{E}_{max}$ (2.29), the square error norm $\mathscr{E}_2$ (2.30), and the relative

error norm $\mathscr{E}_{re}$ (2.31). To demonstrate the exponential convergence of the method, the numerical rate of convergence (the Log slope coefficient according to relative error), $\mathscr{NRC}$ is calculated using the following formula

$$\mathscr{NRC} = \frac{\log(\mathscr{E}_{re}(N_1)) - \log(\mathscr{E}_{re}(N_2))}{\log(N_1) - \log(N_2)}, \tag{3.21}$$

where $\mathscr{E}_{re}(N_1)$ (resp. $\mathscr{E}_{re}(N_2)$) denotes the relative error calculated for $N = N_1$ (resp. $N = N_2$), and $N_2 = N_1 + 2,\ N_1 \geq 2$.
By applying the described method in this paper, we obtain systems of linear and nonlinear equations that can be solved directly by Gauss elimination or by Newton's algorithm, respectively. Several results are presented in tables and figures below to confirm the accuracy of our method.
All results are obtained for $N_x = 50$, and CPU-time is given in seconds. For Newton's method, ϵ is taken 10^{-10}, and the maximum number of iterations is set to be 5.

Example 3.1 *Consider the following nonlinear integral equation*

$$u(x) = -x^2 - \frac{x}{3}(2\sqrt{2} - 1) + 2 + \int_0^1 xt\sqrt{u(t)}\mathrm{d}t. \tag{3.22}$$

The exact solution is $u(x) = 2 - x^2$.
Error values were calculated for different $N \geq 2$, *and we obtain* $\mathscr{E}(x) = 0$, *for all* x *in* $[0, 1]$.

Example 3.2 *Consider the following nonlinear integral equation*

$$u(x) = \sqrt{x+1} - (\mathrm{e} - 1)\sinh(\xi x - 1) + \int_0^1 \sinh(\xi x - 1)\cosh(t - 1)u^2(t)\ \mathrm{d}t, \tag{3.23}$$

where $\xi = \sqrt{2}$. *The exact solution is* $u(x) = \sqrt{x+1}$.

Discussion: Table 3.1 displays various types of approximation errors ($\mathscr{E}_{max}$, $\mathscr{E}_2$ and $\mathscr{E}_{re}$) calculated for increasing values of N, reaching the order of 10^{-16} for $N = 18$. Figure 3.1 illustrates the behaviour of the absolute error for $N = 18$. The obtained results in Table 3.1 and Figure 3.1 are consistent with the values of the numerical rate of convergence $\mathscr{NRC}$, reflecting the exponential convergence.

Table 3.1: $\mathscr{E}_{max}$, $\mathscr{E}_2$, $\mathscr{E}_{re}$ and $\mathscr{NRC}$ for different N and respective CPU-time for Example 3.2

N	$\mathscr{E}_{max}$	$\mathscr{E}_2$	$\mathscr{E}_{re}$	$\mathscr{NRC}$	CPU-time
2	1.30657e − 02	5.52993e − 03	4.46979e − 03	/	10.042
4	1.69372e − 04	5.43398e − 05	4.39223e − 05	−6.6691	24.346
6	3.20565e − 06	8.93187e − 07	7.21954e − 07	−10.132	49.403
8	6.95769e − 08	1.79229e − 08	1.44869e − 08	−13.586	116.59
10	1.62236e − 09	3.99763e − 10	3.23124e − 10	−17.042	210.63
12	3.95414e − 11	9.46293e − 12	7.64880e − 12	−20.532	356.24
14	9.93205e − 13	2.30971e − 13	1.86691e − 13	−24.085	570.10
16	2.55351e − 14	5.71509e − 15	4.61945e − 15	−27.702	885.40
18	8.88178e − 16	2.00619e − 16	1.62158e − 16	−28.437	1329.3

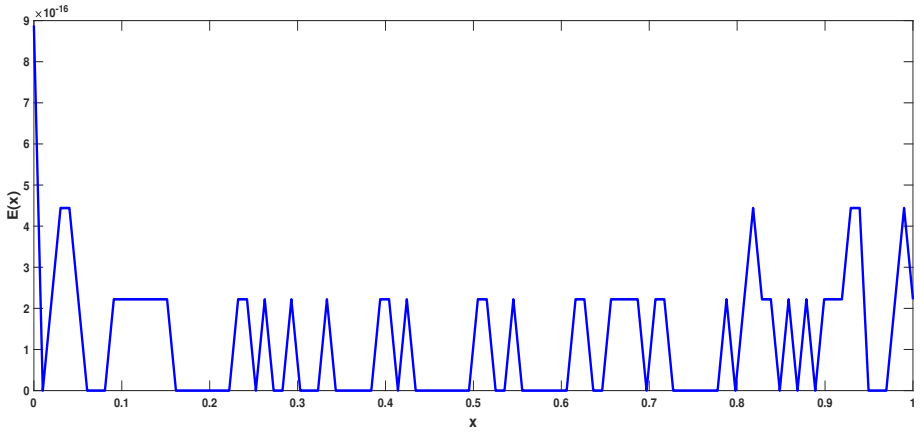

Figure 3.1: Absolute error curve for $N = 18$ for Example 3.2

Example 3.3 *Let's consider the following linear first-order Fredholm integro-differential equation*

$$u'(x) = \mathrm{e}^x - x + x\mathrm{e}^x + \int_0^1 xu(t)\,\mathrm{d}t, \tag{3.24}$$

with the initial condition $u(0) = 0$. *The exact solution is* $u(x) = x\mathrm{e}^x$.

Discussion: Table 3.2 presents some values of the exact solution and the approximate solution calculated in different nodes on $[0, 1]$. The technique is applied using $N = 7$. The absolute error is also calculated for each node and has an order of approximately 10^{-8} all over $[0, 1]$, confirming the global character of the method.

Table 3.2: Exact and approximate solution values in different nodes on $[0, 1]$ when $N = 7$ for Example 3.3

x	Exact solution	Approximate solution	$\mathscr{E}(x)$
0.2	2.442805e − 01	2.442806e − 01	7.099942e − 07
0.4	5.697298e − 01	5.697299e − 01	8.840336e − 08
0.6	1.093271e + 00	1.093271e + 00	8.013137e − 08
0.8	1.780432e + 00	1.780432e + 00	1.056572e − 07
1	2.718281e + 00	2.718281e + 00	1.260678e − 07

Example 3.4 *We consider the following nonlinear first-order Fredholm integro-differential equation of the form*

$$xu'(x) - u(x) = -\frac{1}{6} + \frac{4}{5}x^2 + \int_0^1 (x^2 + t)u^2(t)\,\mathrm{d}t, \tag{3.25}$$

with the initial condition $u(0) = 0$. *The exact solution is* $u(x) = x^2$.

Discussion: Table 3.3 outlines two types of approximation error $\mathscr{E}_2$ and $\mathscr{E}_{re}$ calculated for different values of N from 2 to 8. The values of error are highly accurate, reaching 10^{-17}. These results are of great effectiveness since we obtain this level of accuracy in just under 30 seconds.

Table 3.3: $\mathscr{E}_2$ and $\mathscr{E}_{re}$ for different N and CPU-time for Example 3.4

N	$\mathscr{E}_2$	$\mathscr{E}_{re}$	CPU-time
2	6.86325e − 14	1.49646e − 13	4.2502
4	9.58120e − 15	2.08908e − 14	9.9383
6	4.43580e − 17	9.67181e − 17	18.025
8	5.50628e − 17	1.20059e − 16	29.195

Example 3.5 *We consider the following nonlinear first-order Fredholm integro-differential equation of the form*

$$u'(x) + u(x) = \frac{1}{2}(\mathrm{e}^{-2} - 1) + \int_0^1 u^2(t)\ \mathrm{d}t, \tag{3.26}$$

with the initial condition $u(0) = 1$. *The exact solution is* $u(x) = \mathrm{e}^{-x}$.

Discussion: Table 3.4 provides the values of the exact solution and the approximate solution calculated for different values of x over the interval $[0, 1]$. The corresponding values of the absolute error show a type of homogeneity everywhere in $[0, 1]$. This confirms that the used technique approximates the solution in the same way throughout the interval, illustrating the global character of spectral methods.
Figure 3.2 depicts the behaviour of the logarithmic maximum absolute error according to different increasing values of N. We observe that the different values of the approximation error drop from 10^{-2} to 10^{-12} between $N = 2$ and $N = 10$, reflecting the exponential convergence of the method.

Table 3.4: Exact and approximate solution values in different nodes on $[0, 1]$ when $N = 10$ for Example 3.5

x	Exact solution	Approximate solution	$\mathscr{E}(x)$
0.1	$-9.51625\mathrm{e}-02$	$-9.51625\mathrm{e}-02$	$6.39766\mathrm{e}-15$
0.2	$-1.81269\mathrm{e}-01$	$-1.81269\mathrm{e}-01$	$7.66053\mathrm{e}-15$
0.4	$-3.29679\mathrm{e}-01$	$-3.29679\mathrm{e}-01$	$3.79141\mathrm{e}-14$
0.5	$-3.93469\mathrm{e}-01$	$-3.93469\mathrm{e}-01$	$5.01265\mathrm{e}-14$
0.7	$-5.03414\mathrm{e}-01$	$-5.03414\mathrm{e}-01$	$7.89368\mathrm{e}-14$
0.8	$-5.50671\mathrm{e}-01$	$-5.50671\mathrm{e}-01$	$9.38138\mathrm{e}-14$

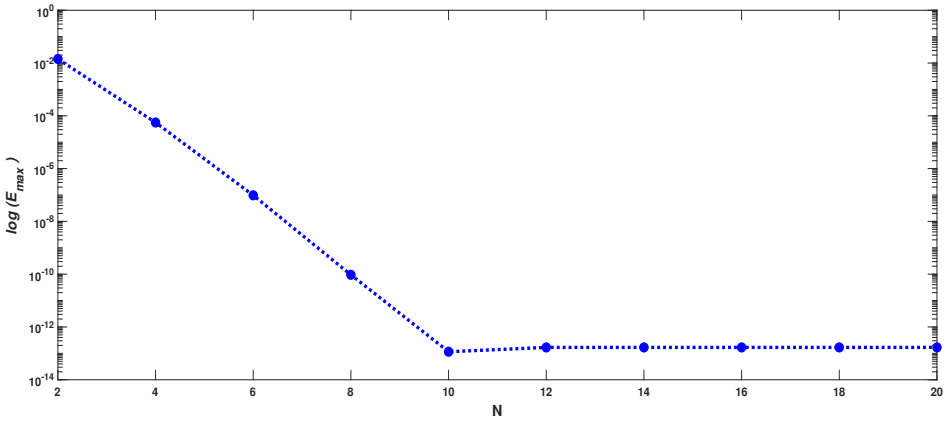

Figure 3.2: Logarithmic maximum absolute error curve for different values of N for Example 3.5

Example 3.6 *We consider the following nonlinear second order Fredholm integro-differential equation of the form*

$$u''(x) + xu'(x) - xu(x) = \mathrm{e}^x - \sin(x) + \int_0^1 \sin(x)\mathrm{e}^{-2t}u^2(t)\,\mathrm{d}t, \tag{3.27}$$

with the initial condition $u(0) = u'(0) = 1$. *The exact solution is* $u(x) = \mathrm{e}^x$.

Discussion: Table 3.5 covers all the diverse types of errors values calculated using $N = 2$ to $N = 14$. The results show great efficiency while approximating by using small values of N. The numerical rate of convergence $\mathscr{NRC}$ confirms the exponential convergence of the method.
Figure 3.3 compares different values of absolute error calculated for different nodes on $[0, 1]$ when $N = 4, 8, 16$. The error is of 10^{-16} order for $N = 16$. The results confirm the accuracy of the method, especially when just taking small values of N.

Table 3.5: $\mathscr{E}_{max}$, $\mathscr{E}_2$ and $\mathscr{E}_{re}$ and $\mathscr{NRC}$ for different N and respective CPU-time for Example 3.6

N	$\mathscr{E}_{max}$	$\mathscr{E}_2$	$\mathscr{E}_{re}$	$\mathscr{NRC}$	CPU-time
2	3.36141e − 01	1.73884e − 01	5.59325e − 01	/	3.3138
4	4.66519e − 03	2.66201e − 03	8.56278e − 03	−6.029	9.0975
6	1.72096e − 05	9.92601e − 06	3.19284e − 05	−13.790	22.375
8	2.86663e − 08	1.65973e − 08	5.33876e − 08	−22.222	67.270
10	2.72220e − 11	1.57900e − 10	5.07908e − 10	−20.861	172.55
12	1.66533e − 14	9.68711e − 15	3.11600e − 14	−53.196	338.74
14	6.66133e − 16	2.59410e − 16	8.34430e − 16	−23.484	581.84

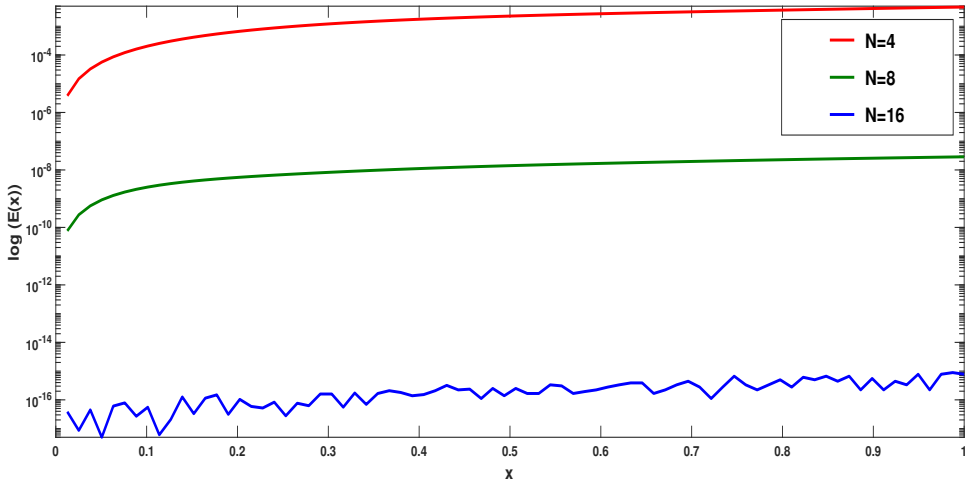

Figure 3.3: Logaritmic absolute error curve for different values of N for Example 3.6

3.4 Concluding remarks

To summarize, the shifted Legendre spectral method is employed to find approximate solutions for both linear and nonlinear integral equations as well as for Fredholm integro-differential equations of n-th order with the initial condition.

Leveraging important properties of shifted Legendre polynomials, a new algorithm is developed, characterised by simplicity and effectiveness in achieving accurate results. The reliability of the method is demonstrated through several examples, with error calculations (including absolute error, maximum absolute error, square error norm and relative error) confirming the accuracy and exponential convergence in terms of relative error for each case.

Chapter 4

Fractional integro-differential equations

Chapter 4

Fractional integro-differential equations

The obtained results in this chapter are the subject of an article entitled "Theoretical and Numerical Study for Volterra-Fredholm Fractional Integro-Differential Equations Based on Chebyshev Polynomials of the Third Kind" published in *Complexity*, **2023**, 2023.

We develop an present numerical method for approximating the solutions of fractional integro-differential equations of mixed Volterra-Fredholm type. This method utilizes spectral collocation approach with shifted Chebyshev polynomials of the third kind. The fractional derivative is defined in the Caputo sense, and Chebyshev-Gauss quadrature is employed to improve the accuracy of integrals. Two categories of equations are examined, leading to algebraic systems solvable using the Gauss elimination method for linear equations, and the Newton algorithm for nonlinear ones. Additionally, we conduct an error analysis, evaluating six numerical examples with different error metrics (maximum absolute error, root mean square error and relative error) to compare the approximate with the exact ones. The experimental rate of convergence is also calculated as well. The results affirm the efficiency, applicability, and performance of the proposed numerical approach.

The chapter is organized as follows. In Section 4.1, we introduce the studied problem and some important mathematical concepts essential for the elaboration of the method. Section 4.2 is devoted to developing the numerical method, with the linear and nonlinear cases explored separately in Section 4.2.1 and Section 4.2.2, respectively. Section 4.3 presents error analysis based on certain definitions and useful lemmas. In Section 4.4, we examine numerical examples presenting and discussing the results in a clear manner. Finally, we summarize all details in the conclusion.

4.1 Description of the problem and preliminaries

In this chapter, our focus lies in the numerical study of fractional integro-differential equations of Volterra-Fredholm type

$$ {}^{C}\mathscr{D}^{\alpha}u(x) = g(x)u(x)+f(x)+\int_0^x \mathscr{K}_1(x,t)\ \mathscr{F}_1(t,u(t))\ \mathrm{d}t+\int_0^1 \mathscr{K}_2(x,t)\ \mathscr{F}_2(t,u(t))\ \mathrm{d}t, \tag{4.1} $$

for $0 \leq x \leq 1$ joined to non-local boundary condition

$$ \mathfrak{a}u(0) + \mathfrak{b}u(1) = 0\,; \quad \mathfrak{a},\mathfrak{b} \in \mathbb{R}, \text{ and } \mathfrak{a}+\mathfrak{b} \neq 0, \tag{4.2} $$

where

- $u(x)$ is the unknown function,
- x and t are in $[0,1]$,
- ${}^{C}\mathscr{D}^{\alpha}$ denotes the α-th Caputo fractional derivative of $u(x)$ with $0 < \alpha < 1$,
- $g, f \in \mathscr{C}([0,1],\mathbb{R})$, $\mathscr{K}_1, \mathscr{K}_2 \in \mathscr{C}([0,1]^2,\mathbb{R})$ and $\mathscr{F}_1, \mathscr{F}_2 \in \mathscr{C}([0,1]\times\mathbb{R},\mathbb{R})$ are given functions.

The existence and uniqueness of the solution of equations of this kind has been widely investigated in numerous studies. The approach involves transforming the problem (4.1)−(4.2) into a fractional integral equation and then applying Banach fixed point theorem and Krasnoselskii fixed point theorem. For a more in-depth understanding, interested readers are encouraged to refer to [35, 90, 47, 68, 40].

Now, in order to elaborate a suitable numerical method for this type of equations, we first need to present the necessary definitions and the mathematical tools related to fractional calculus.
Let be $\alpha > 0$ and $\Gamma(\alpha)$ be the gamma Euler function.

Definition 4.1 [44] *The Riemann Liouville fractional integration of order α of a function $\mathfrak{g} \in L[a,b]$ is*

$$\mathrm{J}_a^{\alpha}\mathfrak{g}(x) = \frac{1}{\Gamma(\alpha)}\int_a^x (x-t)^{\alpha-1}\mathfrak{g}(t)\mathrm{d}t,\ x > a.$$

Definition 4.2 [44] *The Riemann Liouville fractional derivative of order α of a function $\mathfrak{g}$ is*

$$\mathscr{D}_a^{\alpha}\mathfrak{g}(x) = \frac{1}{\Gamma(n-\alpha)}\frac{\mathrm{d}^n}{\mathrm{d}x^n}\int_a^x (x-t)^{n-\alpha-1}\mathfrak{g}(t)\mathrm{d}t,\ x > a.$$

where $n = [\alpha] + 1$, $[\alpha]$ denotes the integer part of α.

Definition 4.3 [44] *The Caputo fractional derivative of $\mathfrak{g}(x)$ of order α is*

$$\begin{aligned} {}^{C}\mathscr{D}_a^{\alpha}\mathfrak{g}(x) =& \mathscr{D}_a^{\alpha}\left(\mathfrak{g}(x) - \sum_{\imath=0}^{n-1}\frac{\mathfrak{g}^{\imath}(a)}{\imath!}(x-a)^{\imath}\right), \\ =& \frac{1}{\Gamma(n-\alpha)}\int_a^x (x-t)^{n-\alpha-1}\mathfrak{g}^{(n)}(t)\,\mathrm{d}t, \end{aligned}$$

where $n-1 < \alpha \leq n,\ n \in \mathbb{N}$.

Some of the basic properties are given by

1. $\mathrm{J}^{\alpha}\mathrm{J}^{\nu} = \mathrm{J}^{\alpha+\nu}$,
2. $\mathrm{J}^{\alpha}\mathrm{J}^{\nu} = \mathrm{J}^{\nu}\mathrm{J}^{\alpha}$,
3. $\mathrm{J}^{\alpha}x^{\nu} = \dfrac{\Gamma(1+\nu)}{\Gamma(1+\nu+\alpha)}x^{\nu+\alpha}$,
4. ${}^{C}\mathscr{D}^{\alpha}(\lambda\mathfrak{g}(x)+\delta\mathfrak{f}(x)) = \lambda\cdot{}^{C}\mathscr{D}^{\alpha}\mathfrak{g}(x)+\delta\cdot{}^{C}\mathscr{D}^{\alpha}\mathfrak{f}(x)$, where λ and δ are constants.
5. ${}^{C}\mathscr{D}^{\alpha}\mathfrak{c} = 0, \quad (\mathfrak{c}$ is a constant);

$${}^{C}\mathscr{D}^{\alpha}x^{\nu} = \begin{cases} 0, & \text{for } \nu \in \mathbb{N}_0 \text{ and } \nu < \lceil\alpha\rceil, \\ \dfrac{\Gamma(1+\nu)}{\Gamma(1+\nu-\alpha)}x^{\nu-\alpha}, & \text{for } \nu \in \mathbb{N}_0 \text{ and } \nu \geq \lceil\alpha\rceil \text{ or } \nu \notin \mathbb{N},\ \nu > \lfloor\alpha\rfloor, \end{cases} \tag{4.3}$$

where the integers $\lceil\alpha\rceil, \lfloor\alpha\rfloor$ satisfy $\alpha \leq \lceil\alpha\rceil$ and $\lfloor\alpha\rfloor \leq \alpha$. Also $\mathbb{N} = \{1, 2, \dots\}$ and $\mathbb{N}_0 = \{0, 1, 2, \dots\}$.

For convenience, we define a first approximation of $u(x)$ by considering the first $(N+1)$ terms of shifted Chebyshev polynomials of the third kind

$$u_N(x) = \sum_{k=0}^{N} \hat{u}_k \widetilde{\mathscr{V}_k}(x), \tag{4.4}$$

For the elaboration of the numerical method, some useful theorems are stated below.

Theorem 4.1 [60] *The error of approximation using the first $N+1$ terms of Chebyshev polynomials of the third kind verifies, for $x \in [-1, 1]$*

$$R_N = |u(x) - u_N(x)| \leq \sum_{k=N+1}^{+\infty} |\hat{u}_k|. \tag{4.5}$$

Theorem 4.2 [60] *Let $u \in L^2[0, 1]$ be a twice-differentiable function such that*

$$\exists M > 0\,; \quad \forall x \in [0, 1], \ \ |\vartheta''(x)| < M.$$

Then $u_N(x)$ defined by (4.4) converges uniformly to $u(x)$ defined by (1.34).

Proof 4.1 *Using $2x - 1 = \cos\theta$, the relation (1.36) becomes*

$$\hat{u}_k = \frac{2}{\pi} \int_0^{\pi} u\left(\cos^2\frac{\theta}{2}\right) \cos\left(k + \frac{1}{2}\right)\theta \cos\frac{\theta}{2} \mathrm{d}\theta,$$

and after two integrations by parts, we get

$$\hat{u}_k = \frac{1}{8\pi} \int_0^{\pi} u''\left(\cos^2\frac{\theta}{2}\right) \sin\theta g_k(\theta) \mathrm{d}\theta,$$

where

$$g_k(\theta) = \frac{\sin k\theta}{k(k+1)} - \frac{\sin(k+2)\theta}{(k+1)(k+2)} - \frac{\sin(k-1)\theta}{k(k-1)} + \frac{\sin(k+1)\theta}{k(k+1)}.$$

Then,

$$|\hat{u}_k| \leq \frac{M}{8} \frac{4k^2 + 4k - 2}{(k-1)k(k+1)(k+2)}.$$

From Theorem 4.1,

$$\left| \sum_{k=0}^{+\infty} \hat{u}_k \widetilde{\mathscr{V}_k}(x) - \sum_{k=0}^{N} \hat{u}_k \widetilde{\mathscr{V}_k}(x) \right| \leq \sum_{k=N+1}^{+\infty} \frac{M}{8} \frac{4k^2 + 4k - 2}{(k-1)k(k+1)(k+2)}$$

Hence the uniform convergence.

Theorem 4.3 [83] *Let $u(x)$ be approximated by (4.4), then*

$$ {}^{C}\mathscr{D}^{\alpha}(u_N(x)) = \sum_{k=\lceil\alpha\rceil}^{N} \sum_{\ell=0}^{k-\lceil\alpha\rceil} \hat{u}_k \mathscr{N}_{k,\ell}^{(\alpha)} x^{k-\ell-\alpha}, \tag{4.6} $$

where

$$ \mathscr{N}_{k,\ell}^{(\alpha)} = (-1)^{\ell} 2^{2k-2\ell} \frac{(2k+1)\Gamma(2k-\ell+1)\Gamma(k-\ell+1)}{\Gamma(\ell+1)\Gamma(2k-2\ell+2)\Gamma(k-\ell+1-\alpha)}. \tag{4.7} $$

Proof 4.2 *Making use of the definition of the approximate function $u_N(x)$ defined in (4.4) and taking into account the properties of the fractional derivation in Caputo sense cited before, we can write*

$$ {}^{C}\mathscr{D}^{\alpha}(u_N(x)) = \sum_{k=0}^{N} \hat{u}_k {}^{C}\mathscr{D}^{\alpha}(\widetilde{\mathscr{V}_k}(x)). \tag{4.8} $$

Making use of the linearity of the Caputo derivative and (4.3) allows us to obtain

$$ {}^{C}\mathscr{D}^{\alpha}(\widetilde{\mathscr{V}_k}(x)) = 0,\ k = 0, 1, \ldots, \lceil\alpha\rceil - 1,\ \alpha > 0. \tag{4.9} $$

Also,

$$ {}^{C}\mathscr{D}^{\alpha}(\widetilde{\mathscr{V}_k}(x)) = \sum_{\ell=0}^{k} (-1)^{\ell} \frac{2^{2k-2\ell}(2k+1)\Gamma(2k-\ell+1)}{\Gamma(\ell+1)\Gamma(2k-2\ell+2)} {}^{C}\mathscr{D}^{\alpha} x^{k-\ell}. \tag{4.10} $$

Using again the properties of the Caputo derivative (4.3), (4.10) can be rewritten as

$$ {}^{C}\mathscr{D}^{\alpha}(\widetilde{\mathscr{V}_k}(x)) = \sum_{\ell=0}^{k-\lceil\alpha\rceil} (-1)^{\ell} \frac{2^{2k-2\ell}(2k+1)\Gamma(2k-\ell+1)\Gamma(k-\ell+1)}{\Gamma(\ell+1)\Gamma(2k-2\ell+2)\Gamma(k-\ell+1-\alpha)} x^{k-\ell-\alpha}. \tag{4.11} $$

Now, by combining (4.8), (4.9) and (4.11), we obtain

$$ {}^{C}\mathscr{D}^{\alpha}(u_N(x)) = \sum_{k=\lceil\alpha\rceil}^{N} \sum_{\ell=0}^{k-\lceil\alpha\rceil} \hat{u}_k (-1)^{\ell} \frac{2^{2k-2\ell}(2k+1)\Gamma(2k-\ell+1)\Gamma(k-\ell+1)}{\Gamma(\ell+1)\Gamma(2k-2\ell+2)\Gamma(k-\ell+1-\alpha)} x^{k-\ell-\alpha}, \tag{4.12} $$

which can be simplified to obtain the form (4.6) with (4.7).

4.2 Shifted Chebyshev-Gauss collocation method

In this section, we apply Gauss-collocation method using shifted Chebyshev polynomials of the third kind to solve the problem (4.1)−(4.2) numerically.

4.2.1 Linear case

We assume that $\mathscr{F}_1(t,u(t)) = \mathscr{F}_2(t,u(t)) = u(t)$. By substituting the relation (4.4) into the equation (4.1) and using Theorem 4.3, we obtain

$$\sum_{k=\lceil\alpha\rceil}^{N}\sum_{\ell=0}^{k-\lceil\alpha\rceil}\hat{u}_k\mathscr{N}_{k,\ell}^{(\alpha)}x^{k-\ell-\alpha} = g(x)\sum_{k=0}^{N}\hat{u}_k\widetilde{\mathscr{V}_k}(x) + f(x) + \sum_{k=0}^{N}\hat{u}_k\int_0^x\mathscr{K}_1(x,t)\widetilde{\mathscr{V}_k}(t)\,\mathrm{d}t + \sum_{k=0}^{N}\hat{u}_k\int_0^1\mathscr{K}_2(x,t)\widetilde{\mathscr{V}_k}(t)\,\mathrm{d}t. \tag{4.13}$$

By replacing in (4.13) the variable x by $\mathfrak{m}$ roots $x_\mathfrak{p}$ defined by (1.33), we obtain

$$\sum_{k=\lceil\alpha\rceil}^{N}\sum_{\ell=0}^{k-\lceil\alpha\rceil}\hat{u}_k\mathscr{N}_{k,\ell}^{(\alpha)}x_\mathfrak{p}^{k-\ell-\alpha} = g(x_\mathfrak{p})\sum_{k=0}^{N}\hat{u}_k\widetilde{\mathscr{V}_k}(x_\mathfrak{p}) + f(x_\mathfrak{p}) + \sum_{k=0}^{N}\hat{u}_k\int_0^{x_\mathfrak{p}}\mathscr{K}_1(x_\mathfrak{p},t)\widetilde{\mathscr{V}_k}(t)\,\mathrm{d}t + \sum_{k=0}^{N}\hat{u}_k\int_0^1\mathscr{K}_2(x_\mathfrak{p},t)\widetilde{\mathscr{V}_k}(t)\,\mathrm{d}t. \tag{4.14}$$

Using the change of variable $\tau = \frac{2}{x_\mathfrak{p}}t - 1$ (resp. $\tau = 2t-1$) to move from $[0,x_\mathfrak{p}]$ to $[-1,1]$ (resp. from $[0,1]$ to $[-1,1]$) gives

$$\begin{aligned}\sum_{k=\lceil\alpha\rceil}^{N}\sum_{\ell=0}^{k-\lceil\alpha\rceil}\hat{u}_k\mathscr{N}_{k,\ell}^{(\alpha)}x_\mathfrak{p}^{k-\ell-\alpha} &= g(x_\mathfrak{p})\sum_{k=0}^{N}\hat{u}_k\widetilde{\mathscr{V}_k}(x_\mathfrak{p}) + f(x_\mathfrak{p}) \\ &\quad + \frac{x_\mathfrak{p}}{2}\sum_{k=0}^{N}\hat{u}_k\int_{-1}^{1}\mathscr{K}_1(x_\mathfrak{p},\tfrac{x_\mathfrak{p}}{2}(\tau+1))\widetilde{\mathscr{V}_k}(\tfrac{x_\mathfrak{p}}{2}(\tau+1))\,\mathrm{d}\tau \\ &\quad + \frac{1}{2}\sum_{k=0}^{N}\hat{u}_k\int_{-1}^{1}\mathscr{K}_2(x_\mathfrak{p},\tfrac{1}{2}(\tau+1))\widetilde{\mathscr{V}_k}(\tfrac{1}{2}(\tau+1))\,\mathrm{d}\tau.\end{aligned} \tag{4.15}$$

Using the Gauss-Chebyshev integration formula, we obtain

$$\sum_{k=\lceil\alpha\rceil}^{N}\hat{u}_k\sum_{\ell=0}^{k-\lceil\alpha\rceil}\mathscr{N}_{k,\ell}^{(\alpha)}x_{\mathfrak{p}}^{k-\ell-\alpha}=g(x_{\mathfrak{p}})\sum_{k=0}^{N}\hat{u}_k\widetilde{\mathscr{V}_k}(x_{\mathfrak{p}})+f(x_{\mathfrak{p}})$$
$$+\frac{x_{\mathfrak{p}}}{2}\sum_{k=0}^{N}\hat{u}_k\sum_{\mathfrak{q}=0}^{N}\omega_{\mathfrak{q}}\mathscr{K}_1(x_{\mathfrak{p}},\frac{x_{\mathfrak{p}}}{2}(\tau_{\mathfrak{q}}+1))\widetilde{\mathscr{V}_k}(\frac{x_{\mathfrak{p}}}{2}(\tau_{\mathfrak{q}}+1))\sqrt{\frac{1-\tau_{\mathfrak{q}}}{1+\tau_{\mathfrak{q}}}}$$
$$+\frac{1}{2}\sum_{k=0}^{N}\hat{u}_k\sum_{\mathfrak{q}=0}^{N}\omega_{\mathfrak{q}}\mathscr{K}_2(x_{\mathfrak{p}},\frac{1}{2}(\tau_{\mathfrak{q}}+1))\widetilde{\mathscr{V}_k}(\frac{1}{2}(\tau_{\mathfrak{q}}+1))\sqrt{\frac{1-\tau_{\mathfrak{q}}}{1+\tau_{\mathfrak{q}}}}. \tag{4.16}$$

Here, $\tau_{\mathfrak{q}}$, $\omega_{\mathfrak{q}}$ correspond to the $N+1$ zeros of $\mathscr{V}_{N+1}$ and their respective weights such that

$$\tau_{\mathfrak{q}}=\cos\frac{\left(\mathfrak{q}+\frac{1}{2}\right)\pi}{N+\frac{3}{2}}\quad\text{and}\quad\omega_{\mathfrak{q}}=\frac{\pi}{N+\frac{3}{2}}(1+\tau_{\mathfrak{q}}).$$

From boundary condition (4.2) and approximation (4.4), we have

$$\mathfrak{a}\sum_{k=0}^{N}\hat{u}_k\widetilde{\mathscr{V}_k}(0)+\mathfrak{b}\sum_{k=0}^{N}\hat{u}_k\widetilde{\mathscr{V}_k}(1)=\sum_{k=0}^{N}((-1)^k(2k+1)\mathfrak{a}+\mathfrak{b})\hat{u}_k=0. \tag{4.17}$$

Now, for numerical resolution, we use a Gauss elimination method to solve (4.16)−(4.17).

4.2.2 Nonlinear case

We assume in this case $\mathscr{F}_1(t,u(t))=(u(t))^s$, $\mathscr{F}_2(t,u(t))=(u(t))^r$ where $r,s\neq 1$. By substituting the relation (4.4) into the equation (4.1) and using Theorem 4.3, we obtain

$$\sum_{k=\lceil\alpha\rceil}^{N}\sum_{\ell=0}^{k-\lceil\alpha\rceil}\hat{u}_k\mathscr{N}_{k,\ell}^{(\alpha)}x^{k-\ell-\alpha}=g(x)\sum_{k=0}^{N}\hat{u}_k\widetilde{\mathscr{V}_k}(x)+f(x)$$
$$+\int_0^x\mathscr{K}_1(x,t)\left(\sum_{\imath=0}^{N}\hat{u}_k\widetilde{\mathscr{V}_k}(t)\right)^s\mathrm{d}t$$
$$+\int_0^1\mathscr{K}_2(x,t)\left(\sum_{k=0}^{N}\hat{u}_\imath\widetilde{\mathscr{V}_k}(t)\right)^r\mathrm{d}t. \tag{4.18}$$

Following the same steps described in the linear case, we obtain the scheme

$$\sum_{k=\lceil\alpha\rceil}^{N}\hat{u}_k\sum_{\ell=0}^{k-\lceil\alpha\rceil}\mathscr{N}_{k,\ell}^{(\alpha)}x_{\mathfrak{p}}^{k-\ell-\alpha}=g(x_{\mathfrak{p}})\sum_{k=0}^{N}\hat{u}_k\widetilde{\mathscr{V}}_k(x_{\mathfrak{p}})+f(x_{\mathfrak{p}})$$
$$+\frac{x_{\mathfrak{p}}}{2}\sum_{\mathfrak{q}=0}^{N}\omega_{\mathfrak{q}}\mathscr{K}_1(x_{\mathfrak{p}},\frac{x_{\mathfrak{p}}}{2}(\tau_{\mathfrak{q}}+1))\left(\sum_{\imath=0}^{N}\hat{u}_k\widetilde{\mathscr{V}}_k(\frac{x_{\mathfrak{p}}}{2}(\tau_{\mathfrak{q}}+1))\right)^{s}\sqrt{\frac{1-\tau_{\mathfrak{q}}}{1+\tau_{\mathfrak{q}}}}$$
$$+\frac{1}{2}\sum_{\mathfrak{q}=0}^{N}\omega_{\mathfrak{q}}\mathscr{K}_2(x_{\mathfrak{p}},\frac{1}{2}(\tau_{\mathfrak{q}}+1))\left(\sum_{k=0}^{N}\hat{u}_k\widetilde{\mathscr{V}}_k(\frac{1}{2}(\tau_{\mathfrak{q}}+1))\right)^{r}\sqrt{\frac{1-\tau_{\mathfrak{q}}}{1+\tau_{\mathfrak{q}}}}. \tag{4.19}$$

joined to the initial equation (4.17).
Now, in order to solve (4.19)−(4.17), we use a Newton method. For this, we define $\mathscr{G}$ as a vectorial function

$$\mathscr{G}=(\mathscr{G}_1(\hat{u}_0,\ldots,\hat{u}_N),\mathscr{G}_2(\hat{u}_0,\ldots,\hat{u}_N),\ldots,\mathscr{G}_{N+1}(\hat{u}_0,\ldots,\hat{u}_N))^{\mathrm{T}} \tag{4.20}$$

such that for all $j=1,\ldots,N$

$$\mathscr{G}_j(\hat{u}_0,\ldots,\hat{u}_N)=\sum_{k=\lceil\alpha\rceil}^{N}\hat{u}_k\sum_{\ell=0}^{k-\lceil\alpha\rceil}\mathscr{N}_{k,\ell}^{(\alpha)}x_{\mathfrak{p}}^{k-\ell-\alpha}-g(x_{\mathfrak{p}})\sum_{k=0}^{N}\hat{u}_k\widetilde{\mathscr{V}}_k(x_{\mathfrak{p}})-f(x_{\mathfrak{p}})$$
$$-\frac{x_{\mathfrak{p}}}{2}\sum_{\mathfrak{q}=0}^{N}\omega_{\mathfrak{q}}\mathscr{K}_1(x_{\mathfrak{p}},\frac{x_{\mathfrak{p}}}{2}(\tau_{\mathfrak{q}}+1))\left(\sum_{k=0}^{N}\hat{u}_\imath\widetilde{\mathscr{V}}_k(\frac{x_{\mathfrak{p}}}{2}(\tau_{\mathfrak{q}}+1))\right)^{s}\sqrt{\frac{1-\tau_{\mathfrak{q}}}{1+\tau_{\mathfrak{q}}}}$$
$$-\frac{1}{2}\sum_{\mathfrak{q}=0}^{N}\omega_{\mathfrak{q}}\mathscr{K}_2(x_{\mathfrak{p}},\frac{1}{2}(\tau_{\mathfrak{q}}+1))\left(\sum_{k=0}^{N}\hat{u}_\imath\widetilde{\mathscr{V}}_k(\frac{1}{2}(\tau_{\mathfrak{q}}+1))\right)^{r}\sqrt{\frac{1-\tau_{\mathfrak{q}}}{1+\tau_{\mathfrak{q}}}}. \tag{4.21}$$

and from boundary condition for $j=N+1$

$$\mathscr{G}_{N+1}(\hat{u}_0,\ldots,\hat{u}_N)=\sum_{k=0}^{N}((-1)^k(2k+1)\mathfrak{a}+\mathfrak{b})\hat{u}_k. \tag{4.22}$$

The Jacobian matrix of $\mathscr{G}$ is

$$\boldsymbol{J}_{\mathscr{G}}(\hat{u}_0,\ldots,\hat{u}_N)=\left(\frac{\partial\mathscr{G}_{\mathfrak{p}}(\hat{u}_0,\ldots,\hat{u}_N)}{\partial\hat{u}_k}\right)_{\mathfrak{p}k},$$

where

$$\frac{\partial\mathscr{G}_{\mathfrak{p}}(\hat{u}_0,\ldots,\hat{u}_N)}{\partial\hat{u}_k}=\sum_{\ell=0}^{k-\lceil\alpha\rceil}\mathscr{N}_{k,\ell}^{(\alpha)}x_{\mathfrak{p}}^{k-\ell-\alpha}-g(x_{\mathfrak{p}})\widetilde{\mathscr{V}}_k(x_{\mathfrak{p}})$$

$$- \frac{x_{\mathfrak{p}}}{2} \sum_{\mathfrak{q}=0}^{N} \omega_{\mathfrak{q}} \mathscr{K}_1(x_{\mathfrak{p}}, \frac{x_{\mathfrak{p}}}{2}(\tau_{\mathfrak{q}}+1))\, s\, \widetilde{\mathscr{V}_k}(\frac{x_{\mathfrak{p}}}{2}(\tau_{\mathfrak{q}}+1)) \left(\sum_{i=0}^{N} \hat{u}_i \widetilde{\mathscr{V}_i}(\frac{x_{\mathfrak{p}}}{2}(\tau_{\mathfrak{q}}+1)) \right)^{s-1} \sqrt{\frac{1-\tau_{\mathfrak{q}}}{1+\tau_{\mathfrak{q}}}}$$
$$- \frac{1}{2} \sum_{\mathfrak{q}=0}^{N} \omega_{\mathfrak{q}} \mathscr{K}_2(x_{\mathfrak{p}}, \frac{1}{2}(\tau_{\mathfrak{q}}+1))\, r\, \widetilde{\mathscr{V}_k}(\frac{1}{2}(\tau_{\mathfrak{q}}+1)) \left(\sum_{i=0}^{N} \hat{u}_i \widetilde{\mathscr{V}_i}(\frac{1}{2}(\tau_{\mathfrak{q}}+1)) \right)^{r-1} \sqrt{\frac{1-\tau_{\mathfrak{q}}}{1+\tau_{\mathfrak{q}}}} \tag{4.23}$$

for $\mathfrak{p} = 1, \ldots, N$.

$$\frac{\partial \mathscr{G}_{N+1}(\hat{u}_0, \ldots, \hat{u}_N)}{\partial \hat{u}_k} = (-1)^k (2k+1)\mathfrak{a} + \mathfrak{b}. \tag{4.24}$$

To solve this system of equations, we use a Newton algorithm defined by

- Initialisation: Let be $\epsilon > 0$, $\mathscr{U}^0 = (\hat{u}_0^0, \hat{u}_1^0, \ldots, \hat{u}_N^0)$, and
$$\mathscr{G}^0 = \Big(\mathscr{G}_0(\hat{u}_0^0, \ldots, \hat{u}_N^0), \mathscr{G}_1(\hat{u}_0^0, \ldots, \hat{u}_N^0), \ldots, \mathscr{G}_{N+1}(\hat{u}_0^0, \ldots, \hat{u}_N^0) \Big)^{\mathrm{T}}.$$
- Iteration: Solve
$$\boldsymbol{J}_{\mathscr{G}}(\mathscr{U}^{m+1} - \mathscr{U}^m) = -\mathscr{G}^m.$$
- Stop: If $\|\mathscr{U}^{m+1} - \mathscr{U}^m\| < \epsilon$, stop the iteration.

4.3 Error analysis

In this section, we formulate an error analysis for the proposed method. To begin, we introduce some fundamental definitions and lemmas that will be useful in the following (for more details see [82]). Here, we use $\mathcal{C}$ to denote a generic positive constant independent of N.

4.3.1 Definitions and lemmas

Definition 4.4 *Let $L^2_w(I) = \{u, u \text{ mesurable and } \|u\|_w < \infty\}$, where $I = [0,1]$ is the weighted space with*

$$\langle u, \theta \rangle_w = \int_0^1 u(x)\theta(x)w(x)\, \mathrm{d}x, \quad \|u\|_w = \langle u, u \rangle_w^{1/2}.$$

We define $\Pi_N : L^2_w(I) \to \mathbb{P}_N$ as the orthogonal projection operator such that

$$\langle u - \Pi_N u, \phi \rangle = 0, \quad \forall u \in L^2_w(I),\ \phi \in \mathbb{P}_N.$$

Definition 4.5 *We define*

$$H_w^s(I) = \{u, \partial_x^\imath u \in L_w^2(I),\ 0 \le \imath \le s\}$$

with

$$\|u\|_{s,w} = \left(\sum_{\imath=0}^{s} \|\partial_x^\imath u\|_w^2\right)^{1/2}, \quad |u|_{s,w} = \|\partial_x^s u\|_w,$$

where s is a non-negative integer.

Lemma 4.1 *Assume that $u \in H^s(I)$, and we denote the interpolation of u at the Chebyshev Gauss points by $\mathscr{I}_N u$, which satisfies*

$$\|u - \mathscr{I}_N u\|_{L_w^2(I)} \le \mathcal{C} N^{-s}\ |u|_{H_w^{s,N}(I)} \tag{4.25}$$

$$\|u - \mathscr{I}_N u\|_{L_\infty(I)} \le \mathcal{C} N^{\frac{1}{2}-s}\ |u|_{H_w^{s,N}(I)} \tag{4.26}$$

Lemma 4.2 *Assume that $u \in H_w^s(I)$, and $\mathscr{I}_N u$ denotes the interpolation of u at $(N+1)$ Chebyshev Gauss points corresponding to the weight function $w(x)$, then*

$$\|{}^C\mathscr{D}^\alpha u - \mathscr{I}_N {}^C\mathscr{D}^\alpha u\|_{L_w^2(I)} \le \mathcal{C} N^{-s} |{}^C\mathscr{D}^\alpha u|_{H_w^{s,N}(I)}. \tag{4.27}$$

4.3.2 Error analysis

Here, we present an error analysis of the method described in 4.2.1 by using previous definitions, lemmas and Sobolev inequality.

Theorem 4.4 *Let $u(x)$ be the exact solution of (4.1), which is assumed to be sufficiently smooth, and $\mathscr{I}_N u(x)$ the approximation defined by (4.4) obtained using the scheme (4.16)−(4.17), then*

$$\begin{aligned}\|e(x)\|_{L_w^2(I)} \le \mathcal{C} N^{-s}\Big(&|{}^C\mathscr{D}^\alpha u|_{H_w^{s,N}(I)} + N^{1/2}\,(\lambda_1+\lambda_2+\lambda_3)\,|u|_{H_w^{s,N}(I)} \\ &+ \Big(|g(x)|_{H_w^{s,N}(I)} + |\mathscr{K}_1(x,t)|_{H_w^{s,N}(I)} + |\mathscr{K}_2(x,t)|_{H_w^{s,N}(I)}\Big)\,\|u\|_{L_w^2(I)}\Big).\end{aligned} \tag{4.28}$$

Proof 4.3 *From* (4.1), *we have*

$$ {}^{C}\mathscr{D}^{\alpha}u(x) - g(x)u(x) - f(x) - \int_0^x \mathscr{K}_1(x,t)u(t)\mathrm{d}t - \int_0^1 \mathscr{K}_2(x,t)u(t)\mathrm{d}t = 0. \quad (4.29) $$

Using $\mathscr{I}_N u(x)$, *we obtain*

$$ \begin{aligned} \mathscr{I}_N {}^{C}\mathscr{D}^{\alpha}u(x) - \mathscr{I}_N g(x)\mathscr{I}_N u(x) - f(x) - \int_0^x \mathscr{I}_N\mathscr{K}_1(x,t)\mathscr{I}_N u(t)\,\mathrm{d}t \\ - \int_0^1 \mathscr{I}_N\mathscr{K}_2(x,t)\mathscr{I}_N u(t)\,\mathrm{d}t = 0. \end{aligned} \quad (4.30) $$

By subtracting (4.29) *from* (4.30), *we obtain*

$$ \begin{aligned} e(x) = (\mathscr{I}_N {}^{C}\mathscr{D}^{\alpha}u(x) - {}^{C}\mathscr{D}^{\alpha}u(x)) + g(x)u(x) - \mathscr{I}_N g(x)\mathscr{I}_N u(x) \\ + \int_0^x \mathscr{K}_1(x,t)u(t)\,\mathrm{d}t - \int_0^x \mathscr{I}_N\mathscr{K}_1(x,t)\mathscr{I}_N u(t)\,\mathrm{d}t \\ + \int_0^1 \mathscr{K}_2(x,t)u(t)\,\mathrm{d}t - \int_0^1 \mathscr{I}_N\mathscr{K}_2(x,t)\mathscr{I}_N u(t)\,\mathrm{d}t. \end{aligned} \quad (4.31) $$

$$ \begin{aligned} e(x) = (\mathscr{I}_N {}^{C}\mathscr{D}^{\alpha}u(x) - {}^{C}\mathscr{D}^{\alpha}u(x)) \\ + g(x)(u(x) - \mathscr{I}_N u(x)) + (g(x) - \mathscr{I}_N g(x))\mathscr{I}_{\mathfrak{m}} u(x) \\ + \int_0^x \mathscr{K}_1(x,t)(u(t) - \mathscr{I}_N u(t))\,\mathrm{d}t + \int_0^x (\mathscr{K}_1(x,t) - \mathscr{I}_N\mathscr{K}_1(x,t))\mathscr{I}_N u(t)\,\mathrm{d}t \\ + \int_0^1 \mathscr{K}_2(x,t)(u(t) - \mathscr{I}_N u(t))\,\mathrm{d}t + \int_0^1 (\mathscr{K}_2(x,t) - \mathscr{I}_N\mathscr{K}_2(x,t))\mathscr{I}_N u(t)\,\mathrm{d}t. \end{aligned} \quad (4.32) $$

Then we write

$$ e(x) = \sum_{i=1}^{7} R_i, \quad (4.33) $$

where

$$ \begin{aligned} R_1 &= \mathscr{I}_N {}^{C}\mathscr{D}^{\alpha}u(x) - {}^{C}\mathscr{D}^{\alpha}u(x), \\ R_2 &= g(x)(u(x) - \mathscr{I}_N u(x)), \\ R_3 &= (g(x) - \mathscr{I}_N g(x))\mathscr{I}_N u(x), \\ R_4 &= \int_0^x \mathscr{K}_1(x,t)(u(t) - \mathscr{I}_N u(t))\,\mathrm{d}t, \end{aligned} $$

$$R_5 = \int_0^x (\mathscr{K}_1(x,t) - \mathscr{I}_N\mathscr{K}_1(x,t))\mathscr{I}_N u(t)\,\mathrm{d}t,$$
$$R_6 = \int_0^1 \mathscr{K}_2(x,t)(u(t) - \mathscr{I}_N u(t))\,\mathrm{d}t,$$
$$R_7 = \int_0^1 (\mathscr{K}_2(x,t) - \mathscr{I}_N\mathscr{K}_2(x,t))\mathscr{I}_N u(t)\,\mathrm{d}t.$$

Hence, we get

$$\|e(x)\|_{L_w^2(I)} \leq \sum_{i=1}^{7} \|R_i\|_{L_w^2(I)}. \tag{4.34}$$

From Lemma 4.2

$$\begin{aligned}\|R_1\|_{L_w^2(I)} &= \|\mathscr{I}_N {}^C\mathscr{D}^\alpha u(x) - {}^C\mathscr{D}^\alpha u(x)\| \\ &\leq \mathcal{C}N^{-s}|{}^C\mathscr{D}^\alpha u|_{H_w^{s,N}(I)}.\end{aligned} \tag{4.35}$$

In addition, from Lemma 4.1

$$\begin{aligned}\|R_2\|_{L_w^2(I)} &= \|g(x)(u(x) - \mathscr{I}_N u(x))\| \\ &\leq \lambda_1 \mathcal{C}N^{\frac{1}{2}-s}\ |u|_{H_w^{s,N}(I)}\end{aligned} \tag{4.36}$$

where $\lambda_1 = \max|g(x)|,\ x \in I$. *Also*

$$\begin{aligned}\|R_3\|_{L_w^2(I)} &= \|(g(x) - \mathscr{I}_N g(x))\mathscr{I}_N u(x)\| \\ &\leq \mathcal{C}N^{-s}|g(x)|_{H_w^{s,N}(I)}\ \mathcal{C}\|u\|_{L_w^2(I)} \\ &\leq \mathcal{C}N^{-s}|g(x)|_{H_w^{s,N}(I)}\|u\|_{L_w^2(I)}.\end{aligned} \tag{4.37}$$

Moreover

$$\begin{aligned}\|R_4\|_{L_w^2(I)} &= \|\int_0^x \mathscr{K}_1(x,t)(u(t) - \mathscr{I}_N u(t))\ \mathrm{d}t\|_{L_w^2(I)} \\ &\leq \|\int_0^x \mathscr{K}_1(x,t)(u(t) - \mathscr{I}_N u(t))\ \mathrm{d}t\|_{L_\infty(I)} \\ &\leq \lambda_2 \mathcal{C}N^{\frac{1}{2}-s}\ |u|_{H_w^{s,N}(I)}\end{aligned} \tag{4.38}$$

where $\lambda_2 = \max|\mathscr{K}_1(x,t)|,\ x \in I$. *Furthermore*

$$\|R_5\|_{L_w^2(I)} = \|\int_0^x (\mathscr{K}_1(x,t) - \mathscr{I}_N\mathscr{K}_1(x,t))\mathscr{I}_N u(t)\ \mathrm{d}t\|$$

$$\leq \mathcal{C}N^{-s}|\mathscr{K}_1(x,t)|_{H_w^{s,N}(I)}\ \mathcal{C}\|u\|_{L_w^2(I)}$$
$$\leq \mathcal{C}N^{-s}|\mathscr{K}_1(x,t)|_{H_w^{s,N}(I)}\|u\|_{L_w^2(I)}. \tag{4.39}$$

Also, R_6 and R_7 can be treated the same way, so we obtain

$$\|R_6\|_{L_w^2(I)} \leq \lambda_3 \mathcal{C}N^{\frac{1}{2}-s}\ |u|_{H_w^{s,N}(I)} \tag{4.40}$$

where $\lambda_3 = \max|\mathscr{K}_2(x,t)|,\ x \in I,$

$$\|R_7\|_{L_w^2(I)} \leq \mathcal{C}N^{-s}|\mathscr{K}_2(x,t)|_{H_w^{s,N}(I)}\|u\|_{L_w^2(I)}. \tag{4.41}$$

Combining (4.35)−(4.41)*, we derive the desired estimate.*

4.4 Numerical results

This section presents various examples to illustrate the effectiveness of the described method. Different cases are addressed. To analyse the obtained results, different error values are calculated ($\mathscr{E}$ (2.27), $\mathscr{E}_{max}$ (2.29), $\mathscr{E}_2$ (2.30) and $\mathscr{E}_{re}$ (2.31)). To assess the numerical convergence of the method, the numerical rate of convergence $\mathscr{NRC}$ according to the relative error (3.21) is also computed .

Example 4.1 *We consider a linear Volterra equation*

$${}^C\mathscr{D}^{1/3}u(x) = f(x) + \int_0^x (xt + x^2t^2)\ u(t)\ \mathrm{d}t, \tag{4.42}$$

with the condition

$$\mathfrak{a}u(0) + \mathfrak{b}u(1) = 0, \quad \mathfrak{a} = 1, \mathfrak{b} = 0, \tag{4.43}$$

where

$$f(x) = \frac{3\sqrt{\pi}}{4\Gamma(13/6)}x^{7/6} - \frac{2}{63}x^{9/2}(9 + 7x^2), \tag{4.44}$$

knowing that the exact solution is $u(x) = x^{3/2}$.

Discussion: Table 4.1 provides the values of $\mathscr{E}_2$ and $\mathscr{E}_{re}$ for various values of N ranging from 2 to 22. It also includes the corresponding numerical rate of convergence, which stabilizes around the average value $avg(\mathscr{NRC}) = -1,6695$. The significance of this value is demonstrated differently in Figure 4.1, depicting

the behaviour of the relative error values $\mathscr{E}_{re}$ with relation to N is illustrated in comparison with the values of $N^{\mathscr{NRC}}$. Both curves exhibits a similar decreasing trend, confirming the linear convergence of the approximate solution to the exact solution.

Table 4.1: $\mathscr{E}_2$, $\mathscr{E}_{re}$ and $\mathscr{NRC}$ for different N for Example 4.1

N	$\mathscr{E}_2$	$\mathscr{E}_{re}$	$\mathscr{NRC}$
2	$1.0030e-02$	$4.2721e-03$	/
6	$1.5195e-03$	$6.4721e-04$	-1.7177
10	$6.2736e-04$	$2.6720e-04$	-1.7318
14	$3.4228e-04$	$1.4578e-04$	-1.8006
18	$2.1545e-04$	$9.1765e-05$	-1.8419
22	$1.6746e-04$	$7.1325e-05$	-1.2557

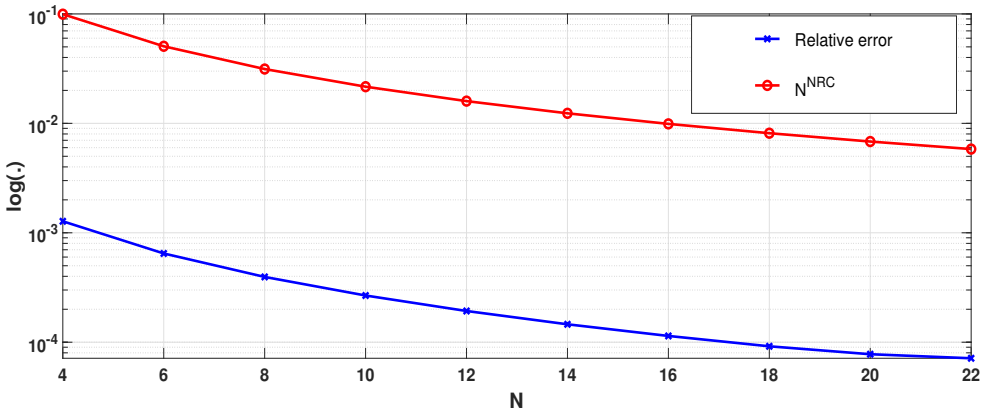

Figure 4.1: Relative error and $N^{\mathscr{NRC}}$ (in log scale) for different N for Example 4.1

Example 4.2 *[5] In this example, a linear Volterra Fredholm equation is studied*

$$ {}^{C}\mathscr{D}^{0.75}u(x) + \frac{x^2\mathrm{e}^x}{5}u(x) = \frac{6x^{2.25}}{\Gamma(3.25)} + \int_0^x \mathrm{e}^x t u(t)\,\mathrm{d}t + \int_0^1 (4 - t^{-3})u(t)\,\mathrm{d}t, \quad (4.45) $$

with $u(0) = 0$. *The exact solution is* $u(x) = x^3$.

Discussion: Table 4.2 provides values for $\mathscr{E}_2$, $\mathscr{E}_{re}$, and $\mathscr{NRC}$ for different N. Comparing with the results obtained in [5], our results show more efficiency when N increases. Figure 4.2 illustrates the behaviour of the exact solution and the approximate solution over the domain $[0, 1]$ using $N = 6$. A clear illustration shows that the two curves exhibit identical behaviour. In Figure 4.3, the curve of the logarithmic absolute error for $N = 18$ is displayed, and the results are in good coherence with those in Table 4.2.

Table 4.2: $\mathscr{E}_2$, $\mathscr{E}_{re}$ and $\mathscr{NRC}$ for different N for Example 4.2

N	$\mathscr{E}_2$	$\mathscr{E}_{re}$	$\mathscr{NRC}$	$\mathscr{E}_2$ in [5]
2	$2.3335e-01$	$1.2689e-01$	/	–
4	$2.2151e-03$	$1.2045e-03$	-6.7189	$4.1433e-03$
6	$8.5977e-04$	$4.6750e-04$	-2.3341	–
8	$4.9534e-04$	$2.6934e-04$	-1.9167	$3.9790e-03$
10	$3.2587e-04$	$1.7719e-04$	-1.8765	–
12	$2.3175e-04$	$1.2601e-04$	-1.8693	–
14	$1.7369e-04$	$9.4445e-05$	-1.8709	–
16	$1.3520e-04$	$7.3517e-05$	-1.8760	$2.2890e-03$
18	$1.0831e-04$	$5.8898e-05$	-1.8822	–
20	$8.8772e-05$	$4.8270e-05$	-1.8887	–

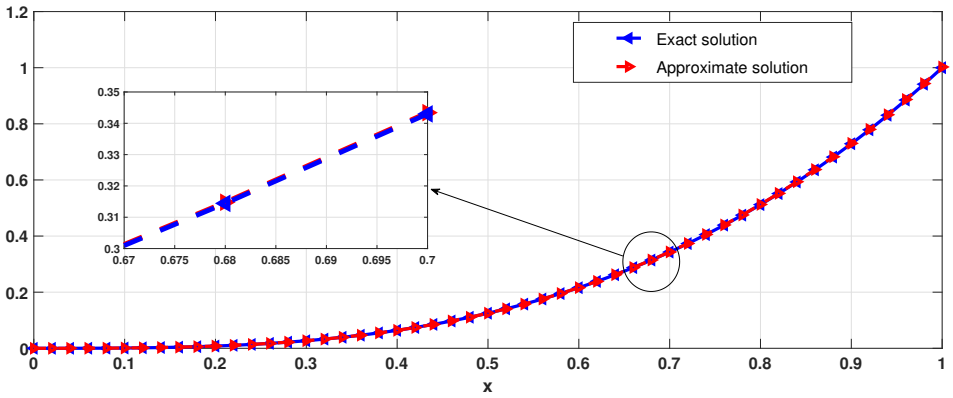

Figure 4.2: Exact and approximate solution for $N = 6$ for Example 4.2

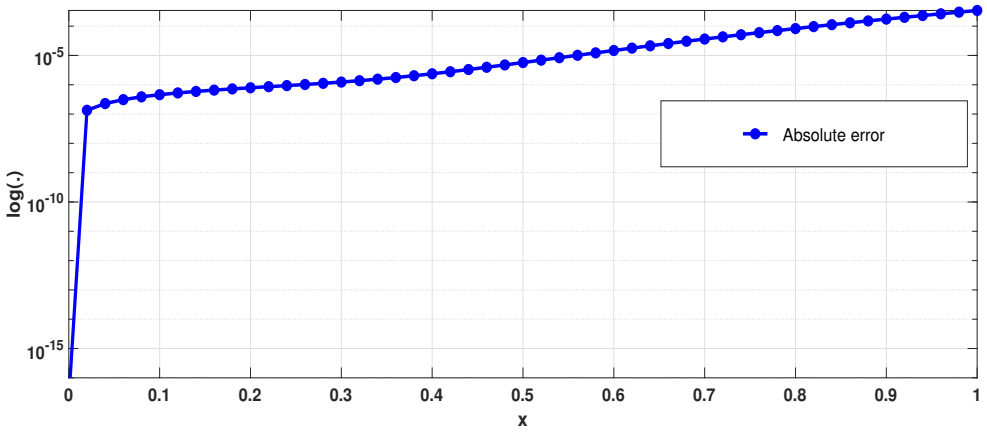

Figure 4.3: Absolute error values for $N = 18$ for Example 4.2

Example 4.3 *[36] We consider another linear Volterra-Fredholm equation with* $u(x) = x$ *being the exact solution*

$$ {}^{C}\mathscr{D}^{0.5}u(x) = \frac{x^{0.5}}{\Gamma(1.5)} - \frac{x^2}{2} - \frac{x^2 e^x}{3}u(x) + \int_0^x e^x t u(t)\mathrm{d}t + \int_0^1 x^2 u(t)\mathrm{d}t, \qquad (4.46) $$

with the condition $u(0) = 0$.

Discussion: In Table 4.3, the values of $\mathscr{E}_2$ and $\mathscr{E}_{re}$ are calculated for different N. Also, the corresponding $\mathscr{NRC}$ is computed, taking uniform values throughout the table with an average value $avg(\mathscr{NRC}) = -1,7688$. Figure 4.4 confirms the obtained results by depicting the curves of $\mathscr{E}_2$ and $\mathscr{E}_{max}$ with different N, showing the decreasing behaviour of error values when N increases.

Table 4.3: $\mathscr{E}_2$, $\mathscr{E}_{re}$ and $\mathscr{NRC}$ for different N for Example 4.3

N	$\mathscr{E}_2$	$\mathscr{E}_{re}$	$\mathscr{NRC}$
2	$1.5353e-02$	$5.7319e-03$	/
6	$2.8405e-03$	$1.0604e-03$	-1.5349
10	$1.1896e-03$	$4.4414e-04$	-1.7037
14	$6.5157e-04$	$2.4325e-04$	-1.7893
18	$4.1074e-04$	$1.5334e-04$	-1.8360
22	$2.8247e-04$	$1.0545e-04$	-1.8656
26	$2.0620e-04$	$7.6982e-05$	-1.8838

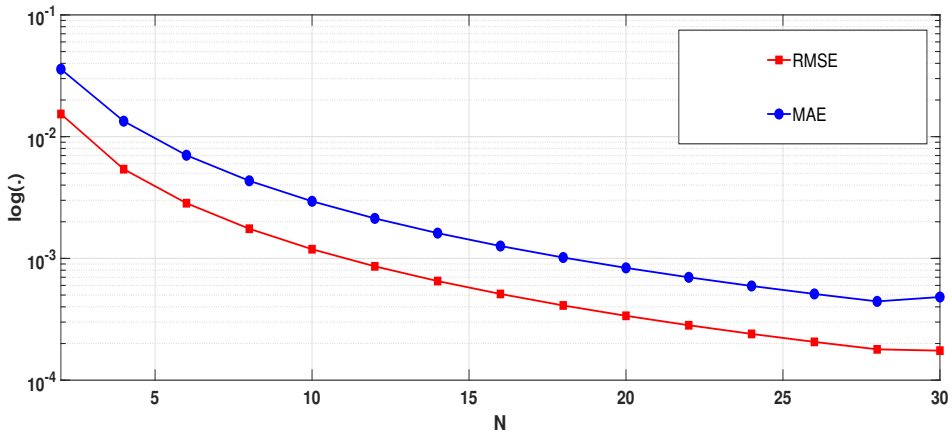

Figure 4.4: $\mathscr{E}_2$ and $\mathscr{E}_{max}$ (in log scale) for different N for Example 4.3

Example 4.4 *Here we discuss the nonlinear Volterra equation*

$$ {}^{C}\mathscr{D}^{3/4}u(x) - \int_0^x xt(u(t))^4 \mathrm{d}t = \frac{1}{\Gamma(1/4)}\left(\frac{32}{5}x^{5/4} - 4x^{1/4}\right) + \frac{x^{11}}{10} + \frac{4x^{10}}{9} - \frac{4x^9}{3} + \frac{4x^8}{7} + \frac{x^7}{6}, \qquad (4.47) $$

with the condition $u(0) + u(1) = 0$*, where the exact solution is* $u(x) = x^2 - x$*.*

Discussion: Table 4.4 provides the values of $\mathscr{E}_2$ and $\mathscr{E}_{re}$ with respect to N. Noting that the results correspond to the example for a nonlinear case so, the parameters used in the Newton's algorithm to solve the nonlinear systems is $\varepsilon = 10^{-10}$ with a maximum of 5 iterations. It is observed that the error values decrease as N increases. The average value of $\mathscr{NRC}$ for Example 4.4 is $avg(\mathscr{NRC}) = -1,9912$ with 3 iterations for Newton's algorithm. In Figure 4.5, the behaviour of the relative error $\mathscr{E}_{re}$ and $N^{\mathscr{NRC}}$ is illustrated, indicating that the error values decrease similarly to $N^{\mathscr{NRC}}$.

Table 4.4: $\mathscr{E}_2$, $\mathscr{E}_{re}$ and $\mathscr{NRC}$ for different N for Example 4.4

N	$\mathscr{E}_2$	$\mathscr{E}_{re}$	$\mathscr{NRC}$
2	$1.3473e-05$	$1.6501e-05$	/
6	$6.8129e-07$	$8.3441e-07$	-2.7165
10	$2.9199e-07$	$3.5761e-07$	-1.6586
14	$6.5157e-07$	$1.9733e-07$	-1.7670
18	$1.0190e-07$	$1.2481e-07$	-1.8227

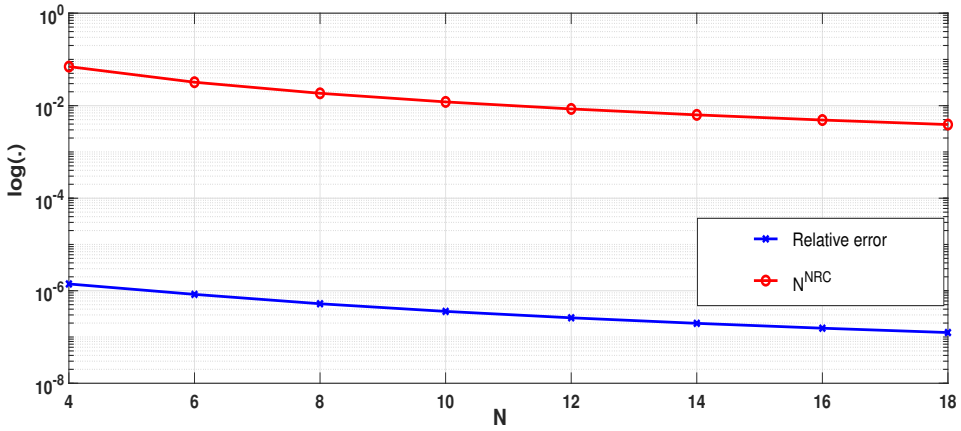

Figure 4.5: Relative error and $N^{\mathscr{NRC}}$ (in log scale) for different N for Example 4.4

Example 4.5 *Here, we study the nonlinear Fredholm equation for different values of* α

$$ {}^{C}\mathscr{D}^{\alpha}u(x) - \int_0^1 xt(u(t))^2 \mathrm{d}t = 1 - \frac{x}{4}, \tag{4.48} $$

with the condition $u(0) = 0$, *noting that for* $\alpha = 1$ *the exact solution is known* $u(x) = x$.

Discussion: For Example 4.5, Table 4.5 presents the values of the approximate solution for different values of α ($\alpha = 0.75$, 0.9, and 1) in comparison with the exact solution calculated for different x ($x = 0.25$, 0.5 and 0.75) and different N ($N = 2$, and 8). For comparison reasons, one can observe the two last columns representing the approximate solution with $\alpha = 1$ and the exact solution, noticing

that they get closer as $N = 8$. Another way to observe this behaviour is shown in Figure 4.6, which depicts the curves of the approximate solution for various values of α (0.5, 0.75, 0.9, 1) when $N = 6$, compared to the exact solution when $\alpha = 1$. The observed behaviour affirms the stability of the solution using the described method.

Table 4.5: Approximate solution values on different x for different α comparing to the exact solution when $\alpha = 1$ for $N = 2$ and 8 for Example 4.5

N	x	$\alpha = 0.75$	$\alpha = 0.9$	$\alpha = 1$	Exact sol.
2	0.25	$3.2486e-01$	$2.7603e-01$	$2.5078e-01$	$2.5000e-01$
	0.5	$6.2166e-01$	$5.4360e-01$	$5.0312e-01$	$5.0000e-01$
	0.75	$8.9042e-01$	$8.0270e-01$	$7.5703e-01$	$7.5000e-01$
8	0.25	$3.8712e-01$	$2.9867e-01$	$2.5009e-01$	$2.5000e-01$
	0.5	$6.6748e-01$	$5.6259e-01$	$5.0036e-01$	$5.0000e-01$
	0.75	$9.2228e-01$	$8.1607e-01$	$7.5081e-01$	$7.5000e-01$

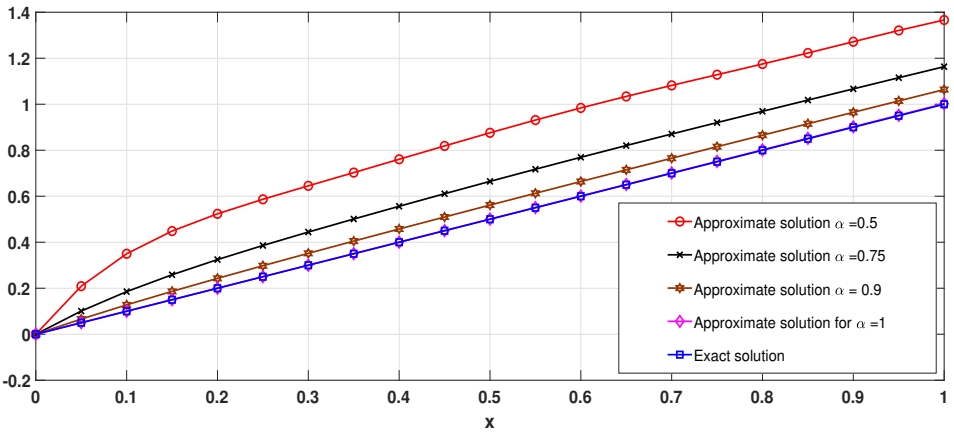

Figure 4.6: Exact and approximate solutions for different α obtained for $N = 6$ for Example 4.5

Example 4.6 *Here, a mixed Volterra-Fredholm equation is discussed*

$$ {}^{C}\mathscr{D}^{1/2}u(x) = f(x) + \frac{1}{10}\int_0^x (3 + x^2 - t^2)u(t)\mathrm{d}t + \frac{1}{24}\int_0^1 (5 + xt)(u(t))^2\mathrm{d}t, \quad (4.49) $$

with the condition $u(0) = 0$, *where*

$$f(x) = \sqrt{\pi}\left(1 + \frac{3x}{4}\right) - \left(\frac{215}{288} + \frac{19x}{180} + \frac{x^{3/2}}{1575}(630 + 189x + 120x^2 + 28x^3)\right),$$

the exact solution is $u(x) = \sqrt{x}(2 + x)$.

Discussion: Table 4.6 depicts $\mathscr{E}_2$ and $\mathscr{E}_{re}$ with respect to N obtained for the same parameters of Newton's algorithm. Also, the values of $\mathscr{NRC}$ with $avg(\mathscr{NRC}) = -1.8907$. Figure 4.7 illustrates the convergence of the approximate solution to the exact solution when N takes the values $2, 6, 12$. The results achieved confirm the effectiveness of the described method for both linear and nonlinear cases.

Table 4.6: $\mathscr{E}_2$, $\mathscr{E}_{re}$ and $\mathscr{NRC}$ for different N for Example 4.6

N	$\mathscr{E}_2$	$\mathscr{E}_{re}$	$\mathscr{NRC}$
2	$2.5722e-01$	$2.9464e-02$	/
6	$3.6918e-02$	$4.2289e-03$	-1.7670
10	$1.2054e-02$	$1.3807e-03$	-2.1912
14	$6.2091e-03$	$7.1124e-04$	-1.9716
18	$4.1190e-03$	$4.7182e-04$	-1.6330

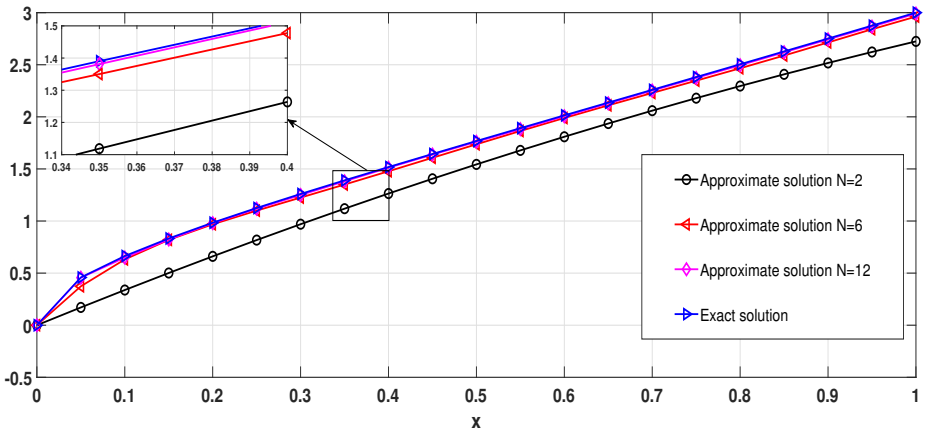

Figure 4.7: Exact and approximate solutions for different N for Example 4.6

4.5 Concluding remarks

The described method demonstrates great efficiency in approximating the solution of the fractional integro-differential equations of different types. Our approach relies on using the shifted Chebyshev polynomials of the third kind as spectral basis with the zeros of Chebyshev polynomials of the third kind as collocation points. This enables us to construct an accurate algorithm applicable to both linear and nonlinear equations.

The obtained results cover a range of integro-differential equation type with fractional order, including linear Volterra equations, linear Volterra-Fredholm equations, nonlinear Volterra equations, nonlinear Fredholm equations, and nonlinear mixed Volterra-Fredholm equations. In all cases, the convergence of the approximate solution to the exact solution is guaranteed, and the method yields significant accuracy compared to other approaches. Furthermore, the experimental rate of convergence calculated for various examples exhibits a consistent behaviour in the relative error obtained for different values of N, thereby validating the convergence results.

Conclusion

Conclusion

The work presented in this thesis focused on the numerical investigation of some mathematical problems using spectral methods. The objective is to demonstrate the significant impact of global approximation when employing the different techniques of spectral methods.
The study primarily addresses partial differential equations and integral equations of integer and fractional order.

In the first part, we examine the advection-diffusion equation as a prototype of parabolic equations. As a first approach, we employ a combination of the Galerkin method with numerical integration and a Crank-Nicolson scheme. This technique combines the advantages of both methods. For the Galerkin method, the presented algorithm utilizes compact combinations of Legendre polynomials as basis functions, satisfying the boundary conditions of the problem and reducing the dimension of the space of approximation to $N-1$ instead of $N+1$. At the same time, the integrals appearing in the weak formulation are evaluated using an integration formula of Gauss-Lobatto type with the Legendre-Gauss-Lobatto points since we prefer to consider both extremities of the interval $[-1,1]$. This latter ensures the highest degree of precision for this type of integration, so we gain more accuracy while calculating the matrices elements that compose the final system to solve. At this stage, a Crank-Nicolson scheme is applied to the resulting system of equations with an appropriate time step, yielding highly efficient and reliable numerical results. In the second approach, we go through the integral form of the advection-diffusion equation and solve it using a Galerkin method based on compact combinations of Legendre polynomials. The technique aims to use the same approach for both spatial and temporal discretizations. The obtained results

show great efficiency and high accuracy.

In the second part, we delve into integral and integro-differential equations using a spectral method based on Legendre polynomials. The proposed technique introduced a novel way of considering the basis functions by incorporating the order of derivation n present in the equation. The basis functions consist of a compact combination of Legendre polynomials that satisfies conditions, reducing the dimension of the space of approximation to $N-n+1$ instead of $N+1$. Linear and nonlinear schemes are proposed using the Gauss-Lobatto quadrature for integral evaluation in the spectral schemes. Numerical results, demonstrated through various examples, showcase exponential convergence with calculated rates of convergence.

In the last part, we explore techniques employed in the previous equations to study an integro-differential equation with a derivation of fractional order in the Caputo sense. Chebyshev polynomials of the third kind are used to approximate the fractional derivative, forming a collocation method using the roots of these polynomials. The technique is developed for the linear and the nonlinear equations, and the numerical examples align with theoretical findings in the error analysis section, confirming the high accuracy of the method.

The results of this modest study underscore the efficiency of spectral methods in solving partial differential equations and extending to other equation types. Future prospects include enhancing matrix calculations for the described techniques in numerical analysis, to address potential error accumulation when using different programming languages.

Bibliography

Bibliography

[1] MA Abdelkawy and Salem A Alyami. Legendre-Chebyshev spectral collocation method for two-dimensional nonlinear reaction-diffusion equation with Riesz space-fractional. *Chaos, Solitons & Fractals*, 151:111279, 2021.

[2] Shazad Shawki Ahmed and Shabaz Jalil MohammedFaeq. Bessel collocation method for solving Fredholm–Volterra integro-fractional differential equations of multi-high order in the Caputo sense. *Symmetry*, 13(12):2354, 2021.

[3] Gregeoire Allaire. *Analyse numérique et optimisation (Éditions de l'École polytechnique)(2007)*.

[4] Ibrahem G Ameen, Mahmoud A Zaky, and Eid H Doha. Singularity preserving spectral collocation method for nonlinear systems of fractional differential equations with the right-sided Caputo fractional derivative. *Journal of Computational and Applied Mathematics*, 392:113468, 2021.

[5] Rohul Amin, Kamal Shah, Muhammad Asif, Imran Khan, and Faheem Ullah. An efficient algorithm for numerical solution of fractional integro-differential equations via Haar wavelet. *Journal of Computational and Applied Mathematics*, 381:113028, 2021.

[6] Kendall E Atkinson. *The numerical solution of integral equations of the second kind*, volume 4. Cambridge university press, 1997.

[7] Lokendra K Balyan, AvinashK Mittal, Mukesh Kumar, and M Choube. Stability analysis and highly accurate numerical approximation of Fisher's equations using pseudospectral method. *Mathematics and Computers in Simulation*, 177:86–104, 2020.

[8] AH Bhrawy, MA Abdelkawy, J Tenreiro Machado, and Ahmed ZM Amin. Legendre–Gauss–Lobatto collocation method for solving multi-dimensional Fredholm integral equations. *Comput. Math. Appl*, 4:1–13, 2016.

[9] Ali H Bhrawy, Mohamed A Abdelkawy, Dumitru Baleanu, and Ahmed ZM Amin. A spectral technique for solving two-dimensional fractional integral equations with weakly singular kernel. *Hacettepe Journal of Mathematics and Statistics*, 47(3):553–566, 2018.

[10] Ali H Bhrawy and Mohammed A Alghamdi. A shifted Jacobi-Gauss-Lobatto collocation method for solving nonlinear fractional Langevin equation involving two fractional orders in different intervals. *Boundary Value Problems*, 2012:1–13, 2012.

[11] Gül Gözde Biçer, Yalçın Öztürk, and Mustafa Gülsu. Numerical approach for solving linear Fredholm integro-differential equation with piecewise intervals by Bernoulli polynomials. *International Journal of Computer Mathematics*, 95(10):2100–2111, 2018.

[12] Haifa Bin Jebreen and Ioannis Dassios. On the wavelet collocation method for solving fractional Fredholm integro-differential equations. *Mathematics*, 10(8):1272, 2022.

[13] Suzan Cival Buranay, Mehmet Ali Özarslan, and Sara Safarzadeh Falahhesar. Numerical solution of the Fredholm and Volterra integral equations by using modified Bernstein–Kantorovich operators. *Mathematics*, 9(11):1193, 2021.

[14] Claudio Canuto, M Yousuff Hussaini, Alfio Quarteroni, and Thomas A Zang. *Spectral methods in fluid dynamics*. Springer, 1988.

[15] Claudio Canuto, M Yousuff Hussaini, Alfio Quarteroni, and Thomas A Zang. *Spectral methods: fundamentals in single domains*. Springer Science & Business Media, 2007.

[16] Bille Chandler Carlson. *Special functions of applied mathematics*. New York, NY (USA) Academic Press, 1978.

[17] Mark H Carpenter and David Gottlieb. Spectral methods on arbitrary grids. *Journal of Computational physics*, 129(1):74–86, 1996.

[18] Dana Černá and Václav Finěk. Galerkin method with new quadratic spline wavelets for integral and integro-differential equations. *Journal of Computational and Applied Mathematics*, 363:426–443, 2020.

[19] Abdeldjalil Chattouh and Khaled Saoudi. Error analysis of Legendre-Galerkin spectral method for a parabolic equation with Dirichlet-Type non-local boundary conditions. *Mathematical Modelling and Analysis*, 26(2):287–303, 2021.

[20] PC Chatwin and CM Allen. Mathematical models of dispersion in rivers and estuaries. *Annual Review of Fluid Mechanics*, 17(1):119–149, 1985.

[21] Jian Chen, Yong Huang, Haiwu Rong, Tingting Wu, and Taishan Zeng. A multiscale Galerkin method for second-order boundary value problems of Fredholm integro-differential equation. *Journal of computational and applied mathematics*, 290:633–640, 2015.

[22] Arman Dabiri and Eric A Butcher. Numerical solution of multi-order fractional differential equations with multiple delays via spectral collocation methods. *Applied Mathematical Modelling*, 56:424–448, 2018.

[23] Eid H Doha, Waleed M Abd-Elhameed, and AH Bhrawy. Efficient spectral ultraspherical-Galerkin algorithms for the direct solution of 2nth-order linear differential equations. *Applied Mathematical Modelling*, 33(4):1982–1996, 2009.

[24] Eid H Doha, Waleed M Abd-Elhameed, and Youssri H Youssri. Fully Legendre spectral Galerkin algorithm for solving linear one-dimensional telegraph type equation. *International Journal of Computational Methods*, 16(08):1850118, 2019.

[25] Eid H Doha, Mohamed A Abdelkawy, Ahmed ZM Amin, and Dumitru Baleanu. Shifted Jacobi spectral collocation method with convergence analy-

sis for solving integro-differential equations and system of integro-differential equations. *Nonlinear Analysis: Modelling and Control*, 24(3):332–352, 2019.

[26] Nehzat Ebrahimi and Jalil Rashidinia. Collocation method for linear and nonlinear Fredholm and Volterra integral equations. *Applied Mathematics and Computation*, 270:156–164, 2015.

[27] Adel A El-Sayed and Praveen Agarwal. Numerical solution of multiterm variable-order fractional differential equations via shifted Legendre polynomials. *Mathematical Methods in the Applied Sciences*, 42(11):3978–3991, 2019.

[28] Mohamed Fathy, Mohamed El-Gamel, and MS El-Azab. Legendre–Galerkin method for the linear Fredholm integro-differential equations. *Applied Mathematics and Computation*, 243:789–800, 2014.

[29] Daniele Funaro. *Polynomial approximation of differential equations*. Springer Science & Business Media, 1992.

[30] Ismail Gad and Paolo Novati. The solution of fractional order epidemic model by implicit Adams methods. *Applied Mathematical Modelling*, 43:78–84, 2017.

[31] Farideh Ghoreishi and Payam Mokhtary. Spectral collocation method for multi-order fractional differential equations. *International Journal of Computational Methods*, 11(05):1350072, 2014.

[32] David Gottlieb and Steven A Orszag. *Numerical analysis of spectral methods: theory and applications*. SIAM, 1977.

[33] Hatıra Günerhan, Hemen Dutta, Mustafa Ali Dokuyucu, and Waleed Adel. Analysis of a fractional HIV model with Caputo and constant proportional Caputo operators. *Chaos, Solitons & Fractals*, 139:110053, 2020.

[34] Mahmoud Hadizadeh and M Asgary. An efficient numerical approximation for the linear class of mixed integral equations. *Applied mathematics and computation*, 167(2):1090–1100, 2005.

[35] Ahmed A Hamoud and Kirtiwant P Ghadle. Some new uniqueness results of solutions for fractional Volterra-Fredholm integro-differential equations.

Iranian Journal of Mathematical Sciences and Informatics, 17(1):135–144, 2022.

[36] Ahmed Abdullah Hamoud, Kirtiwant Ghadle, and Shakir Atshan. The approximate solutions of fractional integro-differential equations by using modified Adomian decomposition method. *Khayyam Journal of Mathematics*, 5(1):21–39, 2019.

[37] Rudolf Hilfer. *Applications of fractional calculus in physics*. World scientific, 2000.

[38] Jordan Hristov. Response functions in linear viscoelastic constitutive equations and related fractional operators. *Mathematical modelling of natural phenomena*, 14(3):305, 2019.

[39] Gigieh Dwi Hutomo, Jeffry Kusuma, Agustinus Ribal, Andi G Mahie, and N Aris. Numerical solution of 2-d advection-diffusion equation with variable coefficient using Du-Fort Frankel method. In *Journal of Physics: Conference Series*, volume 1180, page 012009. IOP Publishing, 2019.

[40] Pakchin S Irandoust. Exact solutions for some of the fractional differential equations by using modification of He's variational iteration method. 2011.

[41] Jerrold Isenberg and Chaim Gutfinger. Heat transfer to a draining film. *International Journal of Heat and Mass Transfer*, 16(2):505–512, 1973.

[42] Reza Jalilian and Tahereh Tahernezhad. Exponential spline method for approximation solution of Fredholm integro-differential equation. *International Journal of Computer Mathematics*, 97(4):791–801, 2020.

[43] Franck Jedrzejewski. *Introduction aux méthodes numériques*. Springer Science & Business Media, 2005.

[44] Anatolii Aleksandrovich Kilbas, Hari M Srivastava, and Juan J Trujillo. *Theory and applications of fractional differential equations*, volume 204. elsevier, 2006.

[45] Naveen Kumar. Unsteady flow against dispersion in finite porous media. *Journal of Hydrology*, 63(3-4):345–358, 1983.

[46] Sunil Kumar, Ajay Kumar, Bessem Samet, and Hemen Dutta. A study on fractional host–parasitoid population dynamical model to describe insect species. *Numerical Methods for Partial Differential Equations*, 37(2):1673–1692, 2021.

[47] Zaid Laadjal and Qing-Hua Ma. Existence and uniqueness of solutions for nonlinear Volterra-Fredholm integro-differential equation of fractional order with boundary conditions. *Mathematical Methods in the Applied Sciences*, 44(10):8215–8227, 2021.

[48] Mehrdad Lakestani, Behzad Nemati Saray, and Mehdi Dehghan. Numerical solution for the weakly singular Fredholm integro-differential equations using Legendre multiwavelets. *Journal of Computational and Applied Mathematics*, 235(11):3291–3303, 2011.

[49] Zineb Laouar, Nouria Arar, and Abdellatif Ben Makhlouf. Spectral collocation method for handling integral and integrodifferential equations of n-th order via certain combinations of shifted Legendre polynomials. *Mathematical Problems in Engineering*, 2022, 2022.

[50] Zineb Laouar, Nouria Arar, and Abdellatif Ben Makhlouf. Theoretical and numerical study for Volterra-Fredholm fractional integro-differential equations based on Chebyshev polynomials of the third kind. *Complexity*, 2023, 2023.

[51] Zineb Laouar, Nouria Arar, and Abdelhamid Talaat. Efficient spectral Legendre Galerkin approach for the advection diffusion equation with constant and variable coefficients under mixed Robin boundary conditions. *Advances in the Theory of Nonlinear Analysis and its Application*, 7(1):133–147, 2023.

[52] Jian Rong Loh, Chang Phang, and Kim Gaik Tay. New method for solving fractional partial integro-differential equations by combination of Laplace transform and resolvent kernel method. *Chinese Journal of Physics*, 67:666–680, 2020.

[53] Xian Ma, Yongxian Wang, Xiaoqian Zhu, Wei Liu, Wenbin Xiao, and Qiang Lan. A high-efficiency spectral method for two-dimensional ocean acoustic propagation calculations. *Entropy*, 23(9):1227, 2021.

[54] Xiaohua Ma and Chengming Huang. Spectral collocation method for linear fractional integro-differential equations. *Applied Mathematical Modelling*, 38(4):1434–1448, 2014.

[55] JA Tenreiro Machado. Fractional order description of dna. *Applied Mathematical Modelling*, 39(14):4095–4102, 2015.

[56] JA Tenreiro Machado, Afshin Babaei, and Behrouz Parsa Moghaddam. Highly accurate scheme for the Cauchy problem of the generalized Burgers-Huxley equation. *Acta Polytechnica Hungarica*, 13(6), 2016.

[57] AMS Mahdy, EMH Mohamed, and GMA Marai. Numerical solution of fractional integro-differential equations by least squares method and shifted Chebyshev polynomials of the third kind method. *Theoretical Mathematics & Applications*, 6(4):87–101, 2016.

[58] Khosrow Maleknejad and Saeed Sohrabi. Numerical solution of Fredholm integral equations of the first kind by using Legendre wavelets. *Applied Mathematics and Computation*, 186(1):836–843, 2007.

[59] Birendra Nath Mandal and Subhra Bhattacharya. Numerical solution of some classes of integral equations using Bernstein polynomials. *Applied Mathematics and computation*, 190(2):1707–1716, 2007.

[60] John C Mason and David C Handscomb. *Chebyshev polynomials*. CRC press, 2002.

[61] Zhijun Meng, Mingxu Yi, Jun Huang, and Lei Song. Numerical solutions of nonlinear fractional differential equations by alternative Legendre polynomials. *Applied Mathematics and Computation*, 336:454–464, 2018.

[62] Behrouz Parsa Moghaddam, Arman Dabiri, and José António Tenreiro Machado. Application of variable-order fractional calculus in solid mechan-

ics. *Applications in Engineering, Life and Social Sciences, Part A*, 7:207–224, 2019.

[63] Behrouz Parsa Moghaddam, A Mendes Lopes, JA Tenreiro Machado, and Zeinab S Mostaghim. Computational scheme for solving nonlinear fractional stochastic differential equations with delay. *Stochastic Analysis and Applications*, 37(6):893–908, 2019.

[64] Behrouz Parsa Moghaddam and Z Salamat Mostaghim. A novel matrix approach to fractional finite difference for solving models based on nonlinear fractional delay differential equations. *Ain Shams Engineering Journal*, 5(2):585–594, 2014.

[65] Akbar Mohebbi and Mehdi Dehghan. High-order compact solution of the one-dimensional heat and advection–diffusion equations. *Applied mathematical modelling*, 34(10):3071–3084, 2010.

[66] Abdelkader Mojtabi and Michel O Deville. One-dimensional linear advection-diffusion equation: Analytical and finite element solutions. *Computers & Fluids*, 107:189–195, 2015.

[67] Payam Mokhtary, Behrouz Parsa Moghaddam, António M Lopes, and JA Tenreiro Machado. A computational approach for the non-smooth solution of non-linear weakly singular Volterra integral equation with proportional delay. *Numerical algorithms*, 83:987–1006, 2020.

[68] Shayma Adil Murad, Hussein Jebrail Zekri, and Samir Hadid. Existence and uniqueness theorem of fractional mixed Volterra-Fredholm integrodifferential equation with integral boundary conditions. *International Journal of Differential Equations*, 2011, 2011.

[69] Anna Napoli and Waleed M Abd-Elhameed. An innovative harmonic numbers operational matrix method for solving initial value problems. *Calcolo*, 54:57–76, 2017.

[70] Tahir Nazir, Muhammad Abbas, Ahmad Izani Md Ismail, Ahmad Abd Majid, and Abdur Rashid. The numerical solution of advection–diffusion problems

using new cubic trigonometric b-splines approach. *Applied Mathematical Modelling*, 40(7-8):4586–4611, 2016.

[71] Somayeh Nemati. Numerical solution of Volterra–Fredholm integral equations using Legendre collocation method. *Journal of Computational and Applied Mathematics*, 278:29–36, 2015.

[72] Jean Yves Parbange. Water transport in soils. *Annual review of fluid mechanics*, 12(1):77–102, 1980.

[73] Alfio Quarteroni, Riccardo Sacco, and Fausto Saleri. *Méthodes Numériques: Algorithmes, analyse et applications*. Springer Science & Business Media, 2008.

[74] Sania Qureshi, Abdullahi Yusuf, Asif Ali Shaikh, Mustafa Inc, and Dumitru Baleanu. Fractional modeling of blood ethanol concentration system with real data application. *Chaos: An Interdisciplinary Journal of Nonlinear Science*, 29(1):013143, 2019.

[75] Marco Raberto, Enrico Scalas, and Francesco Mainardi. Waiting-times and returns in high-frequency financial data: an empirical study. *Physica A: Statistical Mechanics and its Applications*, 314(1-4):749–755, 2002.

[76] Parisa Rahimkhani and Yadollah Ordokhani. Approximate solution of nonlinear fractional integro-differential equations using fractional alternative Legendre functions. *Journal of Computational and Applied Mathematics*, 365:112365, 2020.

[77] Abbas Saadatmandi and Mehdi Dehghan. Numerical solution of the higher-order linear Fredholm integro-differential-difference equation with variable coefficients. *Computers & Mathematics with Applications*, 59(8):2996–3004, 2010.

[78] Prakash Kumar Sahu and S Saha Ray. Legendre spectral collocation method for Fredholm integro-differential-difference equation with variable coefficients and mixed conditions. *Applied Mathematics and Computation*, 268:575–580, 2015.

[79] Mostafa Sakran. Numerical solutions of integral and integro-differential equations using Chebyshev polynomials of the third kind. *Applied Mathematics and Computation*, 351:66–82, 2019.

[80] Jie Shen. Efficient spectral-Galerkin method i. Direct solvers of second-and fourth-order equations using Legendre polynomials. *SIAM Journal on Scientific Computing*, 15(6):1489–1505, 1994.

[81] Jie Shen. Efficient Chebyshev-Legendre Galerkin methods for elliptic problems. In *Proceedings of the third international conference on spectral and hight order methods*, volume 70, pages 233–239, 1998.

[82] Jie Shen, Tao Tang, and Li-Lian Wang. *Spectral methods: algorithms, analysis and applications*, volume 41. Springer Science & Business Media, 2011.

[83] Nasser H Sweilam, Abdelhamid M Nagy, and Adel A El-Sayed. On the numerical solution of space fractional order diffusion equation via shifted Chebyshev polynomials of the third kind. *Journal of King Saud University-Science*, 28(1):41–47, 2016.

[84] Sadiye Nergis Tural-Polat and Arzu Turan Dincel. Numerical solution method for multi-term variable order fractional differential equations by shifted Chebyshev polynomials of the third kind. *Alexandria Engineering Journal*, 61(7):5145–5153, 2022.

[85] Xia Wang, Sanyi Tang, Xinyu Song, and Libin Rong. Mathematical analysis of an HIV latent infection model including both virus-to-cell infection and cell-to-cell transmission. *Journal of biological dynamics*, 11(sup2):455–483, 2017.

[86] Abdul-Majid Wazwaz. *Linear and nonlinear integral equations*, volume 639. Springer, 2011.

[87] Chuanhua Wu and Ziqiang Wang. The spectral collocation method for solving a fractional integro-differential equation. *AIMS Math*, 7(6):9577–9587, 2022.

[88] Yin Yang, Yanping Chen, and Yunqing Huang. Spectral-collocation method for fractional Fredholm integro-differential equations. *Journal of the Korean Mathematical Society*, 51(1):203–224, 2014.

[89] Yang Yin, Chen Yanping, and Yunqing Huang. Convergence analysis of the Jacobi spectral-collocation method for fractional integro-differential equations. *Acta Mathematica Scientia*, 34(3):673–690, 2014.

[90] Muhammed F Younis, Ayoob M Abed, and Ahmed A Hamoud. Existence and uniqueness results for bvp of nonlinear fractional Volterra-Fredholm integro-differential equation. *Advances in Dynamical Systems and Applications*, 16(2):457–467, 2021.

[91] Youssri H Youssri and Waleed M Abd-Elhameed. Numerical spectral Legendre-Galerkin algorithm for solving time fractional telegraph equation. *Romanian Journal of Physics*, 63(107):1–16, 2018.